

Development of Efficient Vibration-based Techniques for Structural Health Monitoring

Ardalan Sabamehr

A thesis

In the Department

of

Building, Civil and Environmental Engineering

Presented in Partial Fulfillment of the Requirements

For the Degree of

Doctor of Philosophy (Civil Engineering) at

Concordia University

Montreal, Quebec, Canada

June 2018

© Ardalan Sabamehr, 2018

CONCORDIA UNIVERSITY
SCHOOL OF GRADUATE STUDIES

This is to certify that the thesis prepared

By: Ardalan Sabamehr

Entitled: Development of Efficient Vibration-based Techniques for Structural Health Monitoring

and submitted in partial fulfillment of the requirements for the degree of

Doctor of Philosophy (Civil Engineering)

complies with the regulations of the University and meets the accepted standards with respect to originality and quality.

Signed by the final examining committee:

_____ Chair
Dr. Muthukumaran Packirisamy

_____ External Examiner
Dr. Mustafa Gul

_____ External to Program
Dr. Ramin Sedaghati

_____ Examiner
Dr. Lucia Tirca

_____ Examiner
Dr. Khaled Galal

_____ Thesis Supervisor
Dr. Ashutosh Bagchi

Approved by _____
Dr. Fariborz Haghghat, Graduate Program Director

Monday, June 18, 2018

Dr. Amir Asif, Dean
Faculty of Engineering and Computer Science

ABSTRACT

Development of Efficient Vibration-based Techniques for Structural Health Monitoring

Ardalan Sabamehr, Ph.D.

Concordia University, 2018

Structural Health Monitoring (SHM) plays a vital role in assessing in-situ the performance of a structure. There are several techniques available for System Identification, Damage Detection and Model Updating. SHM based on the vibration of structures has attracted the attention of researchers in many fields such as: civil, aeronautical and mechanical engineering. This research focuses on the state-of-the art methods for Vibration Testing, Modal Analysis, Model Updating, and Damage Detection in structures. The objective of the thesis is to develop efficient methods in the above areas of SHM using ambient vibration testing. To develop and verify the proposed methods, several case studies are to be developed and implemented a new technique in multi setup merging by use of Random Decrement Technique (RDT). In addition, the preprocessing methods are required for some certain tests like ambient vibration where signal to noise ratio and vibration amplitude are quite low. The RDT is a time domain procedure, where the structural responses to operational loads are transformed into random decrement functions, which are proportional to the correlation functions of a system's operational responses, which can be considered equivalent to free vibration responses. Ambient vibration test of a structure usually produces noisy response and the existing modal identification techniques such as Frequency Domain Decomposition (FDD) and Stochastic Subspace Identifications (SSI) techniques often fail to produce accurate results in such case. Due to contamination of ambient vibration with white Gaussian noise, preprocessing may be required to clean up the vibration signal in order to detect the modal properties accurately. For Operational Modal Analysis (OMA), the multi-setup (or roving sensors) measurement techniques are required due to less number of sensors as compared to the number of degrees of freedom (DOFs) in a structure. The technique is based on selection of DOFs as reference, which is fixed

during all measurements, and the rest of sensors are roved in each setup. Among all available merging techniques, PreGER have been used recently as an alternative method because the merging process have been conducted before parameter estimation. In addition to modal analysis, the measured vibration response of a structure and the results from its Finite Element (FE) model often have some differences because of the idealization and assumptions in representing the structural system, material properties, support conditions, etc., in the FE model. The methods for model updating and damage detection have been classified into Physics-based methods where a mathematical model of a structure needs to be constructed, and data-driven methods where an explicit FE model is used, only the data pattern are used for identifying the changes is a structure. The objective of this research is to develop the hybrid method which is the combination of the physics-based and data-driven methods. The Matrix Update Method (MUM) has been utilized as a physics-based method of model updating, to compare the results between developed method and MUM. Furthermore, damage in structural system is an important concern as it weakens the structure and reduces its functional capacity, and may even cause failure. There are two main challenges in damage detection in the research including baseline free method and the sensitivity analysis. Finally, the proposed merging technique RDT-PreGER shows the efficient method to reduce the number of data and remove the noise in ambient test. In addition, implementing hybrid technique in FE model updating result in providing accurate result by choosing the proper number of groups and well trained network. The result of damage detection technique show that all baseline and baseline free techniques have an uncertainty so the subtle level of damage cannot be detected properly.

Acknowledgements

Foremost, I would like to express my sincere gratitude to my supervisor Prof. Ashutosh Bagchi for the continuous support of my Ph.D study and related research, for his patience, motivation, and immense knowledge. His guidance helped me in all the time of research and writing of this thesis. I could not have imagined having a better advisor and mentor for my Ph.D study.

Besides my advisor, I would like to thank the rest of my thesis committee: Prof. Khaled Galal, Dr. Lucia Tirca, Dr. Ramin Sedaghati and Dr. Mustafa Gul for their encouragement, insightful comments, and hard questions.

Many thanks go to my wife, Niloufar, for her understanding and love during the past few years. She stood by me through all my travails, my absences, my fits of pique and impatience. She gave me support and help, discussed ideas and prevented several wrong turns.

Table of Contents

List of Figures	x
List of Tables	xiii
List of Abbreviations	xiv
Chapter 1. Introduction	1
1.1 Overview	1
1.2 System Identification and Modal Analysis	1
1.3 Problem statement	2
1.4 Research aims and objectives.....	3
Chapter 2. Literature Review	5
2.1 System Identification.....	5
2.1.2 Parametric Methods (Time Domain Methods)	6
2.1.3 Time-Frequency Analysis.....	6
2.1.4 Modal Assurance Criteria (MAC)	7
2.1.5 Random Decrement Technique (RDT).....	7
2.1.6 Merging strategies for multi setup tests	9
2.2 Modal Updating Methods.....	10
2.3 Vibration-based Damage Detection	13
2.3.1 Methods based on frequency changes.....	13
2.3.2 Methods based on mode shape changes.....	13
2.3.3 Mode shape curvature method	14
2.3.4 Methods based on change in flexibility matrix.....	14
2.3.5 Methods based on changes in uniform flexibility shape curvature.....	15
2.3.6 Damage index method	15
2.3.7 Discrete Wavelet Transform.....	17
2.3.8 Summary	17
Chapter 3. Methodology	18
3.1 Overview	18
3.2 Frequency Domain Decomposition (FDD).....	18
3.3 Data-Driven Stochastic Subspace Identification (DD-SSI)	19
3.4 Modified Complex Morlet wavelet.....	20
3.4.1 Parameter selection	21

3.4.2	Modal Properties Identification	22
3.5	Multi Setup Merging Methods	23
3.5.1	Post Separate Estimation Rescaling.....	23
3.5.2	Post Global Estimation Rescaling.....	24
3.5.3	Pre Global Estimation Rescaling	25
3.7	Task details.....	28
3.8	Denosing method for noise reduction	29
3.8.1	Low pass Filter (LPF)	30
3.8.2	Discrete Wavelet Transform (DWT)	30
3.9	Modal updating Methods	31
3.9.1	Neural Networks (NN).....	31
3.9.2	Hybrid method	32
3.9.3	Matrix Update Method (MUM).....	32
3.10	Summary	33
Chapter 4.	Data Collection and Noise Reduction	35
4.1	Overview	35
4.2	Case studies	35
4.2.1	Prestressed Concrete Box (PSCB) Bridge	35
4.2.2	Voided Slab Bridge.....	36
4.2.3	Steel Box (STB) Bridge	37
4.2.4	Three storey scaled steel frame.....	37
4.2.5	Steel cantilever beam	38
4.2.6	Finite Element model of a five storey frame	39
4.2.7	Five storey scaled steel frame	39
4.3	Noise Reduction	40
4.4	Summary	42
Chapter 5.	System Identification and Modal Analysis	43
5.1	Overview	43
5.2	Prestressed Concrete Box (PSCB) Bridge	44
a)	Frequency Domain Decomposition.....	44
b)	Stochastic Subspace Identification (SSI)	45
5.3	Voided Slab Bridge	46

a)	Frequency Domain Decomposition.....	46
5.4	Steel Box (STB) Bridge	48
a)	Frequency Domain Decomposition.....	48
5.5	Three storey scaled steel frame	49
a)	Frequency Domain Decomposition.....	49
b)	Stochastic Subspace Identification.....	49
c)	Time – Frequency Analysis	51
5.6	Cantilever steel beam	54
5.7	Five storey Finite Element model	60
5.8	Five storey scaled steel frame	66
5.9	Other contributions.....	76
5.10	Summary	76
Chapter 6.	Finite Element Model Updating and Vibration-based Damage Detection	77
6.1	Overview	77
6.2	Finite Element Model Updating.....	77
6.2.1	Finite Element Model Updating in PSCB Bridge.....	77
6.2.2	Finite Element Modal updating in Voided Slab Bridge.....	81
6.2.3	Finite Element Model Updating in Steel Box Bridge (STB Bridge).....	84
6.2.4	Finite Element Model Updating in Three storey steel frame.....	87
6.2.5	Finite Element Model Updating in Cantilever steel beam.....	88
6.3	Vibration-based Damage Detection in PSCB Bridge	89
6.3.1	Method based on frequency changes	90
6.3.2	Method based on mode shape changes	91
6.3.3	Mode shape curvature method.....	91
6.3.4	Method base on change in flexibility matrix	92
6.3.5	Methods based on changes in uniform flexibility shape curvature.....	92
6.3.6	Damage index method	93
6.3.7	Wavelet Transform	93
a.	Sensitivity Analysis.....	94
6.4	Summary	95
Chapter 7.	Summary and Conclusions.....	97
7.1	Summary	97

7.2	Conclusions	98
7.3	Contribution	99
7.4	Limitations and Scope for Future Work.....	99
	References.....	101
	Appendix A – FE model of five storey frame.....	108
	Appendix B - FE model of PSCB Bridge	110
	Appendix C – FE model of Voided Slab Bridge	111
	Appendix D – FE model of STB Bridge.....	115
	Appendix E - FE model of Three Storey Scaled Steel Frame	117
	Appendix F - FE model of Steel Cantilever Beam	118
	Appendix G – Publications	119

List of Figures

Figure 2.1 Principle of the Random Decrement Technique (Kölling et al., 2014).....	8
Figure 2.2 Application of RDT technique in modal analysis (Rodrigues et al., 2005)	9
Figure 2.3 Typical three-layer neural network (Chen, 2005)	12
Figure 2.4 MAC values.....	14
Figure 3.1 Post Separate Estimation Rescaling (PoSER) (Felber 1993, Manuel, 2012).....	23
Figure 3.2 Post Global Estimation Rescaling (PoGER) (Manuel, 2012)	25
Figure 3.3 Pre Global Estimation Rescaling (PreGER) (Manuel, 2012).....	26
Figure 3.4 Two-station random response (Ibrahim, 1997)	27
Figure 3.5 Flow chart of PreGER procedure (Parloo, 2003)	27
Figure 3.6 Schematic procedure of RDT – Pre merging multi setup modal analysis.....	28
Figure 3.7 The main classification in vibration based tests	29
Figure 3.8 Additive SNR and calculated SNR after denoising.....	30
Figure 3.9 Procedure of FE model updating (Bagchi, 2005).....	34
Figure 4.1 a) PSCB bridge details b) Data logger	35
Figure 4.2 Sensor location details in PSCB Bridge	36
Figure 4.3 a) Voided Slab Bridge details b) Data logger.....	36
Figure 4.4 Sensor location details (the number inside indicates the channel number).....	36
Figure 4.5 a) STB bridge details b) Data logger	37
Figure 4.6 Sensor Location details in voided slab Bridge	37
Figure 4.7a) Steel frame details b) Micro strain wireless sensor c) Micro strain Gateway	38
Figure 4.8 Steel Cantilever beam details	39
Figure 4.9 Five storey finite element modal in SAP2000.....	39
Figure 4.10 (a) Five storey scale steel frame (b) G link wireless 3D sensor (c) Sensors and data acquisition.....	40
Figure 4.11 (a) top floor acceleration data in 19 second with 512 Hz sampling rate (b) Top floor PSD	41
Figure 4.12 SNR after denoising versus SNR before denoising for (a) bottom floor (b) middle floor (c) top floor	41
Figure 4.13 (a) RMSE in bottom floor (b) RMSE in middle floor (c) RMSE in top floor.....	42
Figure 5.1 Filtered signal of channel #4 in PSCB Bridge.....	44
Figure 5.2 PSCB Bridge modal frequencies	45
Figure 5.3 Corresponding frequencies and mode shapes for PSCB Bridge	45
Figure 5.4 Stabilization chart and mode shapes.....	46
Figure 5.5 Original and filtered signal of channel #1 in Voided Slab Bridge	47
Figure 5.6 Voided Slab Bridge modal frequencies.....	47
Figure 5.7 Identified Modal Properties from Vibration Test in Voided Slab Bridge	47
Figure 5.8 Original and filtered signal of channel #2 in STB Bridge.....	48
Figure 5.9 STB Bridge Modal frequencies	48
Figure 5.10 Identified Modal Properties from Vibration Test in STB Bridge.....	49
Figure 5.11 Modal Properties along long span by use of FDD and SSI methods	50
Figure 5.12 Modal Properties along short span by use of FDD and SSI methods	50

Figure 5.13 MAC values of FDD and SSI methods along both directions.....	51
Figure 5.14 Preliminary result by use of Power spectrum density (PSD)	52
Figure 5.15 Ridge extraction for natural frequency using Scalogram	53
Figure 5.16 Modal properties of three storey steel frame by complex Morlet wavelet.....	53
Figure 5.17 steel Cantilever beam details	54
Figure 5.18 Cantilever beam and sensor location for ambient vibration details	54
Figure 5.19 FDD result for ambient vibration	54
Figure 5.20 RDT – FDD result in ambient vibration.....	55
Figure 5.21 Modal properties of cantilever beam by use of RDT-FDD method.....	55
Figure 5.22 Cantilever beam and sensor location for forced vibration details	55
Figure 5.23 FDD result Force vibration.....	56
Figure 5.24 Modal properties of cantilever beam by use of FDD method	56
Figure 5.25 Manual setup on cantilever beam	58
Figure 5.26 1 st singular value of PSD matrix in (a) pre merging only (b) RDT with pre merging	58
Figure 5.27 Modal analysis along x direction for first three bending mode.....	60
Figure 5.28 WGN applied along x direction.....	61
Figure 5.29 Operational modal analysis along x direction by use of FDD.....	61
Figure 5.30 Apply RDT in acceleration data in level 1 and 5 with the certain trigger value	62
Figure 5.31 Modal Analysis by use of RDT-FDD method.....	62
Figure 5.32 Schematic of multi setup merging in five storey concrete frame	63
Figure 5.33 ARTeMIS output for Post-merging in five storey frame	63
Figure 5.34 Modal properties by use of PreGER.....	64
Figure 5.35 RDT output in each setup	65
Figure 5.36 Modal properties by use of RDT-PreGER technique.....	65
Figure 5.37 1 st singular value along the length.....	66
Figure 5.38 Modal properties along the length.....	66
Figure 5.39 1 st singular value along the width.....	67
Figure 5.40 Modal properties along the width.....	67
Figure 5.41 Stabilization chart along the length	68
Figure 5.42 Modal properties along the length.....	68
Figure 5.43 Stabilization chart along the width	69
Figure 5.44 Modal properties along the width.....	69
Figure 5.45 Ridge detection for frequency along the length	71
Figure 5.46 Mode shape along the length.....	72
Figure 5.47 Ridge detection for frequency along the width	74
Figure 5.48 Mode shape along the width.....	74
Figure 5.49 FDD and SSI outputs for 5 storey building in ARTeMIS	75
Figure 5.50 MAC values in FDD and SSI in ARTeMIS	75
Figure 5.51 Sample results of collaborated projects.....	76
Figure 6.1 Initial Modal properties of PSCB Bridge in SAP 2000.....	78
Figure 6.2 Neural Network Details for PSCB Bridge.....	79
Figure 6.3 Stiffness adjustment factor in PSCB Bridge	80

Figure 6.4 Stiffness adjustment factor in PSCB Bridge in Iteration #12.....	81
Figure 6.5 Initial mode shapes and corresponding frequencies of Voided Slab Bridge in SAP 2000.....	81
Figure 6.6 Neural Network Details for Voided Slab Bridge	82
Figure 6.7 Stiffness adjustment factor voided Slab Bridge	83
Figure 6.8 Stiffness adjustment factor voided Slab Bridge	83
Figure 6.9 Modal properties of STB Bridge in SAP2000.....	84
Figure 6.10 Neural Network Details for STB Bridge	84
Figure 6.11 Stiffness adjustment factor in STB Bridge in iteration #4	86
Figure 6.12 Stiffness adjustment factor in STB Bridge in iteration #4	86
Figure 6.13 Modal properties of three storey Finite Element model.....	87
Figure 6.14 FE model of Cantilever beam and its corresponding modal properties	88
Figure 6.15 Model updating in cantilever steel beam in different conditions	89
Figure 6.16 FEM of the PSCB Bridge	89
Figure 6.17 Damage applied in specified element (a) Elements 166,167, 566, 567 are 20% stiffness reduction (b) Elements 366,367 are 30% stiffness reduction.....	90
Figure 6.18 Modal curvatures of mode 1 and mode 3	91
Figure 6.19 Maximum differences of flexibility matrices of damaged and undamaged bridge...	92
Figure 6.20 Differences in uniform flexibility curvatures of damaged and undamaged bridge...	92
Figure 6.21 Damage indices calculated from equation.....	93
Figure 6.22 (a) 1 st damaged mode shape in PSCB Bridge (b) Damage Detection in Wavelet plot color type 1 (c) Damage Detection in Wavelet plot color type 2	94
Figure 6.23 wavelet coefficient in three different damage states	95

List of Tables

Table 1.1 Modal analysis classification (Brincker et al., 2015).....	2
Table 5.1 Summery of case studies and their applications	43
Table 5.2 Frequencies of ambient vibration test.....	46
Table 5.3 Natural frequency extracted by FDD and SSI	51
Table 5.4 Modal Identification of cantilever beam in different conditions	57
Table 5.5 Modal identification by use of pre merging only and RDT with pre merging	59
Table 5.6 Modal identification of cantilever beam by use of different techniques	59
Table 5.7 Modal identification in five storey frame by use of different methods	65
Table 5.8 Mode shape calculation	71
Table 5.9 Mode shape calculation	72
Table 5.10 Four frequencies of five storey frame using different techniques in MATLAB and ARTeMIS.....	74
Table 6.1 Stiffness modifier by NN in PSCB Bridge	79
Table 6.2 Initial and update modal properties of PSCB Bridge by hybrid model	79
Table 6.3 PSCB bridge initial and updated frequencies (M-FEM)	80
Table 6.4 Stiffness modifier by NN in Voided Slab Bridge	82
Table 6.5 Initial and update modal properties of Voided Slab Bridge by hybrid model	82
Table 6.6 Voided Slab Bridge initial and updated frequencies (MUM).....	83
Table 6.7 Stiffness adjust factor for STB Bridge by hybrid method	85
Table 6.8 Initial and update modal properties of STB bridge by hybrid method	85
Table 6.9 Model updating details of STB Bridge by MUM.....	86
Table 6.10 Model updating three storey frame by hybrid method	87
Table 6.11 Model updating three storey by MUM	88
Table 6.12 Stiffness adjust factor for three storey scaled frame by hybrid method and MUM....	88

List of Abbreviations

OMA	Operational Modal Analysis
EMA	Experimental Modal Analysis
AVT	Ambient Vibration Test
BFD	Basic Frequency Domain
MAC	Modal Assurance Criterion
COMAC	Co-Ordinate Modal Assurance Criterion
DFT	Discrete Fourier Transform
DOF	Degree of Freedom
ERA	Eigensystem realization algorithm
FDD	Frequency domain decomposition
FEM	Finite Element Method
FFT	Fast Fourier Transform
FVT	Forced Vibration Test
ITD	Ibrahim Time Domain
MRPT	Minimum rank perturbation theory
PP	Peak-Picking
PSD	Power Spectral Density
PSCB	Pre-Stressed Concrete Box
SSI	Stochastic Subspace Identification
DD-SSI	Data-Driven Stochastic Subspace Identification
COV-SSI	Covariance Driven Stochastic Subspace Identification
BR	Balanced Realization
CVA	Canonical Variate Analysis
STB	Steel Box
SVD	Singular Value Decomposition
VBDI	Vibration Based Damage Identification
PoSER	Post Separate Estimation Rescaling
PoGER	Post Global Estimation Rescaling
PreGER	Pre Global Estimation Rescaling
RDT	Random Decrement Technique
FE	Finite Element
CF	Correlation Function
WT	Wavelet Transform
HHT	Hilbert–Huang transform
ANPSD	Average Normalized Power Spectral Density
STFT	Short Term Fourier Transform
MRPT	Minimum Rank Perturbation Theory
SHM	Structural Health Monitoring
MUM	Matrix Update Method
NN	Neural Network
CE	Complex Exponential
RC	Reinforced Concrete

Chapter 1. Introduction

1.1 Overview

Structures are generally affected by vibration or dynamics motion. Therefore, applicable analysis tools are essential to measure the response of structures due to dynamic loads. Modal analysis is one the tools that provide the dynamic behavior, modal properties and performance criteria of the structures. It is a reliable technique to provide the global estimation of structure's behavior and to assess the condition of structure. It is worth noting that can be used to detect any damage in structure by applying different algorithms. In addition, measuring modal properties like natural frequency is helpful to avoid resonance in earthquake.

1.2 System Identification and Modal Analysis

The modal testing of structures using forced vibration is often referred to as Experimental Modal Analysis (EMA). It was a common method to find the modal properties until last decades. Modal identification using EMA has become more challenging in case of a large scale structure that requires heavy and expensive devices to excite the structure. For this reason, a new technique called Operational Modal Analysis (OMA), which depends on ambient vibration, is increasing being used. OMA identifies the modal properties of a structure by use of operational and ambient loads only. The ambient vibration, operation loads are the inputs of OMA test which means it has no need to any additional force. So, it is also called ambient modal analysis or output only modal analysis (Rainieri et al., 2014). In Table 1.1, the modal test has been classified by Brincker (Brincker et al., 2015).

Both forced vibration and ambient vibration or in-operation methods can be utilized to determine the dynamic characteristics of structures. Forced vibration method is more complex and costly rather than operational analysis. The positive point of using forced vibration is its controllable excitation which is not possible in ambient vibration tests. The sensitivity of sensors used for ambient vibration measurements should be much higher than those used in forced vibration (Brincker et al., 2015).

Table 1.1 Modal analysis classification (Brincker et al., 2015)

	Mechanical Engineering	Civil Engineering
EMA	Artificial Excitation Impact Hammer shaker (Hydraulic, electromechanical, etc.) Controlled blasts Well-defined measured input	Artificial Excitation Shaker mainly hydraulic Drop weights Pull back tests Eccentric Shakers and exciters Well-defined measured or unmeasured input Controlled blast
OMA	Artificial Excitation Scratching device Air flow Acoustic Emissions Unknown signal, Random in time and space	Natural excitation Wind Waves Traffics Unknown signal, Random in time and space, with some spatial correlation

1.3 Problem statement

- 1) In modal analysis, there are some difficulties and limitations depending on the type of structures. While OMA is an innovative method which is widely used in system identification, it has some drawbacks and limitations in different types of tests. OMA has low amplitude in comparison to EMA, and can be affected by noise easily. On the other hand, monitoring a large scale structure needs large number of sensors. So, the sensing nodes are more than number of sensors which results in dividing the vibration test into several setups covering the entire structure. Then, merging the setups to extract the modal parameters by system identification is quite challenging in large setups. In this research the new technique is developed to merge the large number of setups with less number of data and remove the possible noise in ambient load.
- 2) In Finite Element (FE) Model, there are some differences between FE model and real model which need to be correlated to have same outputs. So, the FE model needs to be updated by use of different techniques which has been classified into two groups such as physics-based and data-driven methods. While there are many available methods for model

updating, there are many limitations including the lack of physically realistic outcome for the updated structural and geometric parameters, and the existing physics-based methods are often complex. To overcome these limitations, there is a need for developing data-driven and hybrid methods of model updating. These methods could be adapted to detecting damage in structures.

- 3) There are lots of algorithms in damage detection. Most of them require a baseline model to compare with the damaged model. It can be a barrier when intact model and corresponding vibration data from the baseline model are not available. Therefore, a baseline free technique is desirable for damage detection when the intact model and corresponding data are not available.

1.4 Research aims and objectives

Based on the problems stated above, the objectives of the present research are identified as follows.

- 1) Develop new techniques for multi setup merging of sensor detains vibration testing of structures for the use in system identification.
- 2) Study the available noise reduction methods in vibration signals and identify the most suitable one for minimizing the error in vibration signals in structures
- 3) Develop a Hybrid method based on Physics-based and Data-Driven methods for model updating using the measured vibration properties of structures
- 4) Study the exiting damage detection techniques of structures using vibration data from the lab and field tests, and develop a baseline free damage detection technique.

To achieve the above objectives, the following tasks, in the broad terms, will be undertaken.

- (a) Both laboratory tests on scaled structures and field tests of real structures will be performed to obtain vibration data for EMA and OMA as appropriate, and data from multi-setup of sensors.
- (b) Frequency domain, time domain and time-frequency domain analysis of system identification will explore to develop a new and efficient system identification technique.
- (c) Effectiveness of RDT in Ambient vibration system identification will be studied and integrated to the developed method.
- (d) Comparative study between three different methods of multi setup merging will be conducted.

- (e) Application of RDT on different types of multi setup merging methods will be studied.
- (f) Noise reduction
- (g) Physics-based method such as the MUM and data-driven method such as the NN-based method will be explored to develop a hybrid method in FE model updating.
- (h) Sensitivity of measurement noise, multi-setup, and incomplete modal information to the model updating and damage detection techniques will be studied in details to test the developed methods.

Chapter 2. Literature Review

2.1 System Identification

Available methods of system identification can be broadly classified in the following three main groups: (i) Non-parametric method (Frequency Domain) (ii) Parametric method (Time Domain) (iii) Time-Frequency Analysis (Turi, 2007). A Nonparametric or Frequency Domain method is fast and relatively simple method to estimate modal parameters from OMA tests. The time domain methods utilize the Correlation Functions (CF) and mathematical transformation from time domain to time-lag domain. On the other hand, the time-frequency methods utilize both frequency domain methods like Fourier analysis and overcome its limitations by capturing the time-varying features of a structure by time domain methods like Wigner–Ville distribution, Wavelet Transform (WT) and Hilbert–Huang transform (HHT). It is worth mentioning that the changes in modal frequencies induced by temperature variation can be more obvious than structural damage, which will have misleading damage identification results. Researchers from Los Alamos National Laboratory monitored the Alamosa Canyon Bridge in New Mexico during 24 hours. They found that the first three modal frequencies varied about 4.7%, 6.6%, and 5.0%, when the temperature of bridge deck changed by about 22° C (Cornwell et al. 1999 and Sohn et al. 1999). It was more significant than the changes of modal frequencies caused by artificial cut in I-40 Bridge (Farrar et al., 1996). Peeters and De Roeck (2001) reported that the first four modal frequencies of Z24 Bridge in Switzerland varied by 14%–18% during monitoring period of 10 months.

2.1.1 Nonparametric methods (Frequency Domain methods)

There are three different methods that can be used in frequency domain modal identification techniques as follows: (1) Basic Frequency Domain (BFD) method which is also called Peak Picking (PP); (2) Frequency Domain Decomposition (FDD) method; and (3) Enhanced Frequency Domain Decomposition (EFDD) method (Brincker et al, 2015). Felber has been attributed for implementation of PP technique. Anderson initiated some basic concept in FDD technique (Anderson, 1997). Then, Brincker presented a completed technique for output only method in modal analysis. He proposed an enhanced FDD method which is called EFDD (Brincker et al, 2015). Estimation of spectral density function is a common procedure in all three methods in frequency domain. When the estimation of spectral density function is done, the analysis type

followed in each of the following methods BFD, FDD and EFDD are different for extracting the modal properties. In BFD technique, Average Normalized Power Spectral Density (ANPSD) is used by normalizing and averaging of auto-spectra to detect all peaks corresponding to the modes of a system. The BFD cannot identify the damping ratio. The half-power bandwidth technique can be added to it (Rodrigues et al., 2004).

2.1.2 Parametric Methods (Time Domain Methods)

The CF based algorithms are the traditional time domain modal analysis techniques which result in changing from time (t) to time-lag (τ) domain. Some of parametric methods are older frequency domain methods. In the early days, several time domain methods applied by use of auto correlation function with no implementation of the Fast Fourier Transform (FFT) (Moller, 2005). The basic time domain methods mentioned above succeed by use of following method Complex Exponential (CE). Ibrahim Time Domain Technique is another method in time domain which developed the complex exponential method (Ewins, 2003). The Stochastic Subspace Identification (SSI) method is time domain system identification which relies on several equations by use of data in time domain.

$$y_t + A_1 y_{t-1} + \dots + A_n y_{t-n} = e_t + B_1 e_{t-1} + \dots + B_n e_{t-n} \quad 2.1$$

In Equation (2.1), Auto Regressive Moving Average (ARMA)-like model is a time discrete model with n samples, and n^{th} order over-determined matrix difference equation. In the model, the model order n can be selected arbitrary (Andersen, 1997). The state space model is the advantage of applying SSI which leads to convert 2^{nd} problem order into two 1^{st} order problems (Moller 2005).

2.1.3 Time-Frequency Analysis

Discrete Fourier Transform (DFT) has some disadvantages like aliasing, leakage, need large number of data, etc. for input data in frequency domain method (Alvin et al., 2003). The DFT is usually applied in stationary signals to extract the frequency content. However, DFT calculates the average of characteristics of signal over the time in the presence of non-stationary signals, and it contaminates its local position globally. So, the modified version of Fourier Transform called Short Term Fourier Transform (STFT) can tackle some of the problems in non-stationary domain, but it still has some limitations (Qian, 2002 and Neild et al, 2003).

The innovative techniques such as Wigner-Ville distribution, Wavelet Transform (WT) and Hilbert-Huang Transform (HHT) are developed to overcome the drawbacks of Fourier-based techniques and provide the time-frequency representation in modal analysis and damage detection (Neild et al., 2001, Staszewski, 2003, Lardies et al., 2002, Kijewski, 2003, Yan, 2004, Yang et al., 2003).

The Morlet wavelet is one of the well-known WT that can decouple multi-component to mono-component in complex-valued shape. Then, system identification for SDOF can be applied to extract the vibration properties. It is worthy to note that identification accuracy is highly depending on time and frequency resolutions. In the presence of operational loads, the well-known algorithm termed Random Decrement Technique (RDT) and WT to extract the modal properties (Kijewski, 2003 and Yan, 2004).

2.1.4 Modal Assurance Criteria (MAC)

The MAC is Modal Assurance Criterion which indicates the orthogonality of two successive modes which can be for the damage and the undamaged structure (measured and/or computed). It can be used to detect damage by use of single number measures of mode shape change in a beam (Fox, 1992). In Equation 2.2, the MAC is mathematically defined as follows (Allemang, 1982).

$$MAC_{cdr} = \frac{|\{\phi_{cr}\}^T\{\phi_{dr}^*\}|^2}{\{\phi_{cr}\}^T\{\phi_{cr}^*\}\{\phi_{dr}\}^T\{\phi_{dr}^*\}} \quad 2.2$$

A MAC value close to 1 shows the independency of two successive modes, however a 0 value indicate that two modes are not correlated well. However, mode shape changes are usually so small that a direct comparison of the mode shapes from the original and the damaged structure in the detection of damage is impractical (Humar et al., 2006).

2.1.5 Random Decrement Technique (RDT)

The Random Decrement Technique (RDT) was introduced by Cole in sixties and seventies during his dynamic analysis conducted with ambient load in NASA project (Cole et al., 1971 and Cole et al., 1973). Gul (2009) applied CMIF with Random Decrement (RD) in order to extract modal properties of a structural system under ambient excitation.

The system response to random input loads or ambient loads is, in each time instant t , composed of the following three parts (1) the response to an initial displacement; (2) the response to an initial velocity; (3) the response to the random input loads between the initial state and the time instant t . Time segmentation and trigger value are two main parameters in RDT. The ambient vibration is zero mean white Gaussian noise which indicate averaging the several time segments with the same initial condition (to avoid time correlation problem), the random part disappear and the response of the system remains close to the initial condition. There is a possibility in experimental test to contaminate with noise especially in OMA test; RDT is very efficient technique to reduce the noise (Rodrigues et al., 2004).

Equation 2.3 shows the relation between RDT and CF;

$$D_{XX}(\tau) = \frac{R_{XX}(\tau)}{\sigma_X^2} a \quad 2.3$$

Where $R_{XX}(\tau)$ is the auto correlation function, $D_{XX}(\tau)$ is auto Random Decrement, a is the trigger value, and σ_X^2 is the variance of process $X(t)$ where $X(t)$ is a stationary stochastic process (Brincker et al., 1991). To minimize the variance of RD function estimation, an optimum trigger value needs to be chosen. The optimum level of triggering condition is defined as $a = \sqrt{2} \sigma_x$, where σ_x is the standard deviation of the time history response (Brincker et al, 2005). Figure 2.1 shows the principle of RDT and two main parameters namely trigger value and time segmentation.

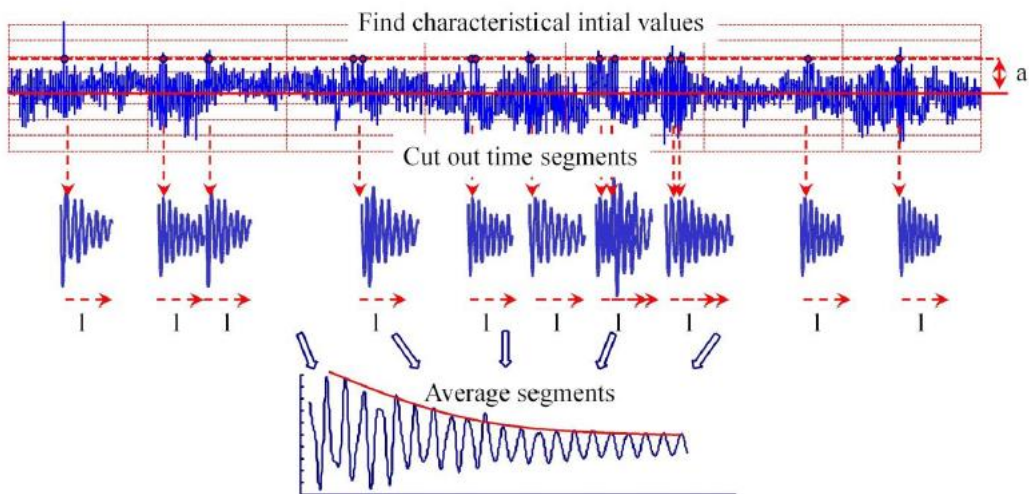


Figure 2.1 Principle of the Random Decrement Technique (Kölling et al., 2014)

The RDT method can be used as a frequency domain modal analysis method that uses spectral estimation (Brincker et al., 1990) and frequency function estimation (Asmussen et al., 1996). Therefore, FFT of the RD functions estimate the spectral density of a system response. Eventually, Welch method is the response time histories, defined as ensemble averaging (Welch, 1967). Spectral densities calculated using FFT from RD functions have been used in a simple example for frequency domain modal analysis technique. It has noticeable advantages regarding estimation of spectral densities by use of common procedure (Brincker et al., 2005). Figure 2.2 shows the application of RDT technique in modal identification in time domain and frequency domain.

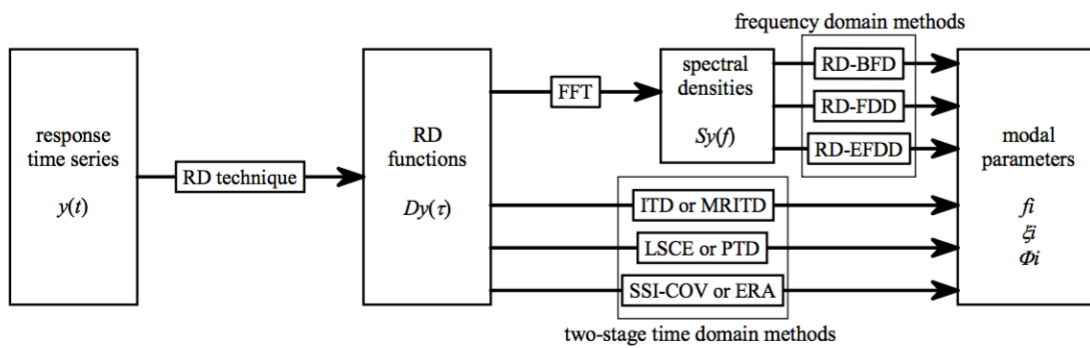


Figure 2.2 Application of RDT technique in modal analysis (Rodrigues et al., 2005)

2.1.6 Merging strategies for multi setup tests

Ambient Vibration test usually have some difficulties in large structure in terms of number of sensors in comparison with degree of freedom. This limitation of available sensors often results error in system identification. To address this, new techniques were proposed in the literature which require multiple setups of sensor arrangements in a structure to capture the vibration patterns corresponding to each setup and then merge the response from all the setups to obtain the global response of the structure (Parloo, 2003). Due to the inherent randomness in ambient vibration due to uncontrolled excitation, some sensors are kept in fixed locations as reference sensors in all setups. The other sensors which are called roving sensors are moved to different locations to cover all degrees of freedom. Generally, there are three different methods for multi-setup merging such as Post Separate Estimation Rescaling (PoSER), Post Global Estimation Rescaling (PoGER) and Pre Global Estimation Rescaling (PreGER). These three approaches are also systematized in (Parloo, 2003).

2.1.7 Noise reduction Methods

In a structural vibration test, reliability and accuracy of the collected signals are very important, as they are contaminated with noise. The noise embedded in the signal could put limits on detection of small defects by affecting the accuracy and reliability of the results (Yi et al., 2012). So far, many techniques have been proposed for denoising such signals. Low pass filter is the most common method for denoising. Low pass filter has the inherent defect that is not able to reduce or remove the in-band noise; it can only be used for out-of-band denoising. In addition, a single scale representation of signals in the time or the frequency domain is not adequate to separate signal from noisy data (Yi et al., 2012). Wavelet is a powerful tool to remove the noise in the signal by combining the time and the frequency domain. The advantage of this method is as follows: (1) decrease the computational complexity in relation to the algorithm; (2) the ability to estimate spectral representation and temporal order of the signal decomposition components simultaneously (Yi et al., 2012). Donoho et al. (1995) and Mohl et al. (2003) proposed a method known as a wavelet transform shrinkage to estimate unknown smoothed signal from data with noise. Adeli and Kim (2004) studied on using of wavelet transform in structural engineering to eliminate dynamic environmental disturbance signals, or the lower frequency components, from ground acceleration signals of civil engineering structures, using Daubechies wavelets with three vanishing moments. Adeli and Jiang (2006) illustrated a signal processing method developed to smoothen the contaminated data of the acceleration response of the structure under earthquakes, based on the discrete wavelet packet transform using a Daubechies wavelet of order 4. Jiang and Mahadevan (2008) also employed the same methodology to remove noise from signals for the nonparametric identification of structures. Rizzo et al. (2005) explained the use of the discrete wavelet transform with Daubechies as a mother wavelet for signal denoising in the tone burst signals of very small structures with dimensions less than 1 mm.

2.2 Modal Updating Methods

A number of methods for updating finite element models are available. Non-iterative methods are one-step approach that directly updates the elements of stiffness and mass matrices (Baruch et al., 1978 and Berman et al., 1983). In the direct method, the updated matrices recreate the modal properties of structures but it includes some drawbacks like loss of the structural connectivity, and

meaninglessness of some parametric changes in terms of structural behaviors. However, iterative method includes the sensitivity analysis of the parameters in model updating model (Friswell et al., 1995 and Link et al., 1999). This approach leads to identify the parameters which have direct effect on modal characteristics of the structure.

Kang et al. (2005) introduced a system identification plan in the time domain to calculate stiffness and damping parameters of a structure using measured acceleration. They introduced an error function defined by the time integral of the least-squared errors between measured and numerical accelerations. They also employed a regularization technique using a geometric mean scheme in the system identification methods. They have validated their method by applying in two-span truss bridge and three storey shear building model (Kang et al., 2005).

Bagchi (2005) utilized iterative process for model updating and correlations using the MUM applied to the Crowchild Bridge in Calgary, Alberta. It shows the difference between initial FE model and measured values affected the performance of FE model updating in stiffness adjustment and correlate the FE model to the real parameters. There is a limitation of stiffness adjustment factors to make the model updating feasible.

Mainly, there are two types of model updating methods such as direct and indirect (iterative) methods. In the direct model updating approach, the system matrices element is updated to correlate the difference between actual model and numerical model. However, the iterative model updating use sensitivity analysis model regularization (Tsai et al., 2002).

Several physic-based formulas are utilized in the matrix updated problem, which can suffer from the nature of the inverse problem. This kind of structural formulate can be significant in terms of estimating modal force errors (Doebling, 1996). Kammer (1988) and Brock (1986) minimized the modal force error by use of property matrix symmetry constraint. Smith (1992) presented an iterative method to update optimal update that applies the sparsity of the matrix which appropriate sparsity pattern multiplying each entry in the stiffness update by zero or one. Zimmerman and Kaouk (1998) proposed Minimum Rank Perturbation Theory (MRPT) algorithm. They developed their algorithm to evaluate perturbation simultaneously by use of complex conjugates of the model force error formula (Brock, 1986, Zimmerman et al., 1994, Kammer, 1988, and Smith, 1992).

The advantage of method of is its capability to be computationally more useful than making the sensitivities at the global matrix level (Doebling et al., 1996, Rhee, 2000, and Ricles, 1991). An eigenstructure assignment method was proposed by Zimmerman and Kaouk (1998) for damage

identification. Li and Smith (1995) proposed a hybrid model update technique for damage identification which combined of the sensitivity and optimal-update approaches. Jaishi and Ren (2005) arranged a test for a practical and sensitivity-based FE model updating technique in structural dynamics for real structures by use of ambient vibration test results. Their main contribution is minimizing using the least-square algorithm by combining the eigenvalue residual, mode shape related function, and modal flexibility residual as an objective function.

In past two decades, one of the powerful techniques, Artificial Neural Networks (ANN) was developed and widely used solving many engineering problems because of its capability in learning and high tolerance to imprecise data. Barai and Pandey (1995) used an ANN to process the vibration signature to detect damage in a steel bridge. Sato et al. (1997) indicated the dynamic response characteristics of a structural system by use of a neural network and Kalman filter algorithm. Xu et al. (2003) and Chen (2005) employed a structural parametric assessment technique by use of neural networks, to identify damage, and monitor the behavior of structure by use of dynamic responses.

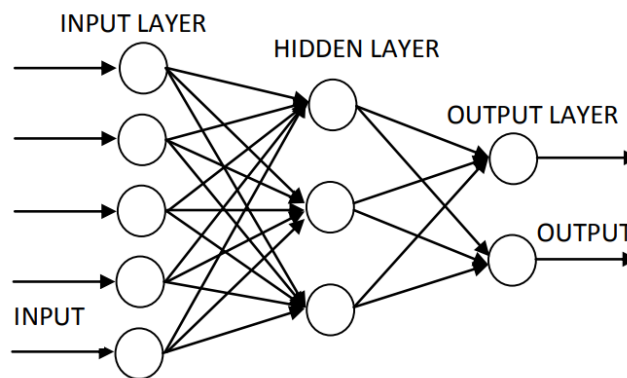


Figure 2.3 Typical three-layer neural network (Chen, 2005)

Figure 2.3 shows the typical three layers in neural network. Hen (2005) and Hasancebi and Dumlupinar (2013) used ANNs to update the model of reinforced concrete (RC) bridges. ANN is known strongly familiar in several topics like diagnosing, forecasting, extracting, identification, and control (Hsu et al., 1993). The principal functions of Back Propagation Network (BPN), which should be connected between physical properties of RC structures and the dynamic parameters, are included of extremely complex mapping relationships. Tsai and Hsu (2002) proposed innovative technique in damage identification domain occurred in existing RC structures using

ANN technique based on the displacement time history. Entezami et al. (2014) proposed a new method to localize the damage in a multi-storey shear building by use of direct model updating method. Therefore, the perturbation matrices should distinguish a damaged structure from and healthy one by use of mass and stiffness matrices of those structural states.

2.3 Vibration-based Damage Detection

Visual and non-destructive inspection are considered traditional damage identification and condition assessment methods. However, the application of these methods requires that the damaged parts of the structure are accessible. Vibration characteristics of a structure, such as frequency, mode shape and damping, are directly affected by the physical characteristics of the structure like mass and stiffness. Damage reduces the stiffness of the structure and changes its vibration characteristics. Therefore, the location and severity of damage can be detected by measuring and monitoring of vibration characteristics. Most of literature deals with the application of theoretical damage identification or laboratory test. Applications on real structures such as bridges or buildings are very rare. There are many analytical methods to identify damage from changes of dynamic parameters. Humar et al. (2006) presented a comprehensive analysis of the performance of existing vibration-based damage detection techniques.

2.3.1 Methods based on frequency changes

Structural property changes such as mass, stiffness and damping result in changing frequency. However, this technique has significant practical limitations for application for real structures. There are two reasons. First, very precise frequency measurements are required to detect small levels of damage. Second, environmental elements, especially temperature, have significant effects on frequency changes. If higher modal frequencies are used, this method may be useful because these modes are associated with local responses. However, it is difficult to excite and extract these higher local modes (Humar et al. 2006).

2.3.2 Methods based on mode shape changes

The MAC has been discussed in section 2.1.4. There is a possibility to identify a damage based on MAC by comparing the intact and damage mode shapes. The changes of MAC values in the

presence of damage is negligible. So, damage detection by MAC might not be applicable when the damage severity is small. Figure 2.5 is an example of MAC value in six mode shapes.

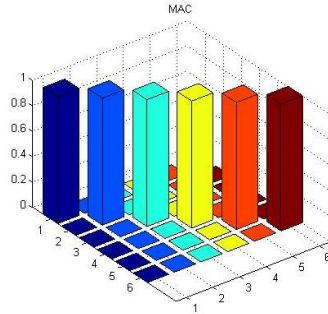


Figure 2.4 MAC values

2.3.3 Mode shape curvature method

Instead of using methods based on mode shape changes to obtain spatial information, mode shape curvature method is an alternative method. This method is better than mode shape changes to detect damage for a beam type structure. The curvature values can be computed from the measured displacement mode shapes by using a central difference operator. Therefore, the curvature $\psi''(x_i)$ at location i along a beam is obtained from following equation.

$$\psi''(x_i) = \frac{y_{i+1} - 2y_i + y_{i-1}}{h^2} \quad 2.4$$

where, y_i is the mode shape displacement at location i and $h = x_{i+1} - x_i$. An advantage of this equation is that an analytical model is not required when healthy mode shapes are obtained from measurement. However, modal curvatures are easily affected by measurement errors and the numerical differentiation of the mode shape vectors (Humar et al. 2006).

2.3.4 Methods based on change in flexibility matrix

In this flexibility change method, damage is detected by comparing the flexibility matrix measured from the mode shapes of the damaged and undamaged structure. The flexibility matrix is the inverse matrix of the static stiffness matrix. Therefore, the flexibility matrix is relations between the applied static force and displacement. The measured flexibility matrix can be estimated from the mass-normalized measured mode shapes and frequencies. The flexibility matrix F of the undamaged structure is obtained from Equation 2.5 (Humar et al. 2006).

$$F \approx \Phi \Omega^{-1} \Phi^T = \sum_{j=1}^{nm} \frac{1}{\lambda_j} \phi_j \phi_j^T \quad 2.5$$

Here, Φ is the modal matrix of the mass-normalized mode shapes ϕ_j and nm is the number of measured mode shapes. This equation of the flexibility matrix is approximate because only the first few modes of the structure can be measured (Doebbling et al. 1998). The flexibility matrix F_d of the damaged structure is obtained from Equation 2.6 (Humar et al. 2006).

$$F_d \approx \Phi_d \Omega_d^{-1} \Phi_d^T = \sum_{j=1}^{nm} \frac{1}{\lambda_{dj}} \phi_{dj} \phi_{dj}^T \quad 2.6$$

where Φ_d is the modal matrix of the damaged structure. The difference between flexibility matrices of the damaged and undamaged structure is obtained from Equation 2.7.

$$\Delta F = F_d - F \quad 2.7$$

Let δ as the row vector whose j^{th} element is equal to the element with the largest absolute value in the j^{th} column of ΔF . The large value of δ is relevant to the location of damage.

$$\delta_j = \max |\Delta F_{ij}| \quad i = 1, \dots, N \quad 2.8$$

2.3.5 Methods based on changes in uniform flexibility shape curvature

The flexibility matrix is relations between the applied static force and the displacement of the corresponding DOF. Therefore, a displacement curvature shape can be obtained corresponding to each column of F and F_d . The difference of curvatures between damaged and undamaged can be obtained from

$$\delta = \sum_j |\psi_{dj} - \psi_j| \quad 2.9$$

where, ψ_{dj} is the j^{th} damaged curvature, ψ_j is the j^{th} undamaged curvature.

2.3.6 Damage index method

Damage index is defined as the change in strain energy of the structure when it is deformed (Stubbs, 1995). This modal strain energy can be derived from the curvature of the measured mode shapes. In a linear elastic beam of NE elements, damage causes reduction in the flexural rigidity

of one or more elements. The lowest nm mode shapes of the structure have been made both of the undamaged and the damaged structure. In the process of the numerical differentiation method such as the central difference operation, modal curvature can be derived. The modal strain energy in the i^{th} mode of the structure and the j^{th} element between a and b are obtained from

$$S_i = \int_0^L EI(x)[\psi_i''(x)]^2 dx, \quad S_{ij} = \int_a^b EI_j[\psi_i''(x)]^2 dx \quad 2.10$$

where, L is the length of the beam, EI is the flexural rigidity, and $\psi''(x)$ is modal curvature. Total strain energy contributed by element j is given by the ratio $F_{ij} = S_{ij}/S_i$. For the damaged structure, the above equations are changed into

$$S_i^d = \int_0^L EI^d(x)[\psi_i^{d''}(x)]^2 dx, S_{ij}^d = \int_a^b EI_j^d[\psi_i^{d''}(x)]^2 dx, \quad F_{ij}^d = S_{ij}^d/S_i^d. \quad 2.11$$

Assuming that damage is limited to a few elements, the damaged and undamaged flexural rigidity would be approximately same, so $EI^d(x) \approx EI(x)$. It is also assumed that

$$F_{ij}^d \approx F_{ij} \quad 2.12$$

Substituting Equations 2.10 and 2.11 in Equation 2.12, we get

$$\gamma_{ij} = \frac{EI_j}{EI_j^d} = \frac{\int_0^L EI(x)[\psi_i''(x)]^2 dx \cdot \int_a^b [\psi_i^{d''}(x)]^2 dx}{\int_0^L EI^d(x)[\psi_i^{d''}(x)]^2 dx \cdot \int_a^b [\psi_i''(x)]^2 dx} \quad 2.13$$

Where, γ_{ij} is the damage index for the j^{th} element in mode no. i . This damage index is changed as follows to use the information available from the nm measured modes.

$$\gamma_j = \frac{\sum_{i=1}^{nm} f_{ij}^d}{\sum_{i=1}^{nm} f_{ij}} \quad 2.14$$

Elements with relatively large γ_j are likely to be damaged. When the strain energy contributed by the j^{th} member in the modes is very small, the denominator will be very small in magnitude too. This may arise numerical problems in the evaluation of Equation 2.12 and Equation 2.13. In that case, Equation 2.14 is modified as follows;

$$\gamma_j = \frac{1 + \sum_{i=1}^{nm} f_{ij}^d}{1 + \sum_{i=1}^{nm} f_{ij}} \quad 2.15$$

2.3.7 Discrete Wavelet Transform

The wavelet is a powerful method to assess the time–frequency content of time series. This transform has a multi-resolution capability deriving from a flexible window that is broader in time for observing low frequencies and shorter in time for observing high frequencies, as required by the Heisenberg uncertainty principle (Sale et al., 2011). This capability is given by the mother wavelet function utilized as the basis of the decomposition. The mother wavelet is defined by two parameters, the scaling parameter a and the translation parameter b (daubechies, 1992). Applied to a time-transient waveform, the CWT yields a scalogram contour plot that retains the time–frequency information of the propagating wave’s energy.

2.3.8 Summary

There is a large volume of literature available on Vibration-based SHM as techniques that have applications in many disciplines including Aerospace, Mechanical, and Civil Engineering. There are various vibration-based system identification techniques developed in frequency and time domains. However, because of the low amplitude of vibration signal in ambient condition, the direct application of these system identification methods generally produce poor results. To mitigate that, the ambient vibration signals are suggested to be preprocessed to reduce the noise level and increase the sensitivity of the signal features. But, such approaches need to be further developed. For vibration-based model updating and damage detection, several physics-based and data-driven methods are available. While a lot attention was given to physics-based methods earlier, their effectiveness was found to be limited because of the inverse nature of the problem and the high level of noise in the data. While data-driven model were found to be promising, further research is required to develop an efficient set of methods that can be used in conjunction with the physics-based methods and thereby develop a hybrid method.

Chapter 3. Methodology

3.1 Overview

Modal Analysis is an important technique to monitor the global behavior of a structure. In modal testing, several algorithms in different domain have been proposed. Frequency Domain Decomposition (FDD), Stochastic Subspace Identification (SSI) and Continuous Wavelet Transform (CWT) are three common algorithms in frequency, time and time-frequency domains respectively. Monitoring large scale structure requires large number of sensors which may not be practical. For the dynamic test of a large scale structure with limited number of sensors, multi setups merging is proved to be an effective technique. Different algorithms have been developed to merge the collected data from sensor in different setups. Apart from modal analysis, there are always some differences between FE models and real structure. To track the structure conditions in FE model, it needs to be updated to have same response as real structure. Model updating is a technique to correlate FE data and measured data using modal properties.

3.2 Frequency Domain Decomposition (FDD)

Equation 3.1 shows the relation between measured response $y(t)$ and unknown input $x(t)$.

$$G_{yy}(j\omega) = \bar{H}(j\omega) G_{xx}(j\omega) H(j\omega)^T \quad 3.1$$

where $G_{xx}(j\omega)$ is the $(r \times r)$ power spectral density (PSD) matrix of the input, r is the number of inputs, $G_{yy}(j\omega)$ is the $(m \times m)$ PSD matrix of the response, m is the number of responses, the Frequency Response Function (FRF) is known by $H(j\omega)$ which is $(m \times r)$ matrix. It is worthy note that overbar and subscript T show the complex conjugate and transpose (Brincker, 2000).

There is partial function to extract FRF as follows;

$$H(j\omega) = \sum_{k=1}^n \frac{R_k}{j\omega - \lambda_k} + \frac{\bar{R}_k}{j\omega - \bar{\lambda}_k} \quad 3.2$$

Where n is the number of modes, $\bar{\lambda}_k$ is the pole and R_k is the residue:

$$R_k = \Phi_k \gamma_k^T \quad 3.3$$

where ϕ_k and γ_k are the mode shape vector and modal participation vector, respectively.

FDD method includes two steps. The first step is calculation of PSD matrix. Estimation of output in PSD, $\widehat{G}_{yy}(j\omega)$, is known as discrete frequencies $\omega = \omega_i$. The second step is decomposed by applying the Singular Value Decomposition (SVD) of the matrix:

$$\widehat{G}_{yy}(j\omega) = U_i S_i U_i^H \quad 3.4$$

where the matrix $U_i = [u_{i1}, u_{i2}, \dots, u_{im}]$ is a unitary matrix holding the singular vectors u_{ij} , and S_i is a diagonal matrix holding the scalar singular values s_{ij} . As it is defined, the real mode should has a peak in frequency domain. Then, near a peak corresponding to the k^{th} mode in the spectrum, this mode or maybe a possible close mode, will be dominating. If only the k^{th} mode is dominating, the first singular vector u_{i1} is an estimate of the mode shape (Brincker, 2000)

$$\widehat{\phi} = u_{i1} \quad 3.5$$

3.3 Data-Driven Stochastic Subspace Identification (DD-SSI)

DD-SSI is a powerful time domain method in order to identify the modal properties of structure in recent years. It requires interesting mathematics tools and robust linear algebra in state-space model using raw data. It relies on well-known mathematic tools like Singular Value Decomposition (SVD), LQ decomposition. In fact, the identification problem is linearized, that is to say it is reduced to a simple least squares problem. Moreover, the use of well-known tools from numerical linear algebra, such as SVD and LQ decomposition, leads to a numerically very efficient implementation. A development of DD-SSI is identifying the state sequence before estimating the state-space model. It can be computed directly from measured data using some geometric operation which are called orthogonal and oblique projection (Van Overschee and De Moor 1996).

$$[H_{0|2i-1}] = \frac{1}{\sqrt{j}} \begin{bmatrix} \{y_0\} & \{y_1\} & \dots & \{y_{j-1}\} \\ \{y_1\} & \ddots & \ddots & \{y_j\} \\ \vdots & \ddots & \ddots & \vdots \\ \{y_{j-1}\} & \{y_j\} & \dots & \{y_{i+j-2}\} \\ \{y_i\} & \{y_{i+1}\} & \dots & \{y_{i+j-1}\} \\ \{y_{i+1}\} & \ddots & \ddots & \{y_{i+j}\} \\ \vdots & \ddots & \ddots & \vdots \\ \{y_{2i-1}\} & \{y_{2i}\} & \dots & \{y_{2i+j-2}\} \end{bmatrix} = \frac{[Y_{0|2i-1}]}{[Y_{i|2i-1}]} = \frac{[Y_p]}{[Y_f]} \quad 3.6$$

3.4 Modified Complex Morlet wavelet

The wavelet is a linear representation which sum all time of signal $x(t)$ multiplied by scaled, shifted version of the mother wavelet $\psi(t)$ in the following form;

$$W(a,b) = \frac{1}{\sqrt{a}} \int_{-\infty}^{+\infty} x(t) \psi^* \left(\frac{t-b}{a} \right) dt, \quad 3.7$$

where a is the scaling factor and b is the time shift. The prototype wavelet is called mother wavelet. The “*” denotes the complex conjugation. The scale index a controls the stretch of the analysis window and parameter b indicates the time shifting. The factor $\frac{1}{\sqrt{a}}$ is used to ensure energy preservation. $W(a,b)$ is the parameter to measure of similarity between the signal and each wavelet function in the form of time-frequency representation. The concept of wavelet transform is the dominant frequency makes the wavelet with prominent amplitudes. There is a number of real and complex-valued wavelet functions for different applications. One of the most well-known and widely used for system identification is complex Morlet wavelet due to its capability in time-frequency localization for analytical signals (Le et al., 2012). The modified complex Morlet is defined as follows,

$$\psi(t) = \frac{1}{\sqrt{\pi f_b}} (e^{j2\pi f_c t} - e^{-f_b(\pi f_c)^2}) e^{-t^2/f_b}, \quad 3.8$$

where f_b is the bandwidth parameter, f_c is the central wavelet frequency, and j is the imaginary unit. To satisfy the admissibility condition, $\sqrt{f_b} f_c \geq \sqrt{2}$ should be considered. So, the term $e^{-f_b(\pi f_c)^2}$ can be negligible, and we have a simplified version as follows,

$$\psi(t) = \frac{1}{\sqrt{\pi f_b}} e^{j2\pi f_c t} e^{-t^2/f_b}, \quad 3.9$$

The wavelet scale, a , and Fourier frequency, f , can be converted by following equation;

$$f = \frac{f_c}{a} \quad 3.10$$

The time and frequency resolution of the wavelet transform are dependent on the basis wavelet $\psi(t)$. They are related by the scale parameter of wavelet as follows;

$$\Delta t_i = a_i \Delta t_\omega \text{ and } \Delta f_i = \frac{1}{a_i} \Delta f_\omega \quad 3.11$$

where Δt_ω and Δf_ω are the time and frequency resolution of the basis function respectively. The Heisenberg uncertainty principle provides a good performance indicator termed the time-frequency resolution rectangle $\Delta t \Delta f \geq 1/4\pi$ to evaluate the time-frequency representation. For the modified Morlet wavelet, the resolution rectangle becomes;

$$\Delta t_\omega \Delta f_\omega = 1/4 \pi \quad 3.12$$

This indicates that an increase in time resolution results in a decrease in frequency resolution and vice versa. For modified Morlet wavelet, the time and frequency resolutions are;

$$\Delta t_\omega = \frac{\sqrt{f_b}}{2} \text{ and } \Delta f_\omega = \frac{1}{2\pi\sqrt{f_b}} \quad 3.13$$

So,

$$\Delta t_i = \frac{f_c}{f_i} \frac{\sqrt{f_b}}{2} \text{ and } \Delta f_i = \frac{f_i}{f_c} \frac{1}{2\pi\sqrt{f_b}} \quad 3.14$$

Which shows that choosing appropriate f_b and f_c result in having good resolution in time and frequency. For ambient vibration, the Random Decrement preprocessing is required for Time-Frequency analysis. However, there is a method that used the correlation function to find the equivalent formula for wavelet without using RDT (Le et al., 2012).

3.4.1 Parameter selection

Generally, in order to select $\sqrt{f_b} f_c$, the values for separate two closely spaced frequency components f_i and f_{i+1} with the difference $\Delta f_{i,i+1} = f_{i+1} - f_i$ and an average of $f_{i,i+1} = (f_i + f_{i+1})/2$ can be calculate according to following formula,

$$(2\alpha) \frac{f_{i,i+1}}{2\pi\Delta f_{i,i+1}} \leq \sqrt{f_b} f_c \leq \left(\frac{2\gamma}{\beta}\right) T f_i \quad 3.15$$

For the signal, the parameters T , f_i , $f_{i,i+1}$ and $\Delta f_{i,i+1}$ are known or predetermined by Fourier transformed. The parameters α , β and γ will be defined in such a way to separate the closed modes properly. The best values for α , β and γ is 2, 4, and 4 respectively (Yel et al, 2006).

3.4.2 Modal Properties Identification

3.4.2.1 Natural Frequency

The wavelet coefficients take on maximum values of instantaneous frequency corresponding to dominant frequency component in the signal at each instant time. The ridge in time-frequency plane, extracting the values of wavelet coefficients along each ridge yields a wavelet skeleton. The square modulus of wavelet is called scalogram that is simplest way to identify the dominant frequency of signal (Kijewski et al., 2003). In order to identify the natural frequency, windows parallel to the frequency axis at the wavelet ridge in time-frequency plot are extracted (Wijesundara et al., 2012).

3.4.2.2 Damping Ratio

A window paralleled to the time axis at the wavelet ridge is extracted from time-frequency plot (semi-logarithmic plot) to estimate the damping ratio of the corresponding mode vibration.

3.4.2.3 Mode shape

The j^{th} mode shape of the structure can be estimated by evaluating the WT of the time signals from all the measured points at the corresponding j^{th} frequency. For example, let $Wh_k(b, a_j)$ and $Wh_r(b, a_j)$ be the WTs of signal at point k and at the reference point r , respectively. The ratio of them,

$$\psi_{kj} = \frac{Wh_k(b, a_j)}{Wh_r(b, a_j)} \quad 3.16$$

The quantity of ψ_{kj} represents the k^{th} component of the j^{th} mode shape of the structure (Yel et al., 2006).

3.5 Multi Setup Merging Methods

When the number of sensing node is more than number of degrees of freedom (DOF), multi setups merging technique is required to cover the response of as DOF as possible by moving or roving some of the sensors while keeping one or two sensors in fixed places as reference. In this method, the sensing test divided to several setups which each setup cover partial section of the structure. When whole of structure is covered, all setups need to be merged using merging algorithm.

3.5.1 Post Separate Estimation Rescaling

The first technique that have been used for ambient vibration test is Post Separate Estimation Rescaling (PoSER) strategy (Felber 1993). In this method, each setup estimates its modal properties individually, then total modes are paired and rescaled to extract the final mode shapes. Figure 3.1 describes schematically the method (Parloo 2003). It is available in some software like ARTeMIS (Structural Vibration Solutions, 1999), MACEC (KU Leuven Structural Mechanics Section, 2014) compiler, and so on.

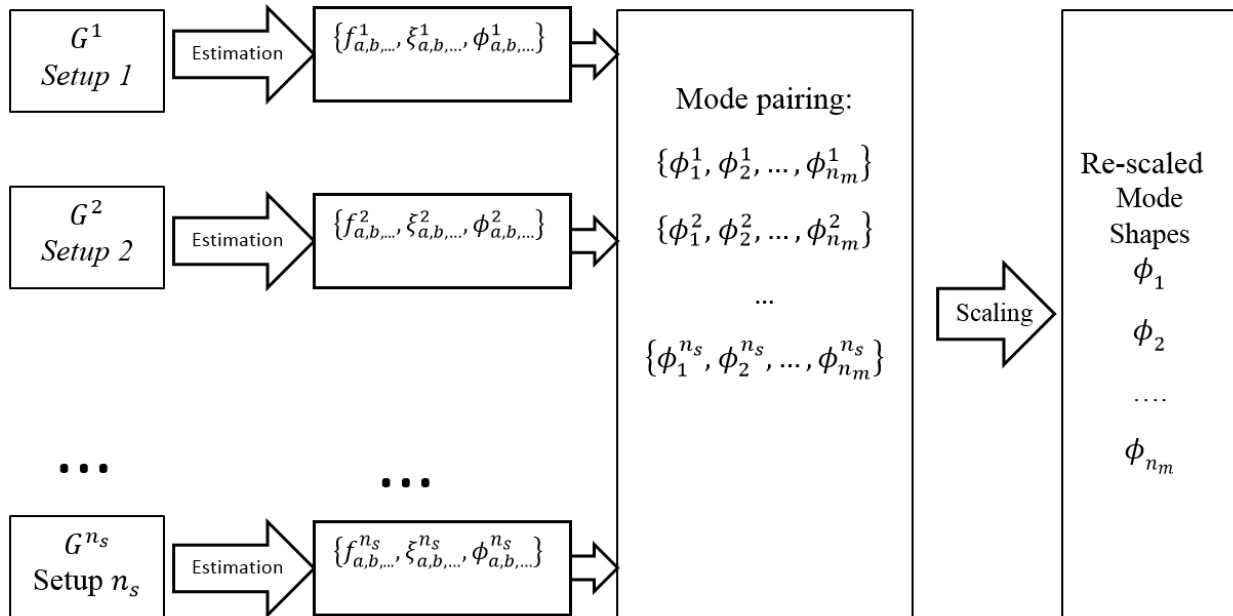


Figure 3.1 Post Separate Estimation Rescaling (PoSER) (Felber 1993, Manuel, 2012)

where, n_s is the total number of setups. Symbol G is related to the inputs of modal parameters. $\{f_{a,b,\dots}^j, \xi_{a,b,\dots}^j, \phi_{a,b,\dots}^j\}$ indicates the modal properties such as natural frequency, f , damping ratio,

ξ , and mode shape φ , in setup j (Manuel, 2012).

As it is mentioned, different setup has been measured in different time. It leads to have different condition in all setups. So, they have to merge and re-scale in such a way that they are measured simultaneously. To find the mode shape, they should be merged and rescaled to have a minimum difference among all segments. Considering the modes of setup k as a reference, the relation for rescaling is expressed in Equations 3.17 and 3.18 (Manuel, 2012).

$$\varphi_i^{j \rightarrow k} = \alpha_i^{j \rightarrow k} \cdot \varphi_i^j \quad 3.17$$

$$\varphi_i^{j \rightarrow k} = \frac{(\varphi_i^{j,ref})^H \cdot (\varphi_i^{k,ref})}{(\varphi_i^{j,ref})^H \cdot (\varphi_i^{j,ref})} \quad 3.18$$

where, vector $\varphi_i^{j,ref}$ includes the mode shape components of mode i at the reference outputs evaluated in setup j . Finally, a complete mode shape of each mode i ($i = 1, \dots, n_m$) can be calculated as follows (Manuel, 2012);

$$\varphi_i = \begin{bmatrix} \varphi_i^{k,ref} \\ \varphi_i^{1 \rightarrow k, mov} \\ \varphi_i^{2 \rightarrow k, mov} \\ \vdots \\ \varphi_i^{n_s \rightarrow k, mov} \end{bmatrix} \quad 3.19$$

where, the scaled mode shape i is expressed by vector $\varphi_i^{j \rightarrow k, mov}$ (Manuel, 2012)

3.5.2 Post Global Estimation Rescaling

The Post Global Estimation Rescaling (PoGER) technique is a new method in order to merge all setups with one analysis. The details of the procedure are shown in Figure 3.2.

Initially, all matrices from G^1 to G^{n_s} have been gathered in a global matrix as follows;

$$G^{tot} = \begin{bmatrix} G^1 \\ G^2 \\ \vdots \\ G^{n_s} \end{bmatrix} \quad 3.20$$

The above modal identification technique is used for extracting all modal properties from the collection of n_m modes. Here, the modal identification has been applied to all data together, and the modal properties of each mode are extracted from that. There is no need for scaling before modal analysis, and the reference sensors have been repeated n_s times in analysis. Consequently, this technique makes the merging of setups more straightforward by the use of a single analysis in all data (Manuel, 2012).

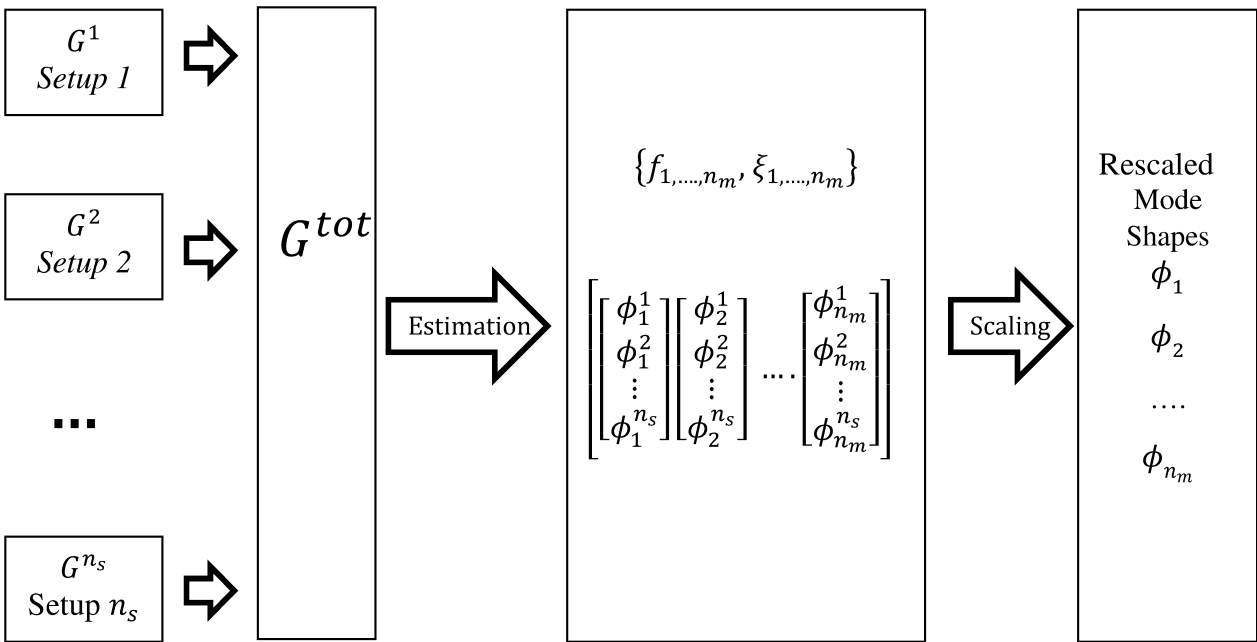


Figure 3.2 Post Global Estimation Rescaling (PoGER) (Manuel, 2012)

3.5.3 Pre Global Estimation Rescaling

This is another alternative technique for merging called Pre Global Estimation Rescaling (PreGER). In this method, sensor data is rescaled before applying for merging. So, the calculated mode shape has no requirement for further rescaling analysis. Figure 3.3 shows the procedure of PreGER algorithm in details.

3.6 Develop New Pre-merging technique using Random Decrement Technique

As it explained in previous section, merging technique used when the number of DOF is greater than available sensors. In this case, the sensors move in order to cover all DOFs using merging technique. By the way, the duration of sensing tests depend on the required modes, type of structure, etc. So, they might collect large amount of data which is not feasible to save it for long term in some cases. Among all merging techniques, PreGER is the state-of-art technique which is used to merge all data. But it can also have large number of data in large scale structure with long sensing test duration. In this research, the new method has been developed for merging data in different setup in sensing test using RDT and PreGER methods. As it was indicated, RDT is a time domain preprocessing technique to increase the efficiency of the algorithm and remove the noise in ambient vibration test. So, the new technique develops the pre-merging method by the use of RDT before processing in frequency domain. RDT is applied on the first channel called leading channel of multiple data which are recorded simultaneously. Then, other channels of data should have the same segment as the leading channel to have a time correlation. RDT is applied to all data to extract the free decay motion. Figure 3.4 shows the details of the choice of the trigger value in the first channel and follows the same pattern for others (Morsy, 2017, and Ibrahim, 1997).

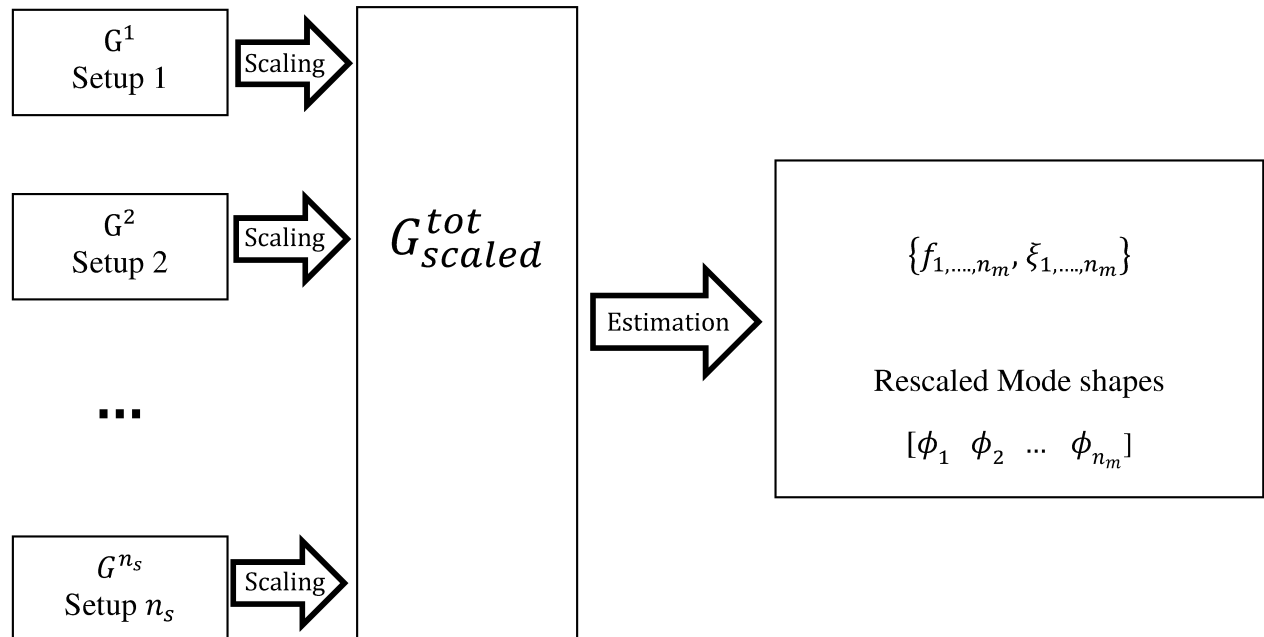


Figure 3.3 Pre Global Estimation Rescaling (PreGER) (Manuel, 2012)

After applying RDT in all channels in each setup, Pre-merging technique merges all data to identify modal properties. The details of Pre-merging technique are shown in Figure 3.5 (Parloo, 2003).

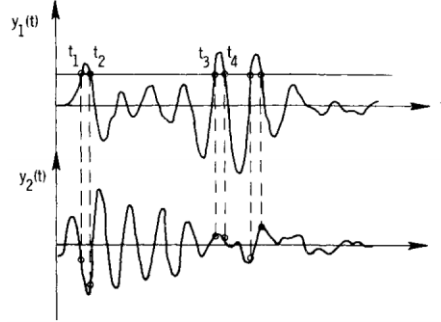


Figure 3.4 Two-station random response (Ibrahim, 1997)

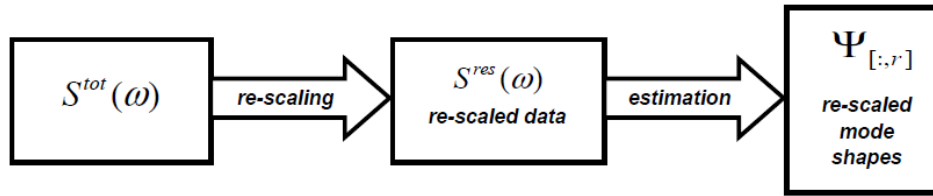


Figure 3.5 Flow chart of PreGER procedure (Parloo, 2003)

If N_{ref} reference responses are used, the $(N_{rov} \times N_{ref})$ matrix $S^{rov}(\omega)|_j$, containing the cross power spectra of setup j ($j = 1, \dots, N_{setup}$), can be re-scaled for all frequencies ω to a common level dictated by, with k ($k = 1, \dots, N_{setup}$) as follows;

$$S^{rov}(\omega)|_{j \rightarrow k} = S^{rov}(\omega)|_j \cdot (S^{ref}(\omega)|_j)^{-1} \cdot S^{ref}(\omega)|_k \quad 3.21$$

Due to an arbitrarily chosen reference setup k , it may possible to have poor quality of parameter estimation. Therefore, it is better to choose an average of all references common to all setups instead of single setup k .

$$S^{rov}(\omega)|_{j \rightarrow k} = S^{rov}(\omega)|_j \cdot (S^{ref}(\omega)|_j)^{-1} \cdot \frac{1}{N_{setup}} \sum_{k=1}^{N_{setup}} S^{rov}(\omega)|_k \quad 3.22$$

The first multiplication of the previous equation eliminates the poles of the system. These are then recovered through the multiplication of the result by an average output spectrum matrix that contains the contributions of the spectra between the reference outputs of all the setups. The total spectrum matrix used in the identification contains the average spectrum matrix of the reference

outputs and the scaled spectrum matrices with the cross-spectra of the outputs measured by the moving sensors:

$$S_{\text{scaled}}^{\text{tot}} = \begin{bmatrix} \frac{1}{n_s} \cdot \sum_{k=1}^{n_s} S^{k,\text{ref}} \\ S_{\text{scaled}}^{1,\text{mov}} \\ \vdots \\ S_{\text{scaled}}^{n_s,\text{mov}} \end{bmatrix} \quad 3.23$$

The procedure of new developed method which is called RDT– PreGER is described schematically in Figure 3.6.

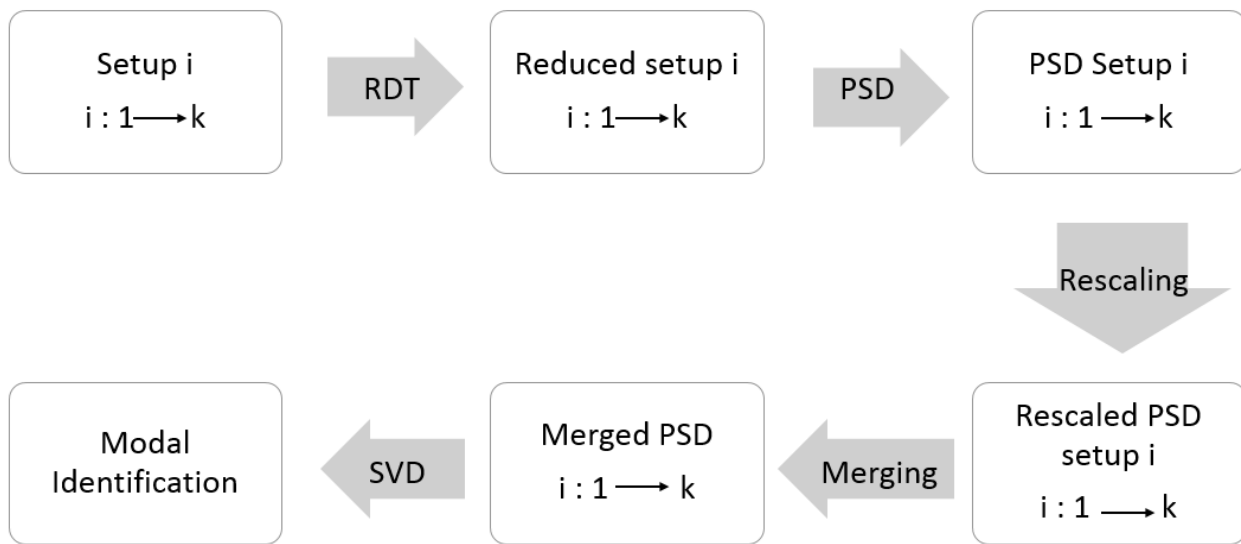


Figure 3.6 Schematic procedure of RDT – Pre merging multi setup modal analysis

3.7 Task details

Figure 3.7 shows the steps in vibration based modal identification and structural health monitoring. It is mainly classified to System Identification, Vibration-based Damage Detection and Finite Element Modal Updating. In System Identification, the new merging technique, RDT-PreGER method, has been developed to merge the data efficiently. In Vibration-based Damage Detection, the available methods have been compared to show the reliability of baseline free technique when there is no record of initial assessment of structure. It explains in following chapters in details. The last part is Finite Element Model Updating, the developed method in this search is called hybrid method using FE model output and Neural Network method which describe in following chapter in details.

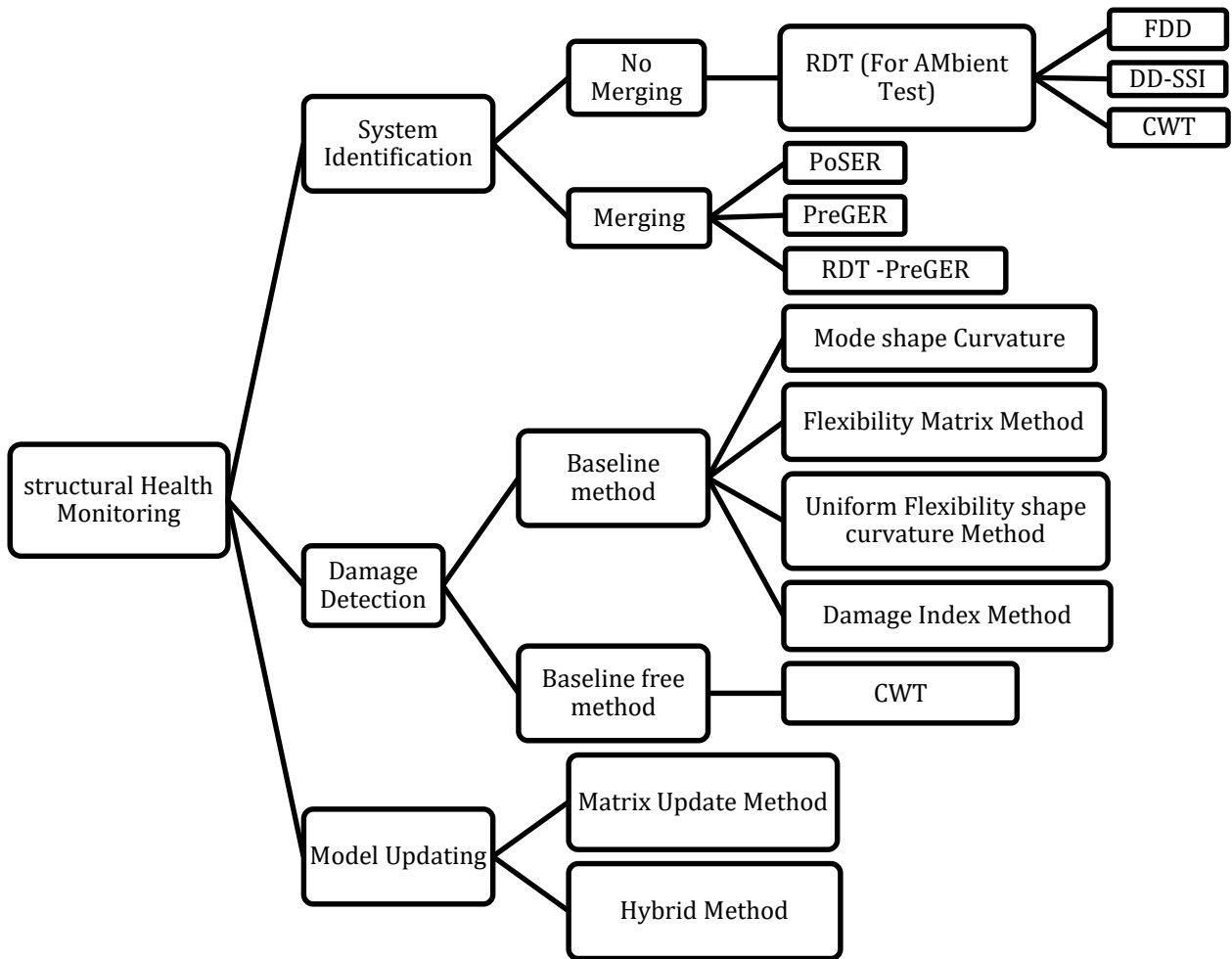


Figure 3.7 The main classification in vibration based tests

3.8 Denoising method for noise reduction

The case study is based on the data obtained from the vibration test of a three storey steel scale frame. In the test, Low Pass Filter (LPF) and Discrete Wavelet Transform (DWT) have been applied to the signal. Two evaluation metrics have been used including Signal Noise Ratio (SNR) and Root Mean Square Error (RMSE) for individual channel (Brincker et al., 2015).

As displayed in Figure 3.8, the additive Gaussian White noise with certain SNR is added to measured data from accelerometers to generate the noisy signal.

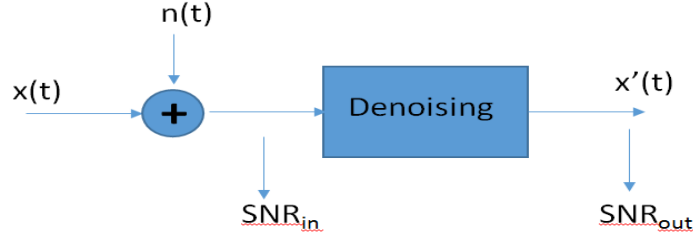


Figure 3.8 Additive SNR and calculated SNR after denoising

3.8.1 Low pass Filter (LPF)

A low pass filter (LPF) is a filter that allows to pass signals with a frequency lower than a specified cut off frequency and weaken signals with frequencies higher than the defined cut off frequency. There are many types of LPF which Butterworth low pass filter is selected in this research. To apply LPF, it needs to define the filter order and cut-off values which is depending on the original data.

3.8.2 Discrete Wavelet Transform (DWT)

Considering a signal x_n ($n = 1, 2, \dots, N$), the Discrete Wavelet Transform (DWT) approach represents the time record x_n using a linear combination of basic functions $\phi_{J,k}$ and $\psi_{J,k}$.

$$x(t) = \sum_k S_{J,k} \phi_{J,k}(t) + \sum_k d_{J,k} \psi_{J,k}(t) + \sum_k d_{J-1,k} \psi_{J-1,k}(t) + \dots + \sum_k d_{1,k} \psi_{1,k}(t) \quad 3.24$$

where $S_{J,k}$, $d_{J,k}, \dots, d_{1,k}$ are the wavelet coefficients; J is a small natural number which depends mainly on N and the basis function; and k ranges from 1 to the number of coefficients in the specified component. The two $\psi(t)$ and $\phi(t)$ are mother and father wavelet respectively which use to translate the data in time and dilating in scale. Equations 3.25 and 3.26 show the mother and father of wavelet.

$$\psi_{j,k}(t) = 2^{-\frac{j}{2}} \psi(2^{-j}t - k) \quad j, k \in Z \quad 3.25$$

$$\phi_{j,k}(t) = 2^{-\frac{j}{2}} \phi(2^{-j}t - k) \quad j, k \in Z \quad 3.26$$

where $k = 1, 2, \dots, N/2$, in which N is the number of data record; $j = 1, 2, \dots, J$, in which j is a small natural number and Z is the set of integers (Yi et al., 2012). Wavelet denoising has three main

steps including: (1) decomposition of input noisy signals into several levels of approximation and details of coefficients, using the selected wavelet basis. (2) Thresholding of coefficients which means to extract the coefficient containing the real signal and discard the others. (3) Reconstruction of the signal using approximation and details coefficients by use of the inverse wavelet transform (Yi et al., 2012).

In the wavelet based denoising procedure, the following parameters should be defined based on the type of measured signal: (1) threshold selection, (2) type of threshold (soft or hard), (3) multiplicative threshold rescaling, (4) wavelet type, (5) level of decomposition. The SNR is calculated in Equation 3.27 as.

$$\text{SNR (dB)} = 10 \log \frac{\sum_{k=1}^N x^2(k)}{\sum_{k=1}^N [x(k) - x'(k)]^2} \quad 3.27$$

where $x'(k)$ is the denoised signal and $x(k)$ is the original signal. The constant N is the number of samples. The Root Mean Square Error is formulated in Equation 3.28.

$$\text{RMSE} = \sqrt{\frac{\sum_{k=1}^N [x(k) - x'(k)]^2}{N}} \quad 3.28$$

3.9 Modal updating Methods

The data-driven and physics-based methods have been presented here. The developed hybrid method includes data-driven and physics-based method. The Neural Network methods have been used for data-driven and MUM as a physics-based (Jaishi et al, 2005).

3.9.1 Neural Networks (NN)

The details of the method using Neural Networks was illustrated in Section 2.3. The NN method is used as a part of hybrid method in FE model updating which is developed in this research. A feed-forward neural network applies a series of functions to the data. The exact functions will depend on the neural network function which mostly these functions each compute a linear transformation of the previous layer, followed by a squashing nonlinearity. In some cases, the functions will do in a different way (like computing logical functions in your examples, or averaging over adjacent pixels in an image). Therefore, the roles of the different layers could

depend on what functions are being computed. In addition, a hidden layer in an artificial neural network is a layer in between input layers and output layers, where artificial neurons take in a set of weighted inputs and produce an output through an activation function. It is a typical part of nearly any neural network in which engineers simulate the types of activity that go on in the human brain.

3.9.2 Hybrid method

This method is a combination of physics-based and data-driven methods. The ANN method is used to update the initial model by use of trained model. The ANN model is composed of input and corresponding output which are defined stiffness modification factor and corresponding modal properties (frequency, mode shape or both), respectively. Therefore, the FE model provides the modal properties when applying the stiffness modifier in particular element or elements. It means changing the stiffness in some elements and find the corresponding frequency of the structure. It creates the data including the stiffness modification factor in some elements and modal properties of the structure. Then, the collected data are used as the input and output in ANN for training purpose. The frequency of the structure under different conditions (different stiffness modification factors) is defined as an input and the stiffness modification factors is assigned as an output. When the network is trained well, it can be used to analyze in further data. It means that the real modal properties of the structure are given to the algorithm and it provided the stiffness adjustment factors to reach to the frequencies. This technique is helpful when there is no access to FE model to apply physics-based method.

3.9.3 Matrix Update Method (MUM)

The MUM is a physics-based technique which is used here to compare the results of the proposed hybrid method. It has been developed by Kabe (1985), which is briefly explained below (Bagchi, 2005). The eigenvalue equation of a dynamic system for a structure is describe as follows;

$$K\phi_i = \lambda_i M \phi_i \quad 3.29$$

In this equation, ϕ_i is the i^{th} mass-orthonormal mode shape, K is a stiffness, M is a mass matrix and λ_i is the corresponding eigenvalue (squared frequency). There two parameters mainly affected on

modal properties termed mass and stiffness. So, it means a small perturbation in those parameters change the modal properties like frequency and mode shape as it is shown in Equation 3.30.

$$\mathbf{K} \delta\phi_i + \delta\mathbf{K} \phi_{di} = \lambda_i \mathbf{M} \delta\phi_i + \delta\lambda_i \mathbf{M} \phi_{di} \quad 3.30$$

Consider a small model, so $\phi_{di} \approx \phi_i$,

$$\phi_i^T \delta\mathbf{K} \phi_{di} = \delta\lambda_i \quad 3.31$$

In this equation, $\delta\mathbf{K}$ indicates any change in the stiffness matrix. If this perturbation is shown by factor β , then the equation has been updated by follows.

$$\delta\lambda_i = - \sum_{j=1}^{n_e} \phi_i^T \mathbf{K}_j \phi_{di} \beta_j \quad 3.32$$

which is $\mathbf{D} \beta = - \delta\lambda$.

In this equations, \mathbf{D} is as $m \times n_e$ matrix, n_e is the number of element, β is the n_e -vector of the changes in element stiffness matrices and $\delta\lambda$ is the m -vector difference between FE model and real eigenvalues (Bagchi, 2005). Figure 3.9 shows the summary of model updating technique (Bagchi, 2005).

3.10 Summary

All in all, the proposed methods have been described in different parts including system identification, model updating, damage detection and pre-processing techniques. In system identification, the developed technique in multi setups merging has been introduced called RDT-PreGER technique. In model updating, the proposed hybrid method is used to update FE model with combination of data-driven and physics-based method. In addition, the sensitivity of different denoising techniques like LPF, DWT have been studied to compare their efficiency in a presence of noise.

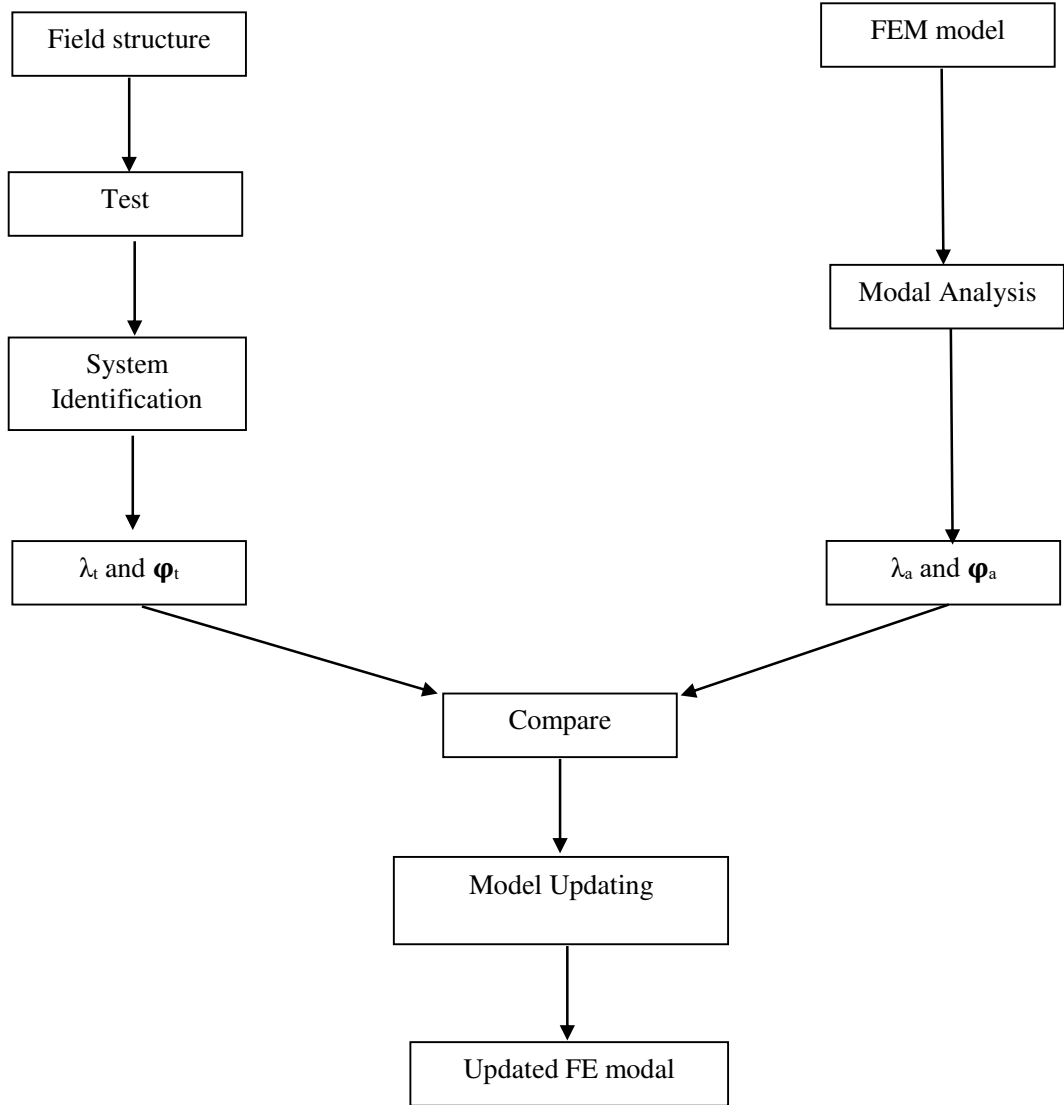


Figure 3.9 Procedure of FE model updating (Bagchi, 2005)

Chapter 4. Data Collection and Noise Reduction

4.1 Overview

As it mentioned in chapter 2, there are two main categories in Vibration Based Test including Force Vibration and Ambient Vibration tests. The Ambient vibration is also called Output only or Operational Modal Analysis (OMA). The ambient vibration is mostly applicable for in-service structures and it has some difficulties because of low amplitude and noise contamination. In laboratory experiments, ambient vibration may not work well. In the present research, an exciter or impact hammer have been used in the laboratory tests. Different real and scaled structures have been studied by use of forced and ambient vibration. There are several case studies which have been used in this research to verify the efficiency and reliability of proposed and developed methods.

4.2 Case studies

4.2.1 Prestressed Concrete Box (PSCB) Bridge

The PSCB Bridge is a 16-span bridge which is 40 m in first and last span and the rest are 50 m. The total length is 780 m with the deck width 12 m and its curve radius is 3000 m. The bridge details are shown in Figure 4.1. It was built in 1994 in Gangwon province of South Korea. The sensing test has been performed by Korean Express Inc (Lim, 2016).



Figure 4.1 a) PSCB bridge details b) Data logger

The wireless data acquisition was used for ambient vibration test. The test has been done by Korea Expressway Corporation on 2012. To measure the ambient vibration of the bridge, 30 wireless accelerometers PCB 393B12 with 10000 mV/g sensitivity and ± 0.5 g range were spaced along the full-length of the bridge for the duration of 100 minutes with sampling rate of 256 Hz in order

to collect sufficient vibration data for modal parameter extraction. As it is shown in Figure 4.2, the number of sensor is 2 for each span except the first and last spans, which have only one sensor. The data logger has 24 bit A/D resolution and maximum sampling rate is 1000 Hz.

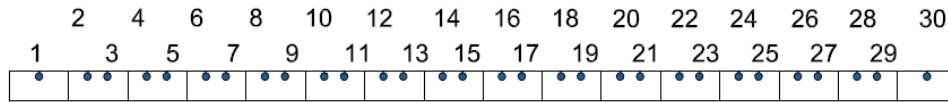


Figure 4.2 Sensor location details in PSCB Bridge

4.2.2 Voided Slab Bridge

The Voided Slab Bridge as shown in Figure 4.3 is a 3-span bridge with 65 m length and 12 m width. The middle span is 25 m and two others are 20 m. The bridge was constructed in 1991 in Gyeonggi province in South Korea. The Korean Express Inc. has performed the sensing test for this bridge (Lim, 2016).



Figure 4.3 a) Voided Slab Bridge details b) Data logger

Figure 4.4 shows the sensor location. 18 wireless sensors were used to measure ambient vibration for 100 minutes with 128 Hz.

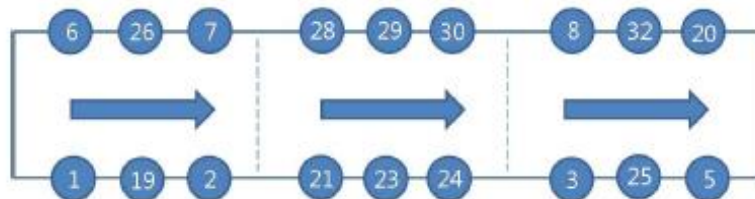


Figure 4.4 Sensor location details (the number inside indicates the channel number)

4.2.3 Steel Box (STB) Bridge

The bridge was constructed on 1995 with 380m total length and 12m width. There are 8 spans with 47.5m length. Figure 4.5 displays the detail of STB Bridge. . The Korean Express Inc. has performed the sensing test for this bridge (Lim, 2016)..



Figure 4.5 a) STB bridge details b) Data logger

Figure 4.6 shows the sensor location. 24 wireless sensors were used to measure ambient vibration for 100 minutes with 128 Hz.

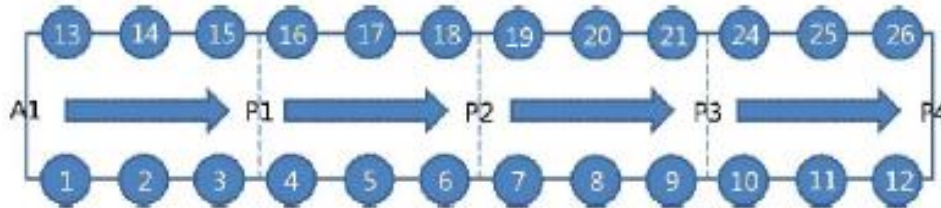


Figure 4.6 Sensor Location details in voided slab Bridge

4.2.4 Three storey scaled steel frame

A three storey galvanized steel frame with 60 cm width, 27 cm depth and 133 cm height have been analyzed. The structure has been built and tested in the structures laboratory at Concordia University by ourselves. The structure and wireless sensor nodes are shown in Figure 4.7. The frame is fixed fully to the floor. Micro strain Tri-axial MEMS wireless sensors having the sensitivity of 10 mV/g have been installed on each floor. The sensors are connected to data acquisition system to transfer the data. The data acquisition system can be connected to maximum four sensors simultaneously. Apart from 3 accelerometer channels, each wireless sensor has an internal temperature channel. All nodes transfer the data to the base station, which is connected to the computer. Micro strain Node Commander Software is used here for establishing the

communication between the base station and the wireless sensors. A sample rate of 512 Hz has been used for acquiring the acceleration data (Sabamehr et al, 2015).

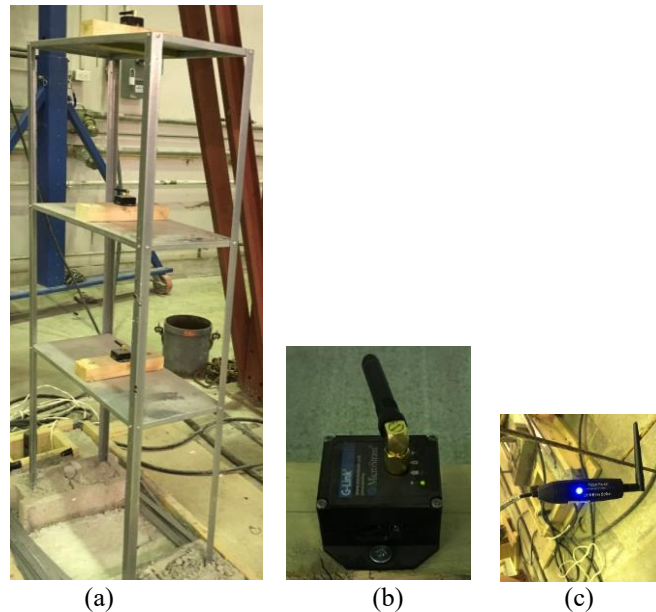


Figure 4.7a) Steel frame details b) Micro strain wireless sensor c) Micro strain Gateway

The structure has been excited using an impact hammer and the free vibration signal is recorded for 20 seconds. The accelerometers are located in the center of each floor to measure the floor acceleration. The tests have been repeated five times along both axes. As it is defined, the sampling frequency is the number of collected data per second. The sampling frequency is chosen initially as 256 Hz using Micro Strain MEMS wireless and National Instrument wired piezo sensor. After testing, it is realized that only first two bending modes can be identified because the third mode is close to Nyquist frequency (half of sampling frequency). Then the sampling frequency was increased to 512 Hz to cover all bending modes. The details of modal identification methods are shown in following chapter.

4.2.5 Steel cantilever beam

The cantilever beam has been tested in Central Building Research University of Roorkee in India. It has 1000 mm length with 10 mm height and 65 mm width. Five wireless sensors were attached in every 200 mm in the beam to measure the vibration response in different conditions such as mass variation in different location (Figure 4.8). Two tests include of ambient vibration and forced vibration have been applied in the beam (Sabamehr et al, 2017).

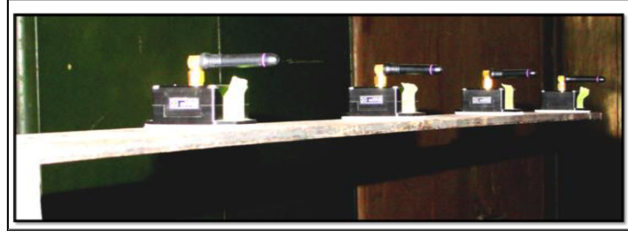


Figure 4.8 Steel Cantilever beam details

4.2.6 Finite Element model of a five storey frame

A five storey concrete frame of 10 m length, 5 m width and 15 m height (3m height in each floor) is modelled in SAP2000. The frame is considered massless and the concentrated mass is located in the center of each floor.

To simulate the ambient vibration, the White Gaussian Noise (WGN) which is simulated in MATLAB, has been applied to all nodes in each direction. The length of the test is 1000 s with the sampling rate 100 Hz. Figure 4.9 shows the modal analysis and operational modal analysis with WGN.

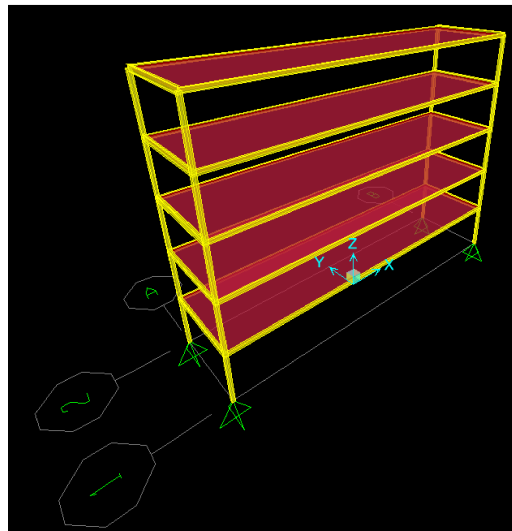


Figure 4.9 Five storey finite element modal in SAP2000

4.2.7 Five storey scaled steel frame

In this study, the five storey scaled steel frame has been tested in Roorkee, India. The frame has 350 mm height in each floor, 350 mm width, and 350 mm height. The MicroStrain 3D wireless sensor single hub accelerometer is used to collect data and send it to data acquisition. All sensors need to collect to data acquisition system to transfer the data. Each data acquisition can be

connected to four sensors wireless. The sensors are located in the middle of each floor for ambient vibration test. Due to low frequency of ambient load, impact hammer is used to excite the structure to have better response. Figure 4.10 shows the details of frame, sensor and data acquisition (Sabamehr et al, 2018).



Figure 4.10 (a) Five storey scale steel frame (b) G link wireless 3D sensor (c) Sensors and data acquisition

4.3 Noise Reduction

The collected data from the sensors have been considered as an original signal and Additive White Gaussian Noise (AWGN) is added to the signal. Then, two different denoising methods are applied to compare their accuracy in various SNRs. Here, two common types of wavelet are used for denoising in two levels of decompositions. It should be noted that the adjustment of rescaling using a single estimation of level noise based on first-level coefficients and heursure threshold selection (Yie et al. 2012) are the same in all types. Figure 4.11 shows the collected data and its PSD in top

floor of the structure (Sabamehr et al., 2017).

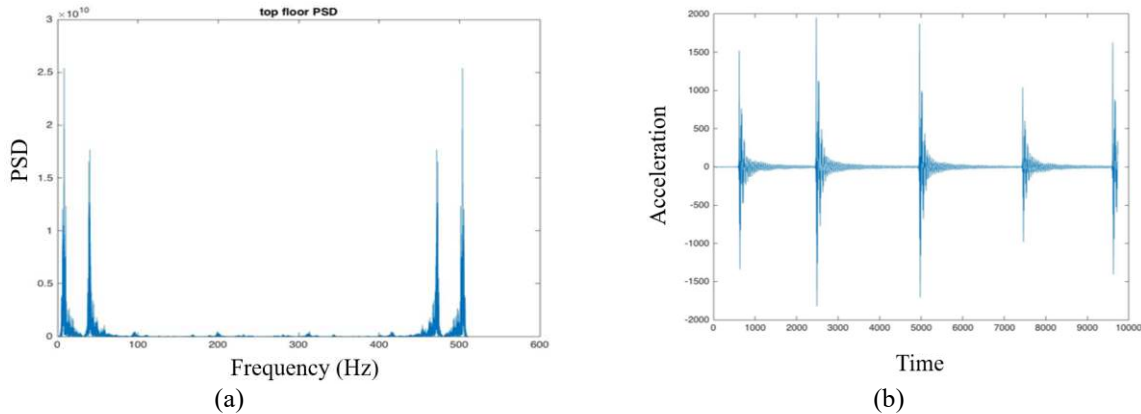


Figure 4.11 (a) top floor acceleration data in 19 second with 512 Hz sampling rate (b) Top floor PSD

The SNR after adding white Gaussian noise (SNR0) is varied between -10 dB to 40 dB by changing the noise variance. The SNR is calculated after denoising by wavelet db4 and sym8 algorithms (Yie et al. 2012) in 1 and 4 level of decompositions and low pass filter. The details of SNR in each floor are shown in Figure 4.12.

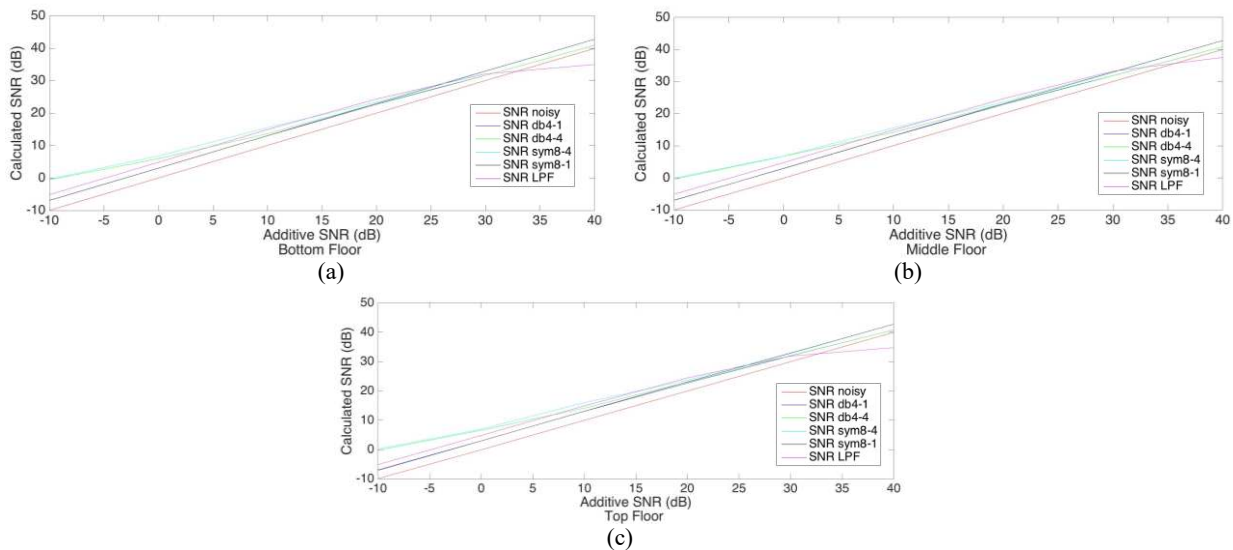


Figure 4.12 SNR after denoising versus SNR before denoising for (a) bottom floor (b) middle floor (c) top floor

Another parameter that has been considered is Root Mean Square Error (RMSE). Figure 4.13 shows the variation of RMSE in three floors by use of different denoising techniques. It is observed from studying the effect of denoising technique on RMSE that the denoising methods by use of symlet8 wavelet has the lowest error as compared to Daubechies wavelet and LPF methods applied to acceleration data on all floors.

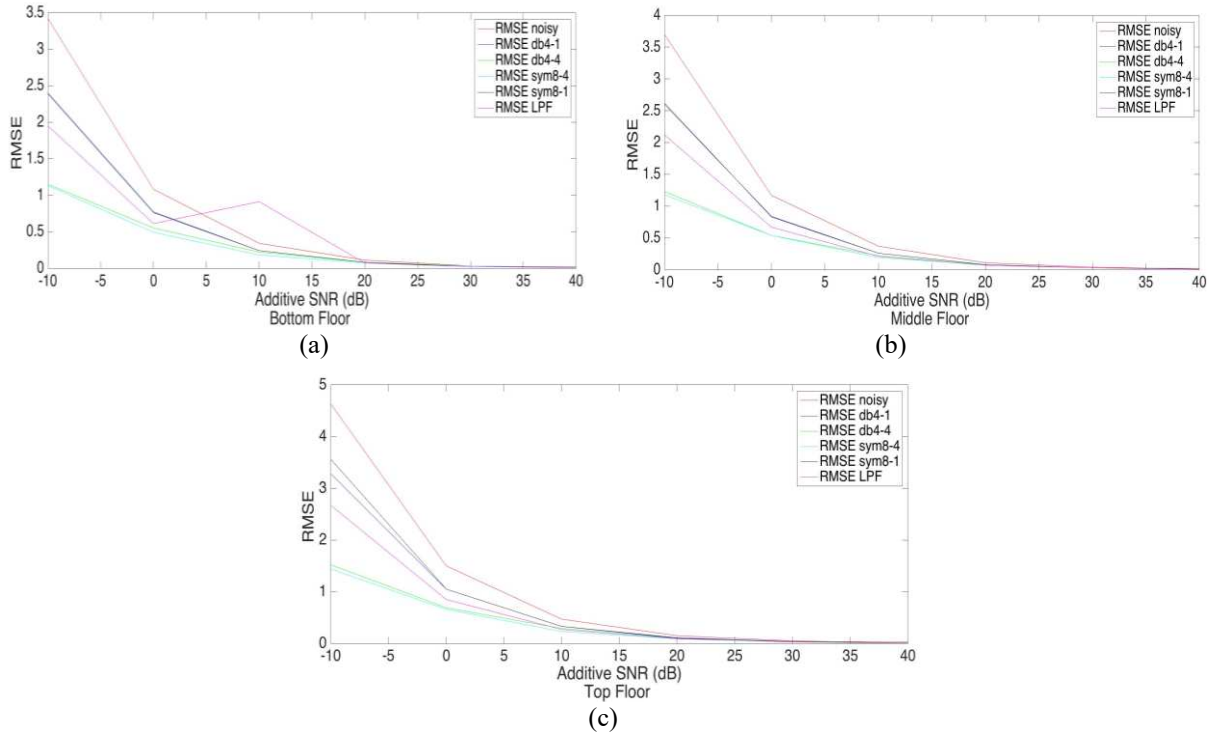


Figure 4.13 (a) RMSE in bottom floor (b) RMSE in middle floor (c) RMSE in top floor

4.4 Summary

In this chapter, all case studies have been introduced with their details. It includes the real, scaled, and FE model of different structures included in the study to verify the proposed methods in different domains. In addition, the different pre-processing techniques for noise reduction have been studied. The efficiency of noise reduction techniques has been compared using two standard metrics, such as, SNR and RMSE. It is observed that selection of appropriate mother wavelet with proper decomposition level is more efficient rather than LPF or other types of wavelets.

Chapter 5. System Identification and Modal Analysis

5.1 Overview

There are several techniques in modal identification in different domains which are mentioned in section 2.2. All techniques are used to extract the modal properties of the structure (Frequency, Mode shape and Damping Ratio). The number of modes depend of number of degrees of freedom in the structure. So, there are many modes in multi-storey building, bridges, etc. The number of chosen modes depends on the type, flexibility importance of the structure. The most important mode having the highest mass participation in the structure is the first mode or fundamental mode. Usually, the first lateral modes and torsion mode are the most important mode in the building. The effective modal mass provides a method for evaluating the significance of a vibration mode. Modes with relatively high effective masses can be readily excited by base excitation. On the other hand, modes with low effective masses cannot be readily excited in this manner. In this study, most common algorithms in each domain have been studied termed FDD, SSI and CWT. In addition, the efficiency of RDT as a pre-processing method have been analyzed in the case study. Then, the RDT-PreGER method is applied to cantilever beam and hypothetical model in SAP2000 for multi setups merging. Table 5.1 shows the summary of all case studies used in this research.

Table 5.1 Summary of case studies and their applications

Case study	Performed by	System Identification	FE model Updating	Damage Detection
Prestressed Concrete Box (PSCB) Bridge	Korean Express Inc.	FDD SSI	MUM Hybrid Method (proposed method)	Baseline methods Baseline free method
Voided Slab Bridge	Korean Express Inc.	FDD	MUM Hybrid Method (proposed method)	-----
Steel Box (STB) Bridge	Korean Express Inc.	FDD	MUM Hybrid Method (proposed method)	-----
Three storey scaled steel frame	Myself	FDD SSI CWT	MUM Hybrid Method (proposed method)	-----
Cantilever steel beam	Research group in Roorkee, India	FDD RDT-FDD PreGER RDT-PreGER (proposed technique)	MUM	-----
Five storey Finite Element model	Myself in SAP2000	Modal Analysis in Sap2000 FDD RDT-FDD PoSER PreGER RDT-PreGER (proposed technique)	-----	-----
Five storey scaled steel frame	Research group in Roorkee, India	FDD SSI CWT	-----	-----

5.2 Prestressed Concrete Box (PSCB) Bridge

In this bridge, FDD technique is applied to extract the modal properties of the structure. In addition, the common LPF called Butterworth is used to reduce the noise level before system identification. The details of modal analysis are showed in following subsections.

a) Frequency Domain Decomposition

Figure 5.1 shows the original raw data and filtered signal by use of Butterworth low pass filter of PSCB Bridge channel #4. The filter type is Butterworth which is one of the most common filter. The filter is low pass filter with 50 Hz cutoff frequency.

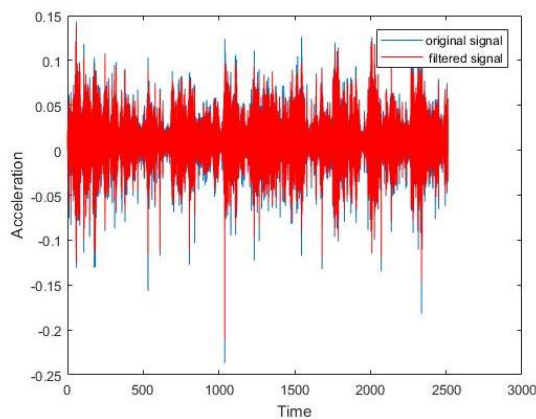


Figure 5.1 Filtered signal of channel #4 in PSCB Bridge

Generally, the number of modes of structure are equal to degree of freedoms. The first six modes of the bridge are considered to assess the modal properties of the structure. The importance of the mode depends on mass participation ratio. Mostly, the first mode includes largest part of mass participation. FDD algorithm is performed to extract the frequencies and mode shapes. As it is displayed in Figure 5.2, the frequencies are calculated by use of FDD. First six peaks have been selected in frequency domain. It is possible to choose higher modes, however for simplicity only first six modes are selected.

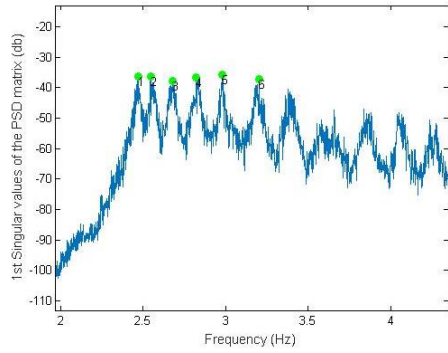


Figure 5.2 PSCB Bridge modal frequencies

Figure 5.3 shows mode shapes and the bridge which is a somewhat slender and all of six modes are bending modes.

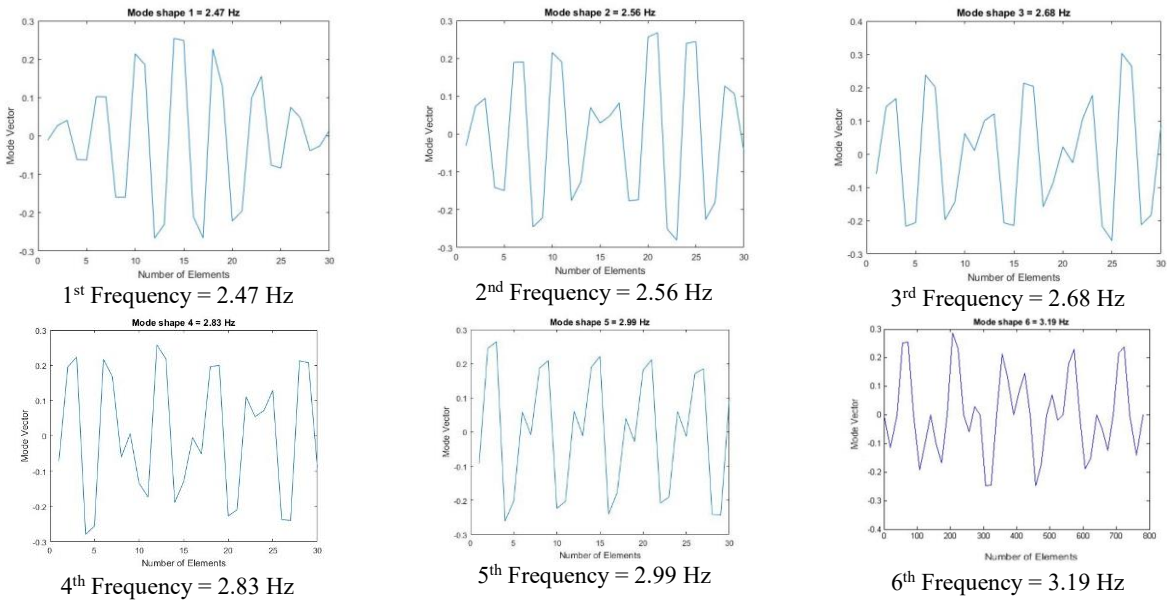


Figure 5.3 Corresponding frequencies and mode shapes for PSCB Bridge

b) Stochastic Subspace Identification (SSI)

Figure 5.4 shows SSI results for the PSCB Bridge. The SSI algorithm works in time domain. In Figure 5.4, the stabilization chart shows the stable mode with vertical lines. Two mode shapes have shown in Figure 5.4.

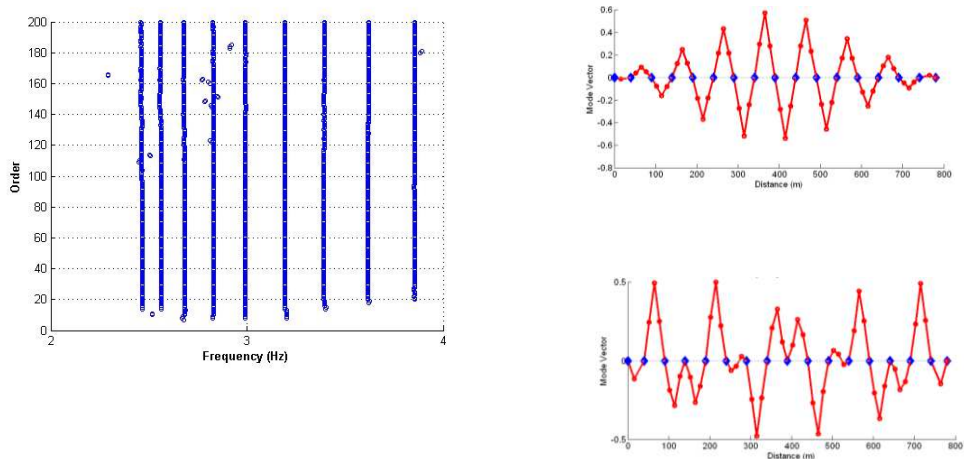


Figure 5.4 Stabilization chart and mode shapes

Table 5.2 shows frequencies obtained by FDD and SSI methods. Frequencies are very similar in two techniques. Six vertical modes are considered and these modes are surrounded between 2.4 and 3.2 Hz. Although the difference between modes are small, the mode shapes clearly show each mode is evident.

Table 5.2 Frequencies of ambient vibration test

Mode no.	FDD (Hz)	SSI (Hz)	Difference (%)
1	2.46	2.46	0.40
2	2.56	2.56	-0.39
3	2.68	2.68	0.00
4	2.83	2.83	-0.35
5	2.99	2.99	-0.34
6	3.19	3.19	0.31

5.3 Voided Slab Bridge

a) Frequency Domain Decomposition

The original and Butterworth filtered data file of channel #1 for Voided Slab Bridge is shown in Figure 5.5. The Butterworth filter type is low pass filter with 50 Hz cutoff frequency.

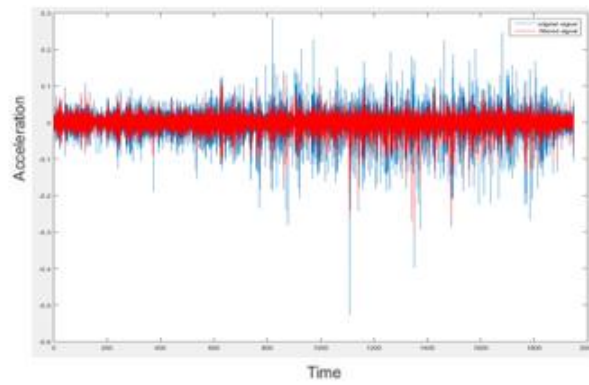


Figure 5.5 Original and filtered signal of channel #1 in Voided Slab Bridge

The real modes should have peaks in frequency domain. So, the frequencies are computed by applying the FDD, as it is shown in Figure 5.6, three natural frequencies are calculated for the Voided Slab Bridge.

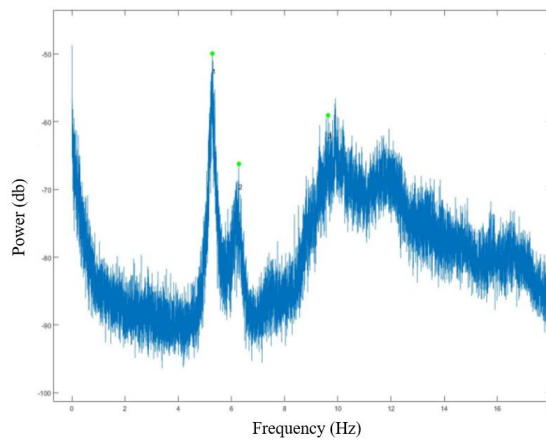


Figure 5.6 Voided Slab Bridge modal frequencies

Figure 5.7 indicates the frequencies and corresponding mode shapes in Voided Slab Bridge.

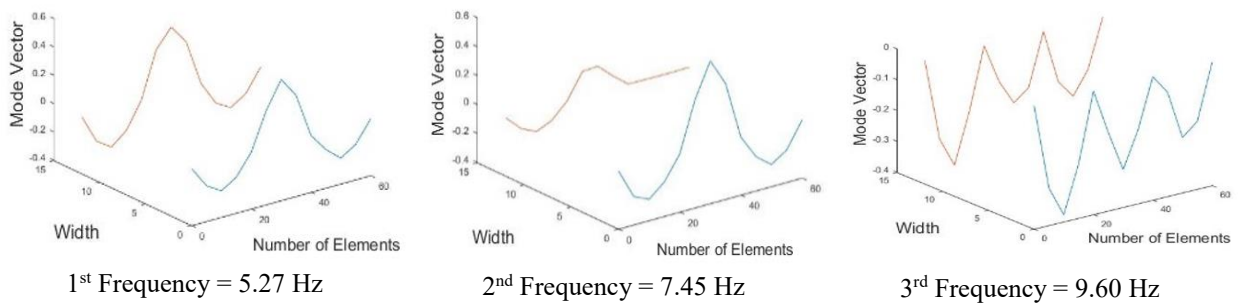


Figure 5.7 Identified Modal Properties from Vibration Test in Voided Slab Bridge

5.4 Steel Box (STB) Bridge

a) Frequency Domain Decomposition

Figure 5.8 shows the original and Butterworth low pass filtered data file of Channel #1. The cutoff frequency is 50 Hz in Butterworth low pass filter.

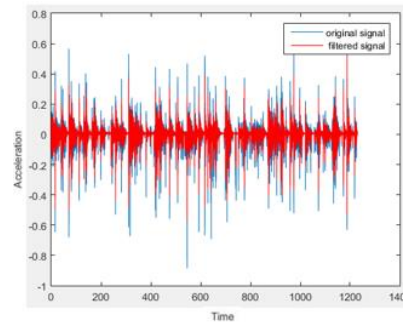


Figure 5.8 Original and filtered signal of channel #2 in STB Bridge

In frequency domain, FDD algorithm is used to extract modal properties of STB Bridge. Figure 5.9 indicates modal frequencies of STB Bridge.

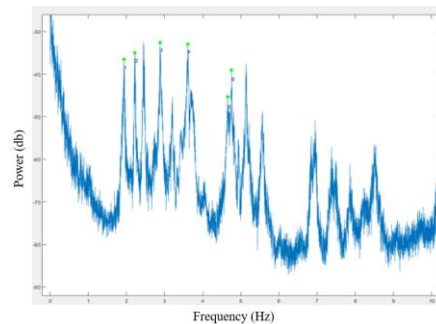


Figure 5.9 STB Bridge Modal frequencies

After, choosing the peaks in frequency domain, six modes have been selected. Then, all mode shapes have been drawn in both side of the bridge. Figure 5.10 displays first six modes of STB Bridge including four bending and two torsion modes.

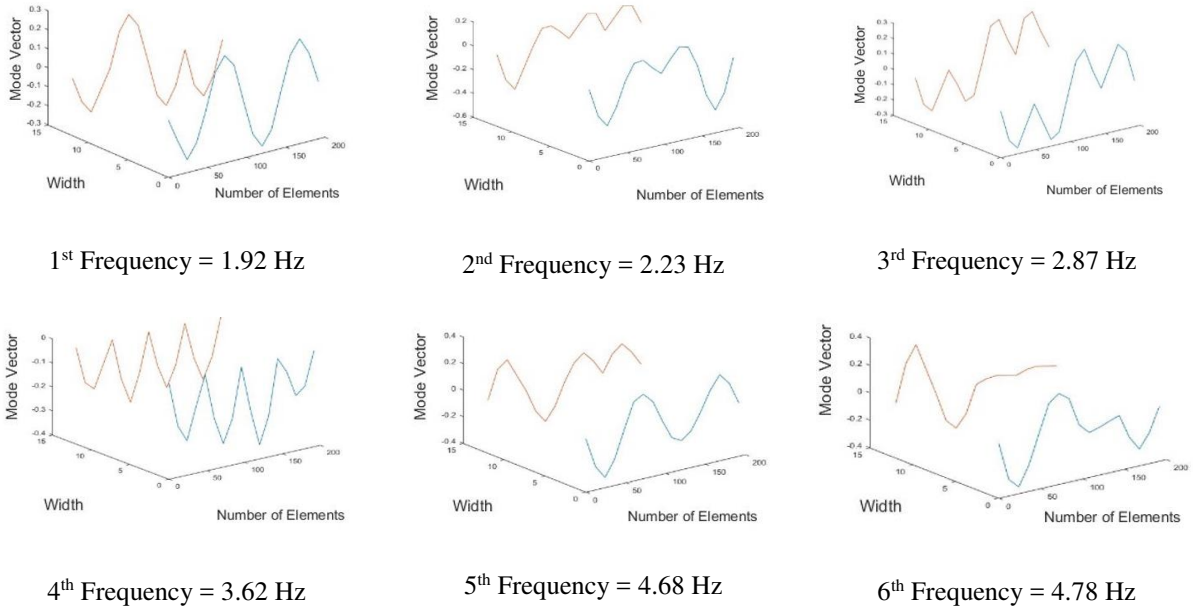


Figure 5.10 Identified Modal Properties from Vibration Test in STB Bridge

5.5 Three storey scaled steel frame

a) Frequency Domain Decomposition

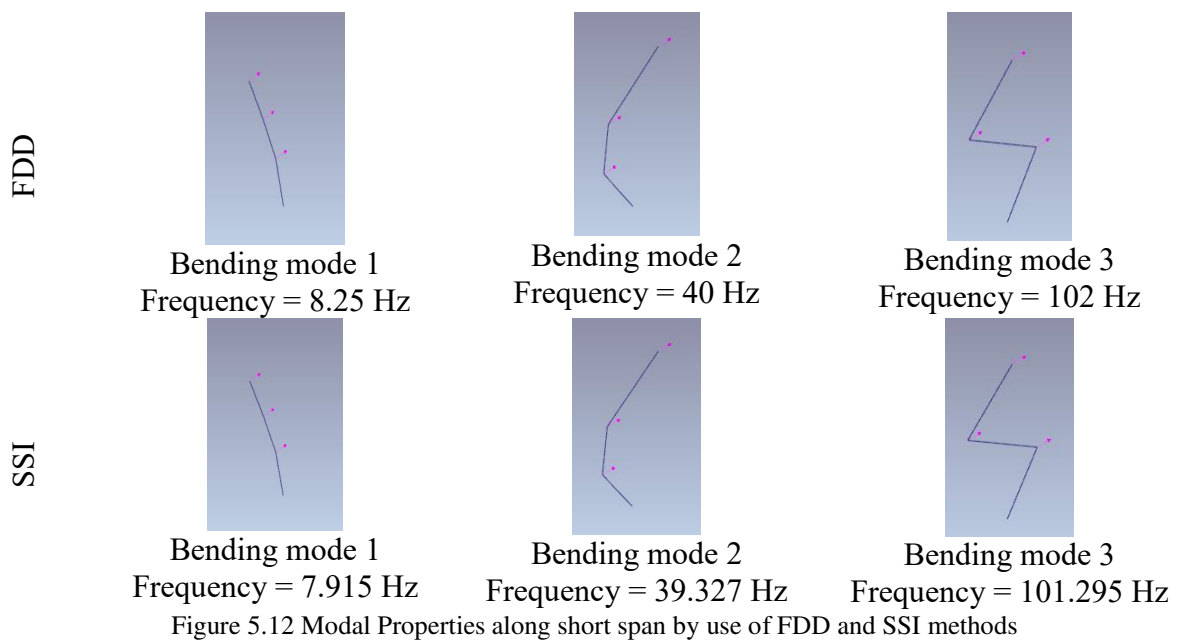
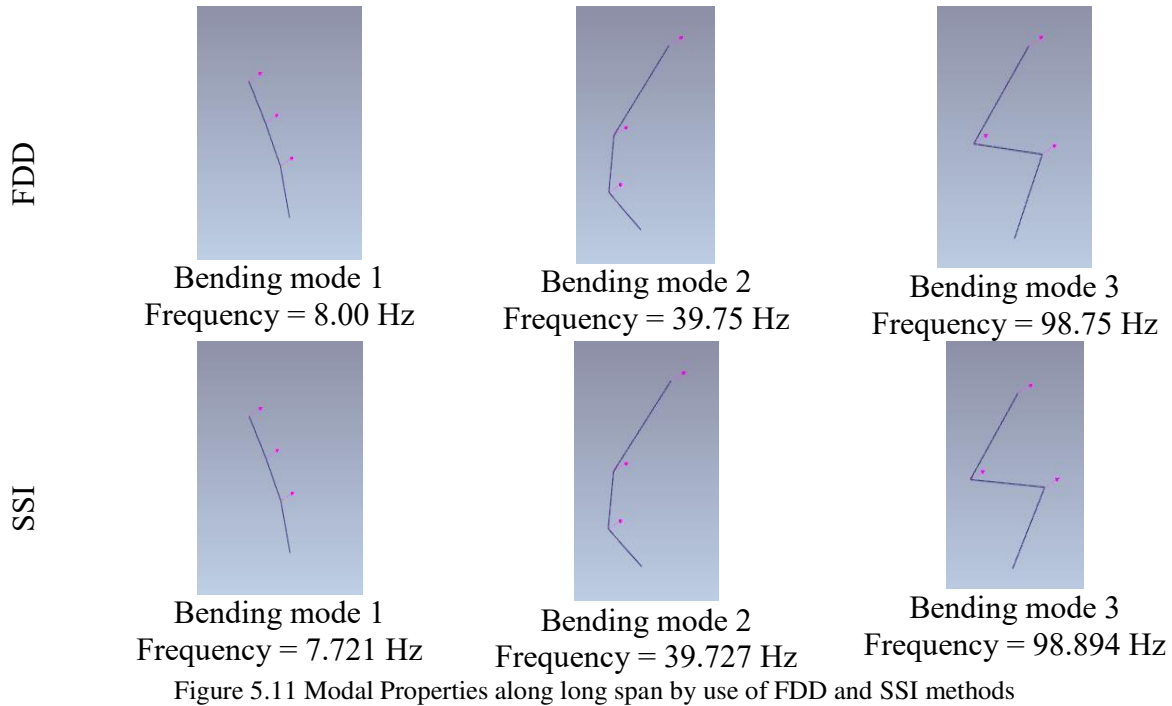
The first three peaks in FDD display the first three natural frequencies and corresponding mode shapes. The ambient vibration test has been done in both directions. The result along long span has been shown in Figure 5.11 by use of FDD.

b) Stochastic Subspace Identification

The stabilization diagram of estimated state space model has been used to get the stable modes in SSI method. The modal analysis results by use of SSI along the long span are shown in Figure 5.11 for first three bending modes and natural frequencies of galvanized steel frame in ARTeMIS (Structural Vibration Solutions, 1999).

After applying the ambient vibration, the test was repeated along short span, so the FDD and SSI methods have been used to find the first three frequencies and mode shape of the frame. The details of result along short span have been shown in Figure 5.12.

After obtaining the modal properties by using both methods, the Modal Assurance Criterion (MAC) is applied to verify the accuracy and closeness of each mode obtained by different methods (Figure 5.13).



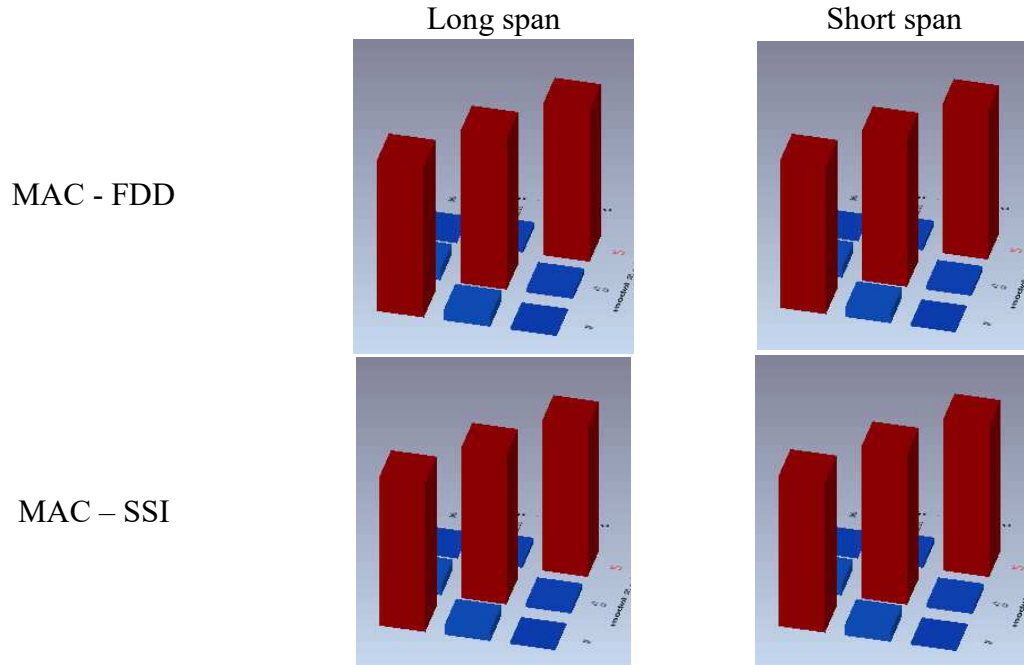


Figure 5.13 MAC values of FDD and SSI methods along both directions

In Table 5.3, it can be seen the modal analysis result of the steel frame obtained from the FDD and SSI methods in both directions. As can be seen the natural frequencies extracted are very close to each other. The frequencies and mode shapes in both directions are similar as the stiffness of the frame is similar in these directions.

Table 5.3 Natural frequency extracted by FDD and SSI

	FDD		SSI	
	Long Span	Short Span	Long Span	Short Span
Frequency 1st (Hz)	8.00	8.25	7.721	7.915
Frequency 2nd (Hz)	39.75	40	39.727	39.327
Frequency 3rd (Hz)	98.75	102	98.894	101.295

c) Time – Frequency Analysis

The time-frequency has been applied on three storey steel frame. The data was collected for 19 seconds with sampling rate 512 Hz along long span. The Power Spectral Density (PSD) has been used to estimate the preliminary results for natural frequency. The modified complex Morlet wavelet has been selected with 4 Hz and 100 Hz for wavelet central frequency and bandwidth, respectively. Figure 5.14 shows the collected data in time domain and frequency domain by use of PSD.

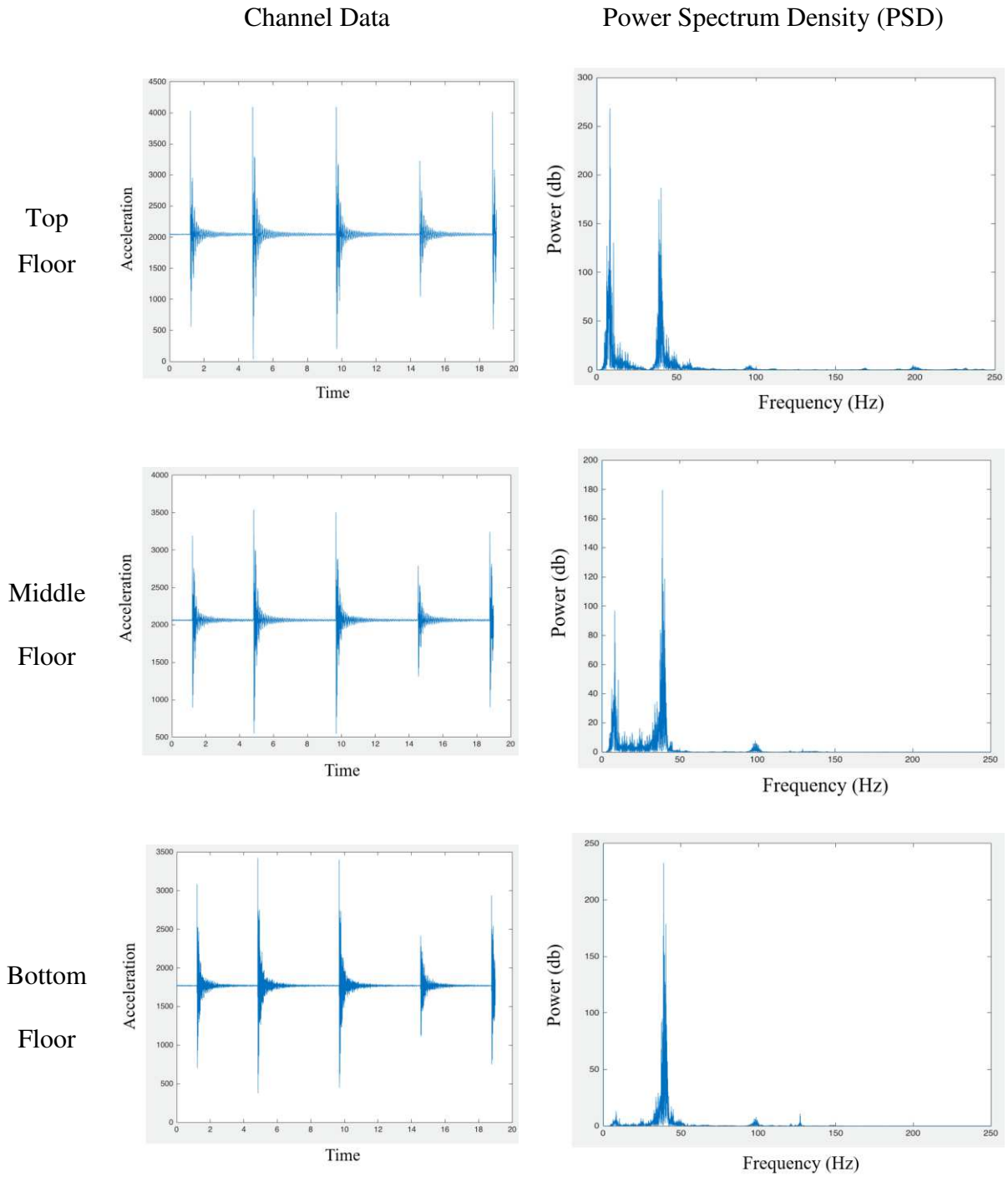


Figure 5.14 Preliminary result by use of Power spectrum density (PSD)

As can be seen in Figure 5.15, three frequencies can be detected in PSD, but the frequency spectrum is very low in the third frequency. The scale range is between 1 to 256.

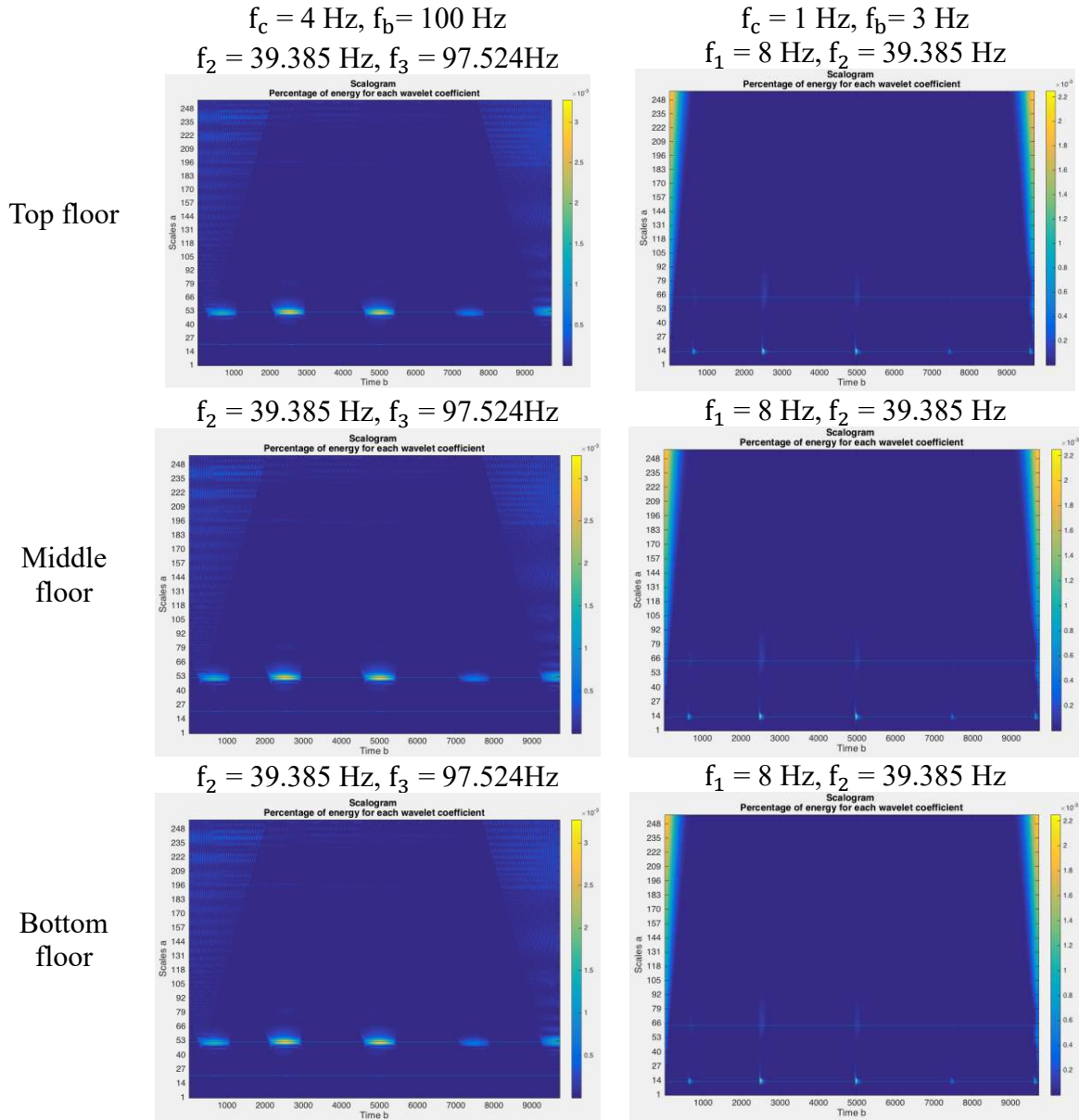


Figure 5.15 Ridge extraction for natural frequency using Scalogram

The natural frequency and corresponding mode shape from complex Morlet wavelet in three storey steel frame along long span are shown in Figure 5.16.

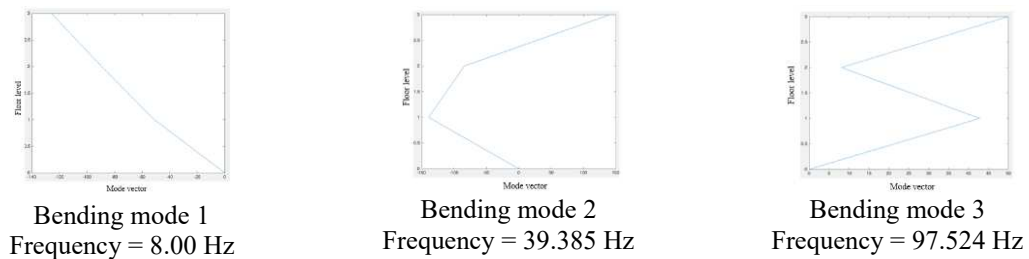


Figure 5.16 Modal properties of three storey steel frame by complex Morlet wavelet

5.6 Cantilever steel beam

The steel beam with the following details and solid cross-section has been tested under ambient and force vibration.

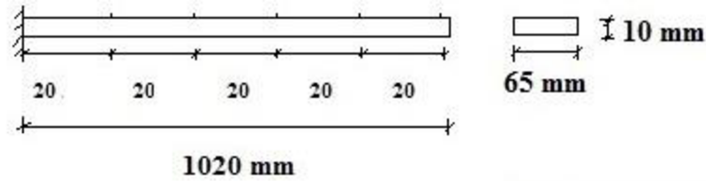


Figure 5.17 steel Cantilever beam details

5.6.1 Ambient vibration

The ambient test has done with 256 Hz sampling rate for 30 seconds. Five accelerations have been placed in every 200 mm to measure the acceleration. The sensor details are as follows;

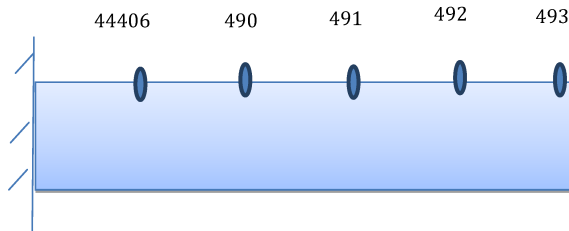


Figure 5.18 Cantilever beam and sensor location for ambient vibration details

The frequency domain decomposition has been applied to extract the modal properties. The result of FDD shows that the data has no peaks in frequency domain to detect the modes (Figure 5.19).

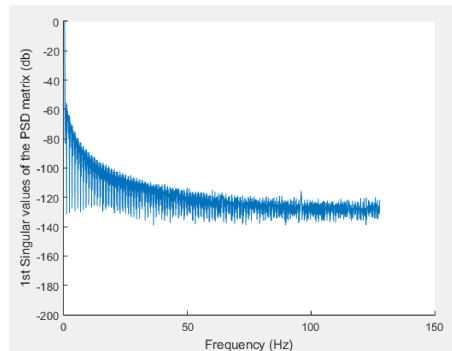


Figure 5.19 FDD result for ambient vibration

To tackle the problem, Random Decrement Technique (RDT) has been applied in order to remove the noise using average of time segments. The two main parameters are selected in such a way that

they cover all modes when RDT is used. The Trigger value is equal to the standard deviation of the time series, and the time segment is chosen 10 sec. The time segment should be selected in such a way that cover all modes. The results of FDD after using RDT are shown below.

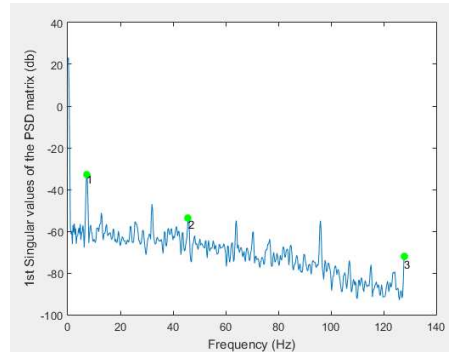
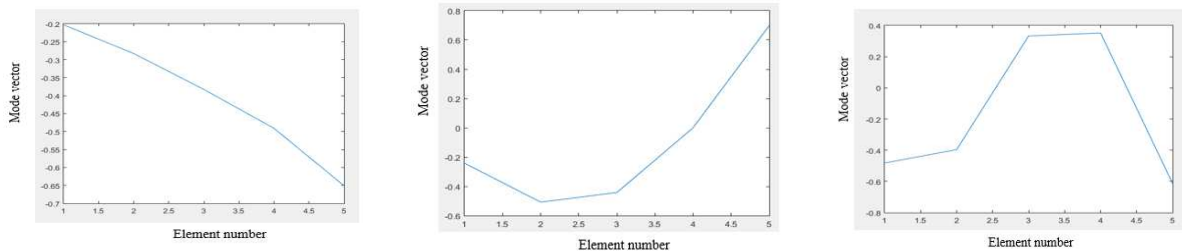


Figure 5.20 RDT – FDD result in ambient vibration

Then, the frequency and corresponding mode shape are as follows;



1st Frequency = 7.25 Hz

2nd Frequency = 45.75 Hz

3rd Frequency = 127.75 Hz

Figure 5.21 Modal properties of cantilever beam by use of RDT-FDD method

5.6.2 Forced vibration

The cantilever beam has been tested with forced vibration as well. The forced vibration has been applied with 256Hz sampling rate for 30 seconds.

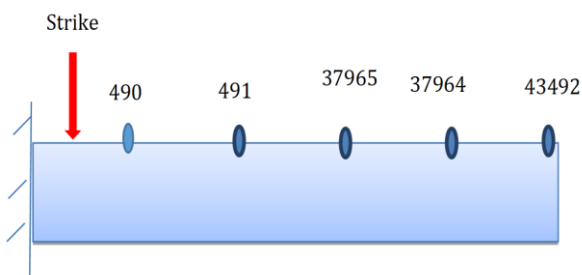


Figure 5.22 Cantilever beam and sensor location for forced vibration details

In forced vibration, there is a high level of amplitude in data, so the real mode can be detected easier than ambient test. The possibility of noise contamination in force vibration is lower than ambient test. Then, the FDD is able to measure the modal properties in forced vibration without using RDT. The peaks are shown in Figure 5.23.

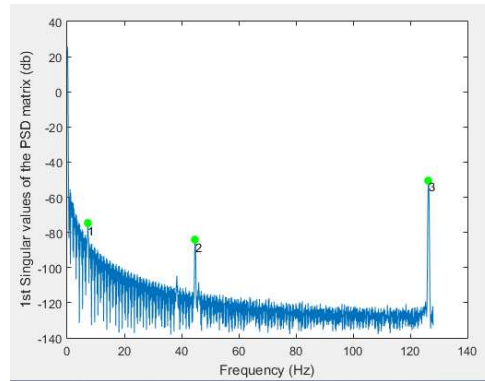
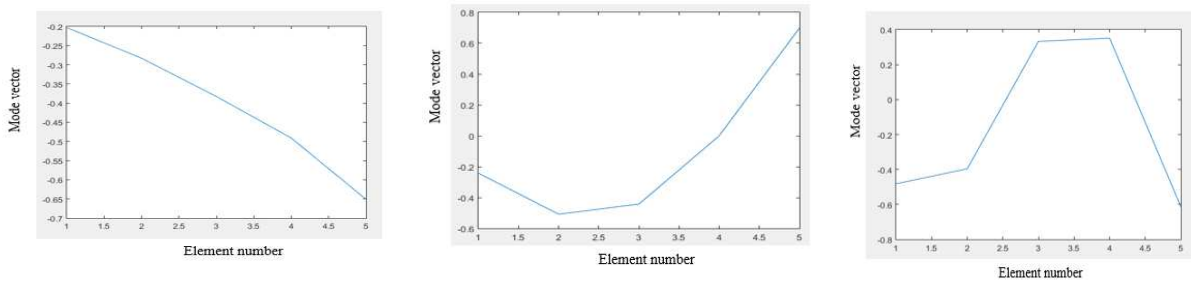


Figure 5.23 FDD result Force vibration

The frequencies and mode shapes are displayed in Figure 5.24;



1st Frequency = 7.25 Hz

2nd Frequency = 45.75 Hz

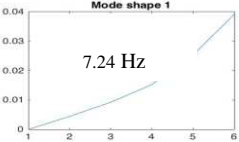
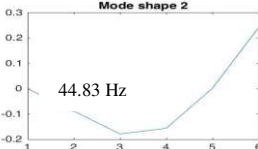
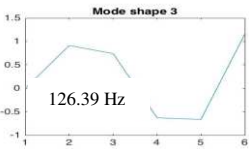
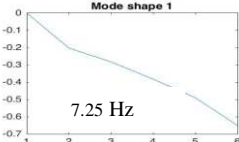
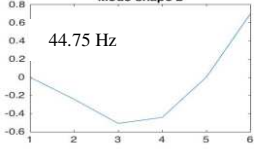
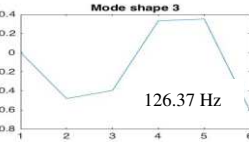
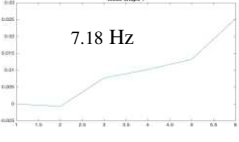
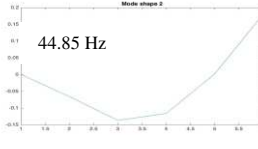
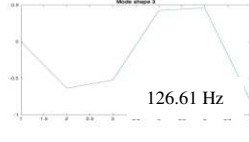
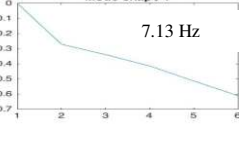
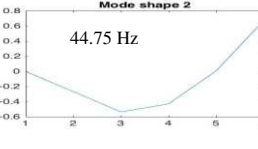

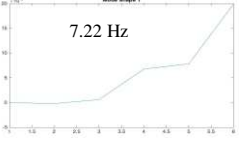
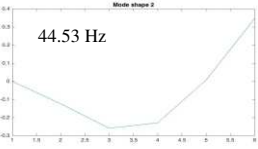
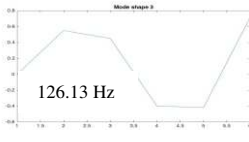
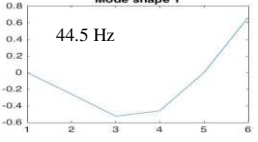
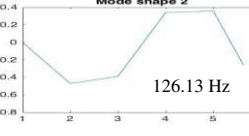
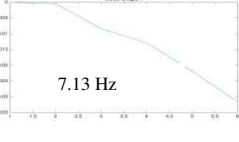
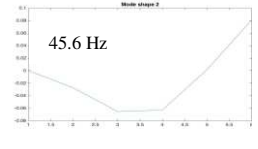
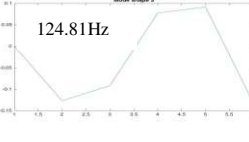
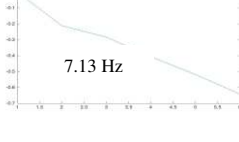
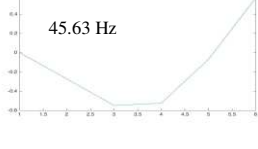

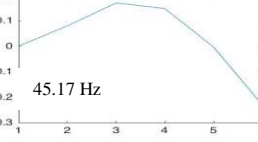
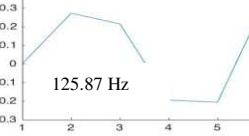
3rd Frequency = 127.75 Hz

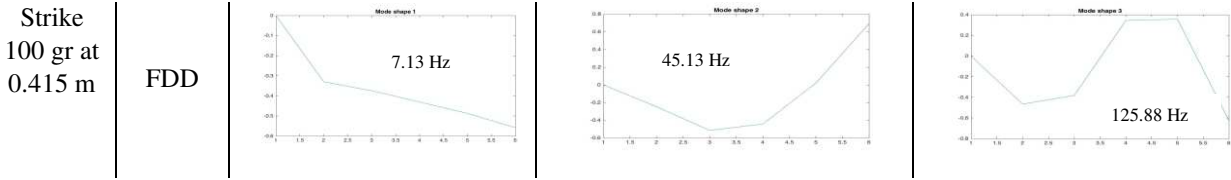
Figure 5.24 Modal properties of cantilever beam by use of FDD method

5.6.3 Forced Vibration with mass variation in different locations

As it mentioned, two main parameters effect on frequency and mode shape of the structure. The beam has been tested with two different masses in two locations. So, there are different tests using mass variation in different locations to compare the results. The FDD and DD-SSI have been used to analyze the modal properties of the data. Table 5.4 shows the output of mentioned algorithms.

Table 5.4 Modal Identification of cantilever beam in different conditions

	Type	Mode 1	Mode 2	Mode 3
C beam with Strike No additional load	SSI	 7.24 Hz	 44.83 Hz	 126.39 Hz
	FDD	 7.25 Hz	 44.75 Hz	 126.37 Hz
C beam with Strike 50 gr at 0.75 m	SSI	 7.18 Hz	 44.85 Hz	 126.61 Hz
	FDD	 7.13 Hz	 44.75 Hz	 125.63 Hz
C beam with Strike 50 gr at 0.415 m	SSI	 7.22 Hz	 44.53 Hz	 126.13 Hz
	FDD	Cannot be detected	 44.5 Hz	 126.13 Hz
C beam with Strike 100 gr at 0.75 m	SSI	 7.13 Hz	 45.6 Hz	 124.81 Hz
	FDD	 7.13 Hz	 45.63 Hz	 124.75 Hz
C beam with	SSI	Cannot be detected	 45.17 Hz	 125.87 Hz



5.6.4 RDT-PreGER technique

As it was discussed in chapter 2, the developed Pre-merging technique called RDT-PreGER is applied to increase the efficiency of the algorithm in the structure. For this purpose, the cantilever beam data is divided into two setups with one reference channel which is same in both setups. Figure 5.25 illustrates that detail of setups in cantilever beam.

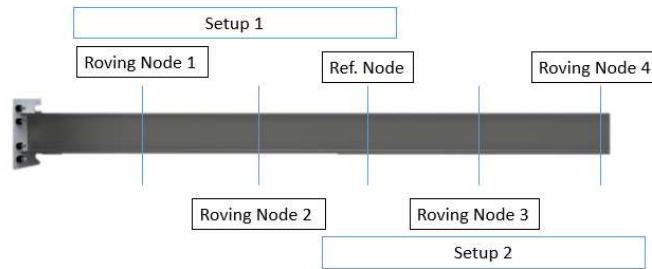


Figure 5.25 Manual setup on cantilever beam

The RDT is applied with 10 s time length and the trigger value is standard deviation of data multiplied by square root of 2. It is applied to the time domain data collected from sensors. Then, PSD is applied in each channel to convert time domain to frequency domain. To identify the modal properties by use of frequency domain decomposition (frequency domain method), SVD is used for assemble PSD matrix. Figure 5.26 shows 1st Singular value versus frequency in pre merging only and RDT with pre merging.

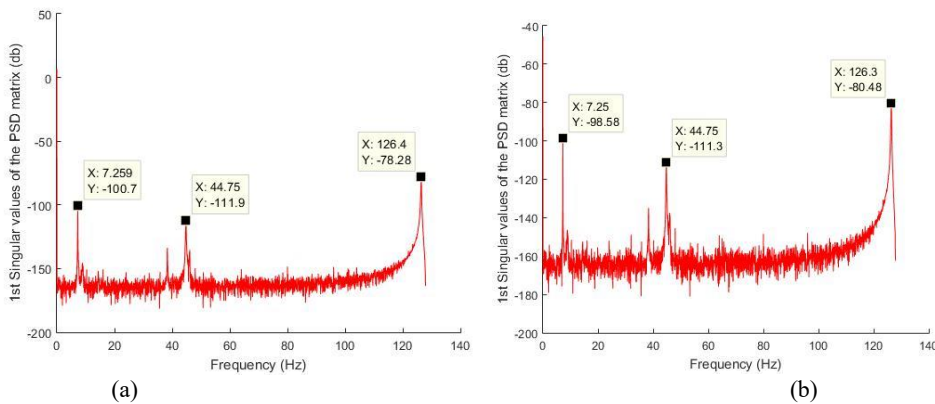


Figure 5.26 1st singular value of PSD matrix in (a) pre merging only (b) RDT with pre merging

After finding the frequencies, the modal properties are compared for the two different methods such as multi setup pre merging only and RDT with multi setup pre merging. Table 5.5 illustrates the modal properties of steel cantilever beam by use of three different algorithms in one setup and multi setups.

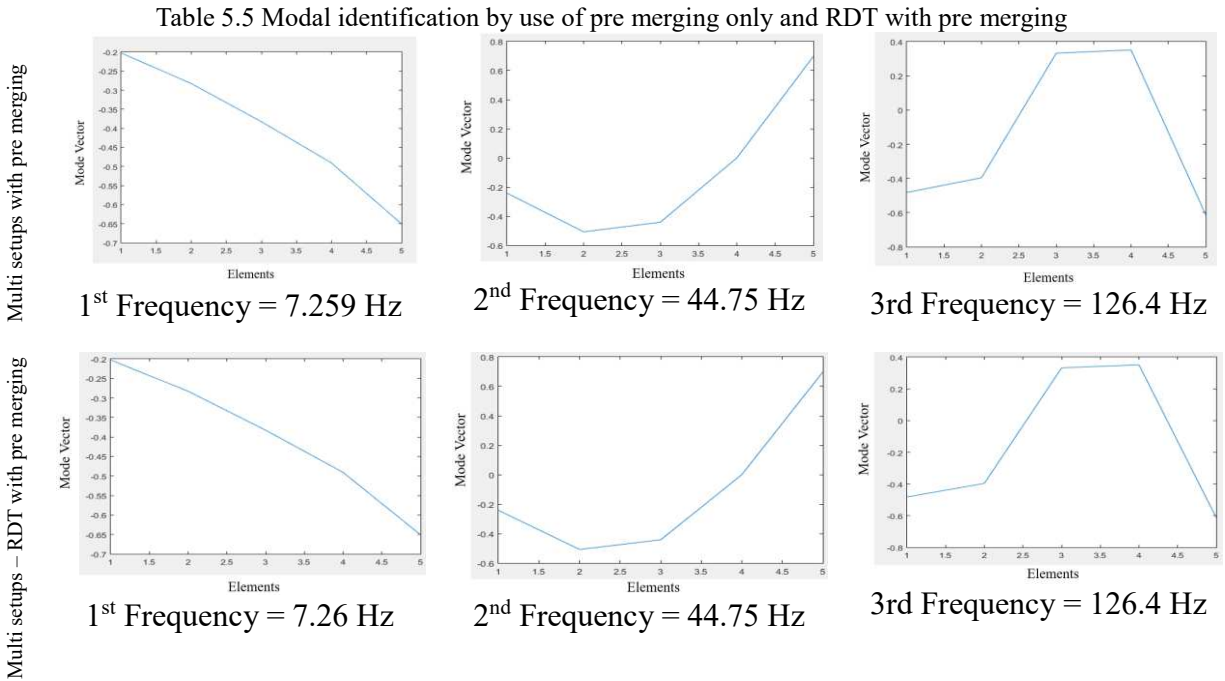


Table 5.6 shows the modal identification of Cantilever beam by use of different techniques. As it mentioned in chapter 3, the cantilever beam has been tested using all sensors together in one setup. To verify the accuracy of developed method, the sensor data is manually divided into two parts to simulate the sensing test with two setups.

Table 5.6 Modal identification of cantilever beam by use of different techniques

	Mode 1	Mode 2	Mode 3
RDT-FDD	7.25 Hz	45.75 Hz	127.75 Hz
PreGER	7.259 Hz	44.75 Hz	126.4 Hz
RDT-PreGER	7.26 Hz	44.75 Hz	126.4 Hz

5.7 Five storey Finite Element model

5.7.1 Modal Analysis in SAP 2000

The frame is modelled in SAP 2000 for modal analysis. The details of SAP model is shown in Appendix A. The frequencies and mode shapes are recorded along x direction and they show in Figure 5.27.

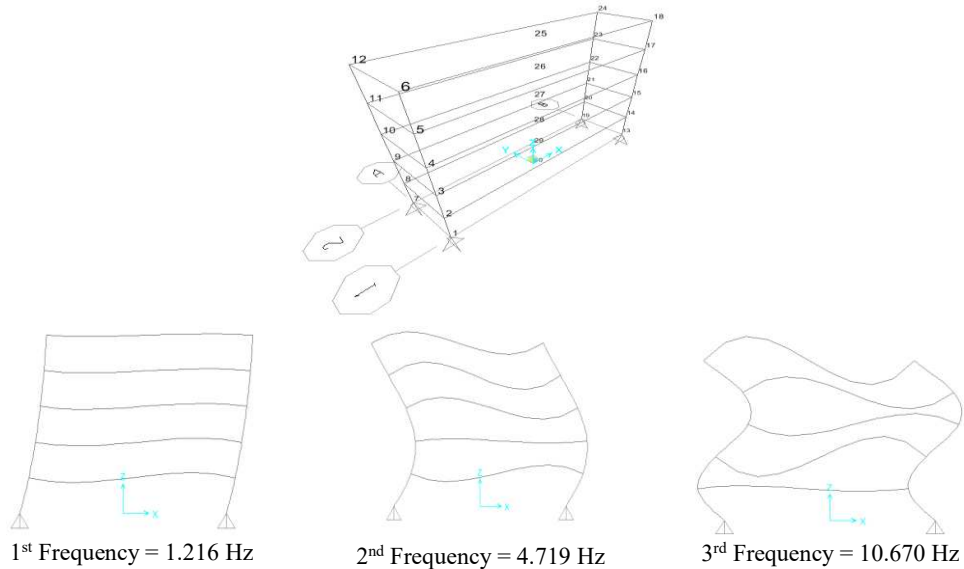


Figure 5.27 Modal analysis along x direction for first three bending mode

5.7.2 Modal Analysis by use of FDD

As it is clear, the ambient load is the type of random noise which can be simulated by use of White Gaussian Noise (WGN). So, the WGN is generated in MATLAB for 100000 data to simulate in 1000 second with 100 Hz sampling rate. The WGN is illustrated in Figure 5.28. The WGN is applied along x direction of the frame.

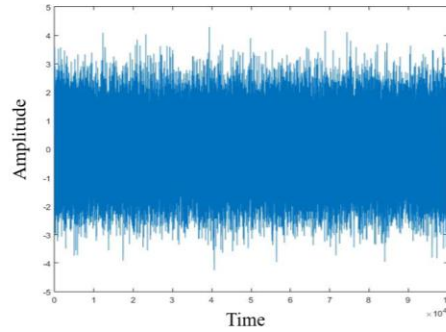


Figure 5.28 WGN applied along x direction

Then, the structure's response should be recorded for modal analysis. The acceleration response is collected from the middle of each floor. The data are used for the modal analysis by use of FDD technique in MATLAB (Farshchin, 2015). Figure 5.29 indicates the frequencies and mode shapes.

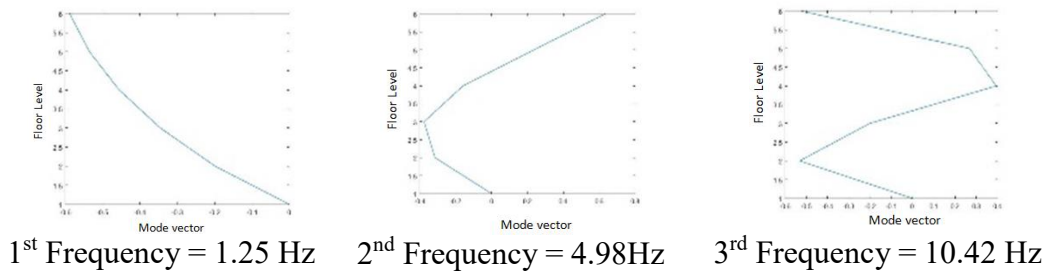


Figure 5.29 Operational modal analysis along x direction by use of FDD

5.7.3 Modal Analysis by use of RDT-FDD

Due to high volume of data in an ambient vibration test, and their contamination with noise, RDT can apply to remove the noise and increase the efficiency of algorithm by decreasing the number of data. In this way, two main parameters should be defined such as trigger value and time segments which should be long enough to cover all modes. The trigger value is defined as a square root of two multiplied by the standard deviation of the input data, and the time segment is 10 s which contains 1000 data. As RDT is the time domain method, so it first applies to the data individually. Figure 5.30 shows the collected data from level 1 and 5 before and after RDT with the certain trigger value.

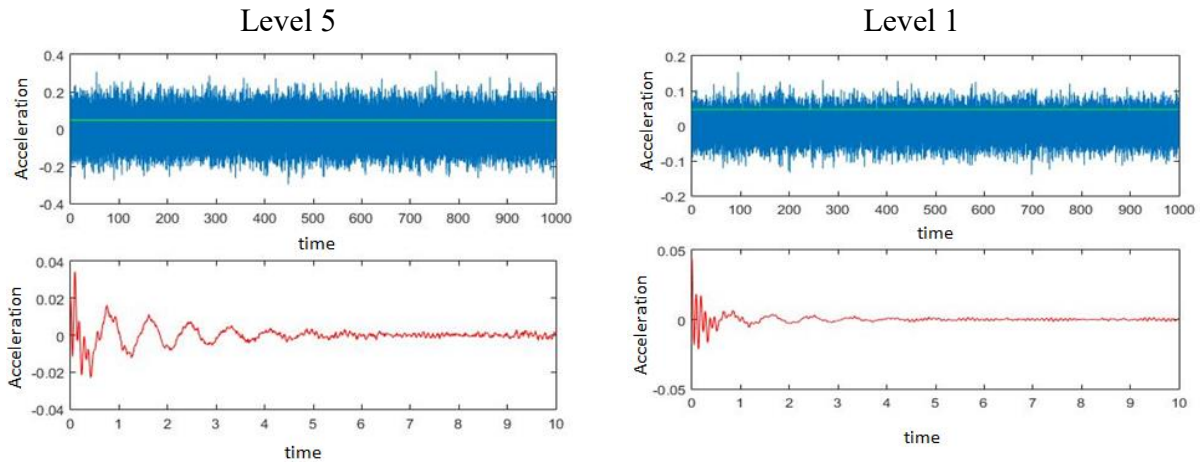


Figure 5.30 Apply RDT in acceleration data in level 1 and 5 with the certain trigger value

As it shown in Figure 5.30, the response resulting from RDT to a random response output of a structure under ambient test is the free decay response. To find the modal properties, FDD is applied in RDT output with 10 s. Figure 5.31 displays the modal properties by use of RDT-FDD.

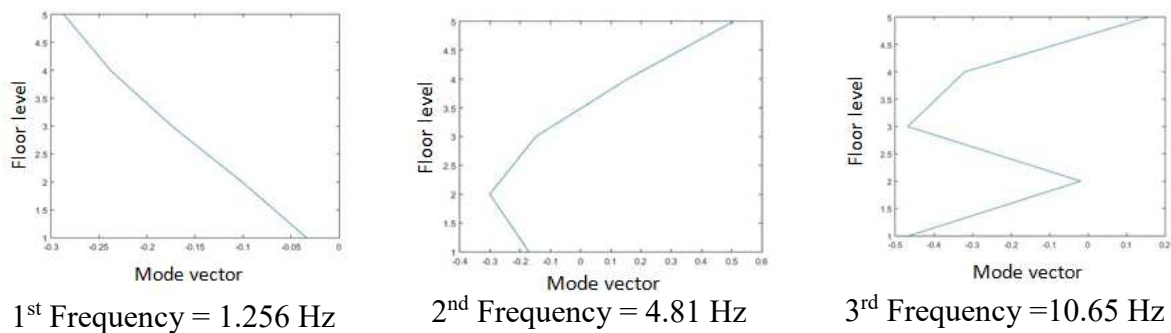


Figure 5.31 Modal Analysis by use of RDT-FDD method

5.7.4 Modal Analysis by use of post-merging (PoSER)

Now, two parts of the total 100000 data are selected as two setups with 20000 number of data points (20s length) in each one. Each setup includes two roving and one reference sensors. Therefore, the new data in two setups are generated to merge the data by use of different techniques. Each setup includes two roving and one reference sensors. The details of setups are shown in Figure 5.32.

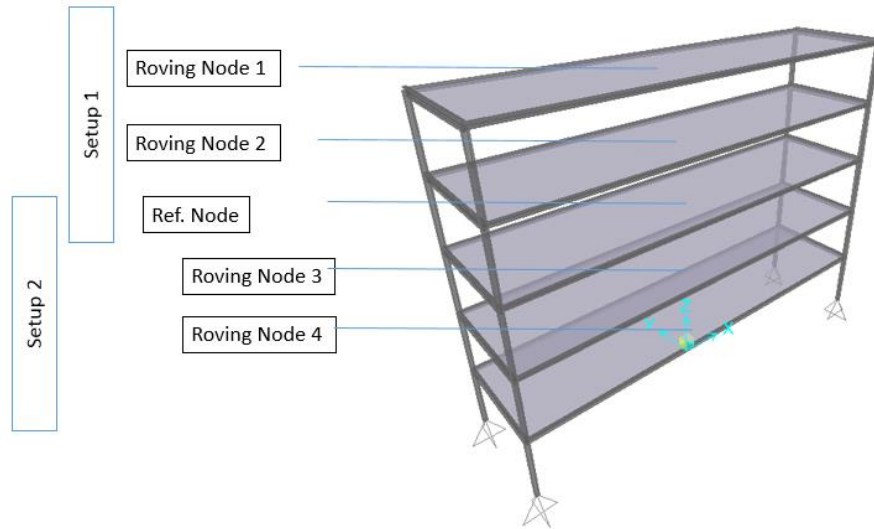


Figure 5.32 Schematic of multi setup merging in five storey concrete frame

The Post-merging method which is called PoSER is used to merge the data. ARTeMIS software is used to merge data by use of PoSER. Figure 5.33 indicates the modal properties in ARTeMIS for five storey frame.

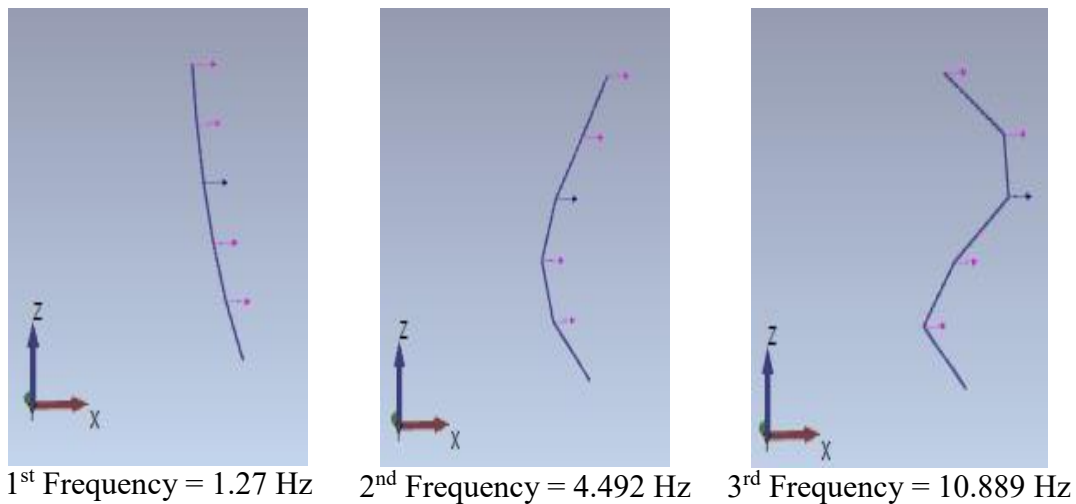


Figure 5.33 ARTeMIS output for Post-merging in five storey frame

5.7.5 Modal Analysis by use of Pre-merging (PreGER)

In PreGER method, first, the collected sensor data should be scaled before modal identification. So, one setup is defined as a main setup, and other setups should be rescaled their output to the main setup by use of reference sensor data. In this manner, the power spectrum density of each data is required for rescaling the setups. In this test, the first setup is used as the main setup. So, the setups should be rescaled by use of reference sensors in each setup. Then, the frequency domain

method like FDD can be applied to the rescaled data to identify modal properties. Figure 5.34 shows the Pre-merging modal properties by use of FDD.

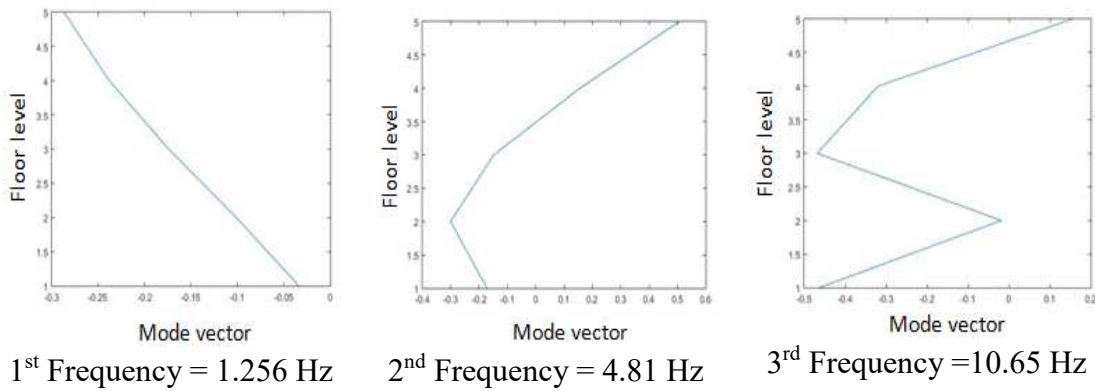


Figure 5.34 Modal properties by use of PreGER

5.7.6 Modal Analysis by use of developed Pre-merging (RDT-PreGER)

Then, the developed PreGER method, which includes RDT technique for noise reduction and high efficiency is applied to the setups. Initially, RDT is applied to each channel in all setups. It should be noted that the trigger value of data should be chosen in such a way that has time correlation between all channels in a setup. Figure 5.35 shows the RDT outputs in the setups for roving and reference sensors.

As it shows, RDT is a free decay recorded data. Now the power spectrum is applied to change time domain to frequency domain. The PSD results of all channels are merged base on Equation 3.65. Figure 5. 36 shows the modal properties obtained using RDT-PreGER technique.

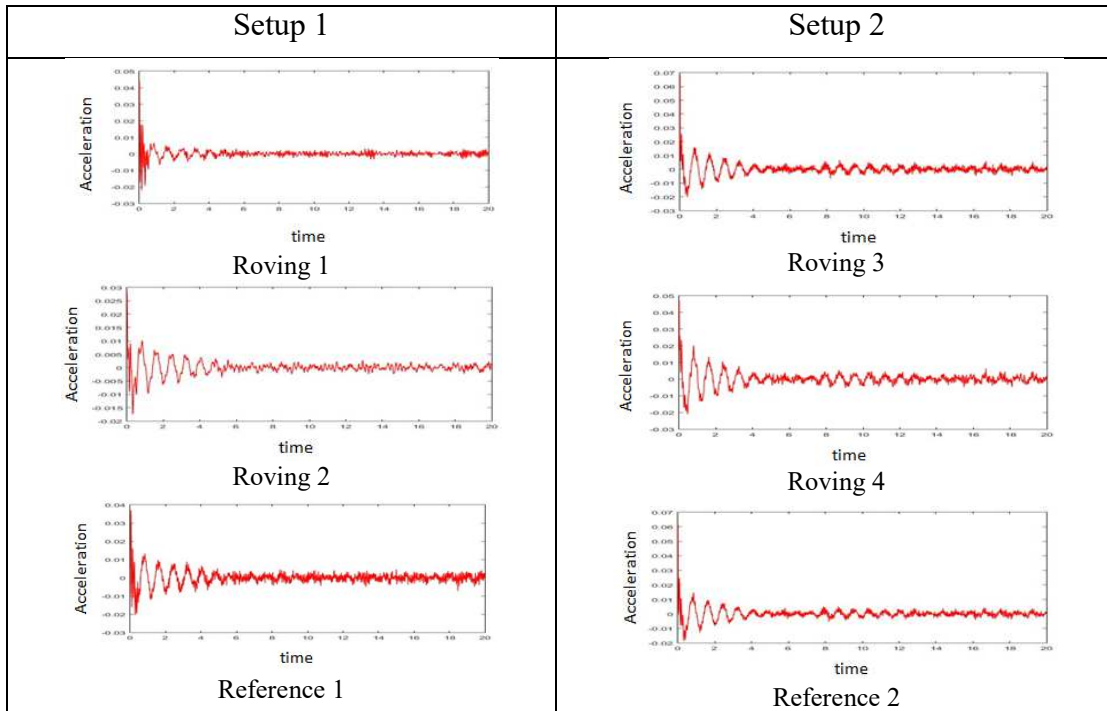


Figure 5.35 RDT output in each setup

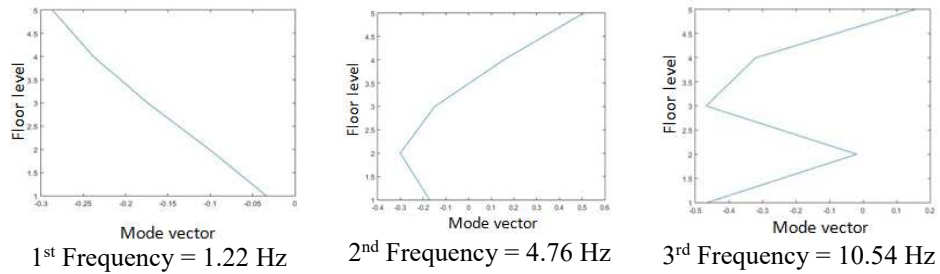


Figure 5.36 Modal properties by use of RDT-PreGER technique

Table 5.7 indicates the total modal identification in the frame in different methods and their differences with SAP 2000 output.

Table 5.7 Modal identification in five storey frame by use of different methods

	Mode 1	Difference	Mode 2	Difference	Mode 3	Difference
SAP 2000	1.216 Hz	-----	4.719 Hz	-----	10.67 Hz	-----
FDD	1.251 Hz	-2.88%	4.981 Hz	-5.55%	10.419 Hz	%3.17
RDT-FDD	1.256 Hz	-3.29%	4.81 Hz	-1.93%	10.65 Hz	1.02%
PoSER	1.27 Hz	-4.44%	4.492 Hz	4.81%	10.889 Hz	-1.02%
PreGER	1.265 Hz	-4.03%	4.83 Hz	-2.35%	10.54 Hz	2.04%
RDT-PreGER	1.22 Hz	-0.33%	4.76 Hz	-0.87%	10.54 Hz	2.04%

5.8 Five storey scaled steel frame

5.8.1 Modal identification along length by use of FDD in MATLAB

FDD method is used as a frequency domain or nonparametric method for modal identification. The algorithm is provided in MATLAB by Farshchin (Farshchin, 2015). Figure 5.37 shows the 1st singular values of power spectrum density (PSD) Matrix. There are four peaks which shows the frequencies of the frame.

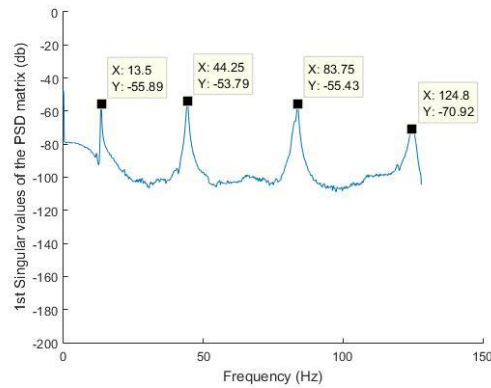


Figure 5.37 1st singular value along the length

After finding frequencies, the corresponding mode shape of each frequency can be detected. Figure 5.38 displays the frequency and corresponding mode shapes along long span in scale steel frame.

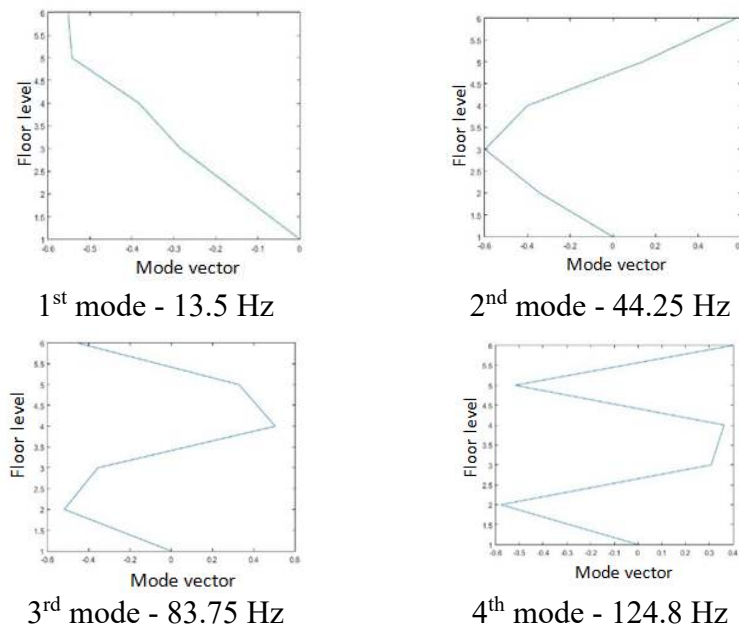


Figure 5.38 Modal properties along the length

5.8.2 Modal identification along width by use of FDD in MATLAB

The sensor can collect the data along x, y and z directions. So, the modal of the frame along other direction can be detected as well. Figure 5.39 shows the 1st singular value of PSD matrix at every frequency.

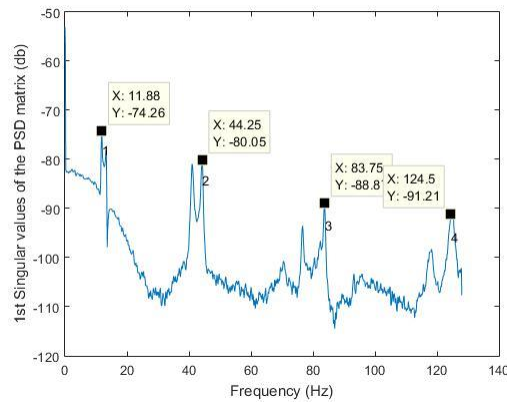


Figure 5.39 1st singular value along the width

Figure 5.40 indicates the corresponding mode shape in each frequency.

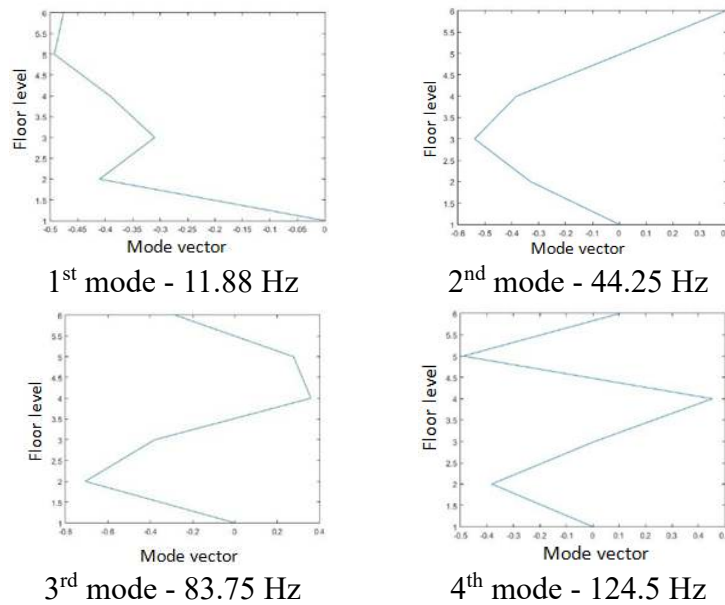


Figure 5.40 Modal properties along the width

5.8.3 Modal identification along length by use of DD-SSI in MATLAB

The time domain modal identification by use of DD-SSI is provided in MATLAB. The number of block Hankel matrix rows is chosen 20. Figure 3.41 shows the stabilization chart and stable modes.

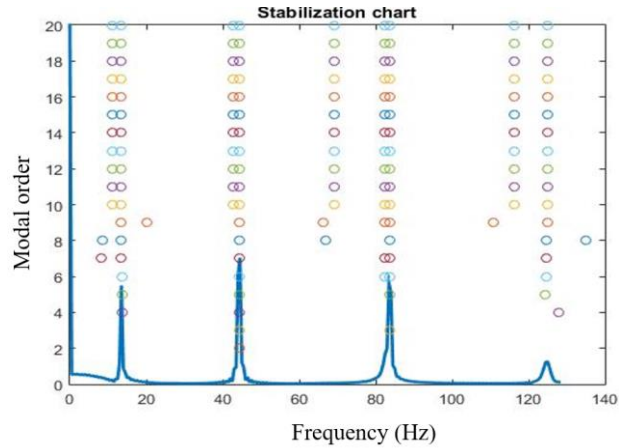


Figure 5.41 Stabilization chart along the length

The frequency and corresponding of mode shapes are shown in Figure 5.42.

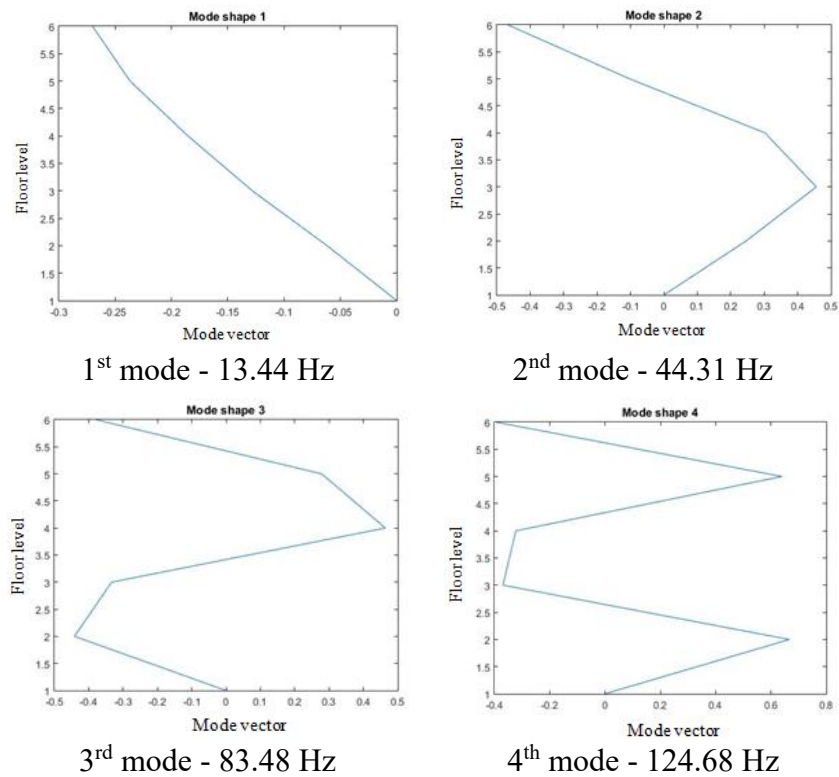


Figure 5.42 Modal properties along the length

5.8.4 Modal identification along width by use of DD-SSI in MATLAB

The DD-SSI also applied along width for modal identification. Figure 5.43 illustrates the stabilization chart and stable modes.

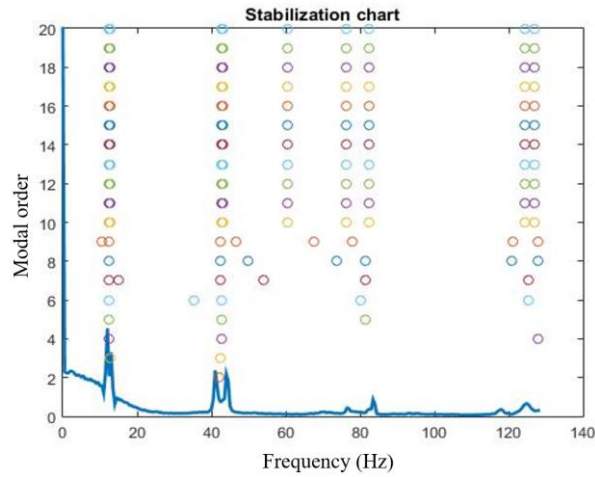


Figure 5.43 Stabilization chart along the width

Then, the frequencies and mode shapes can be detected as it shown in Figure 5.44.

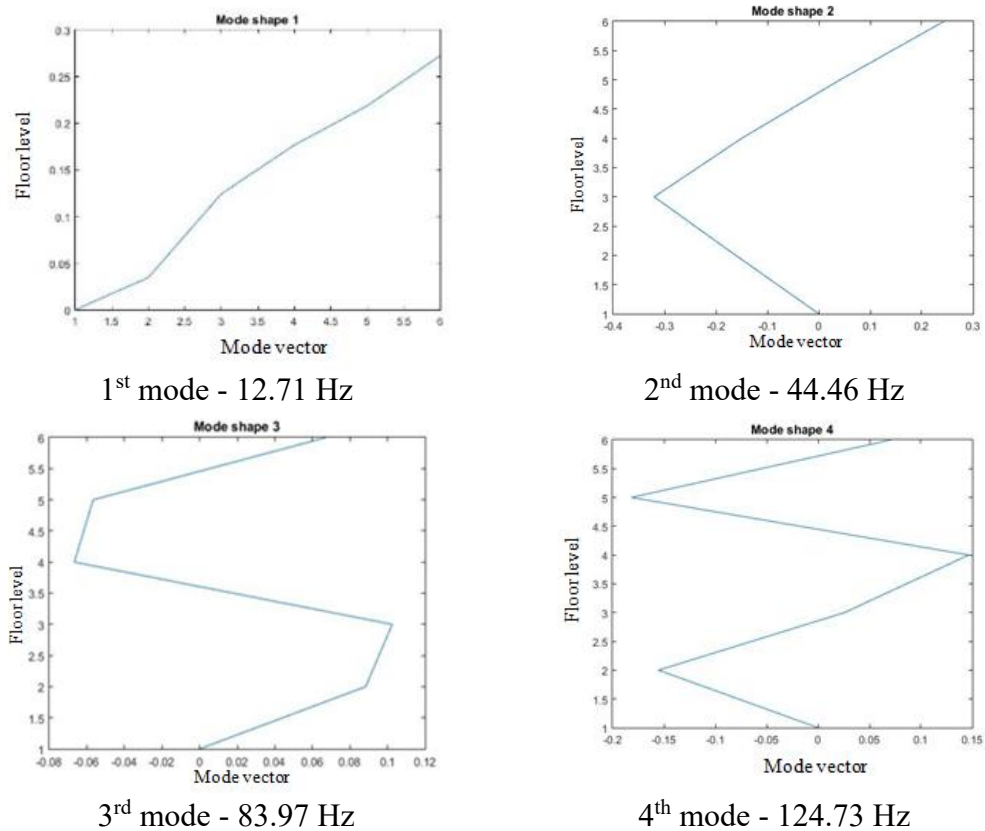
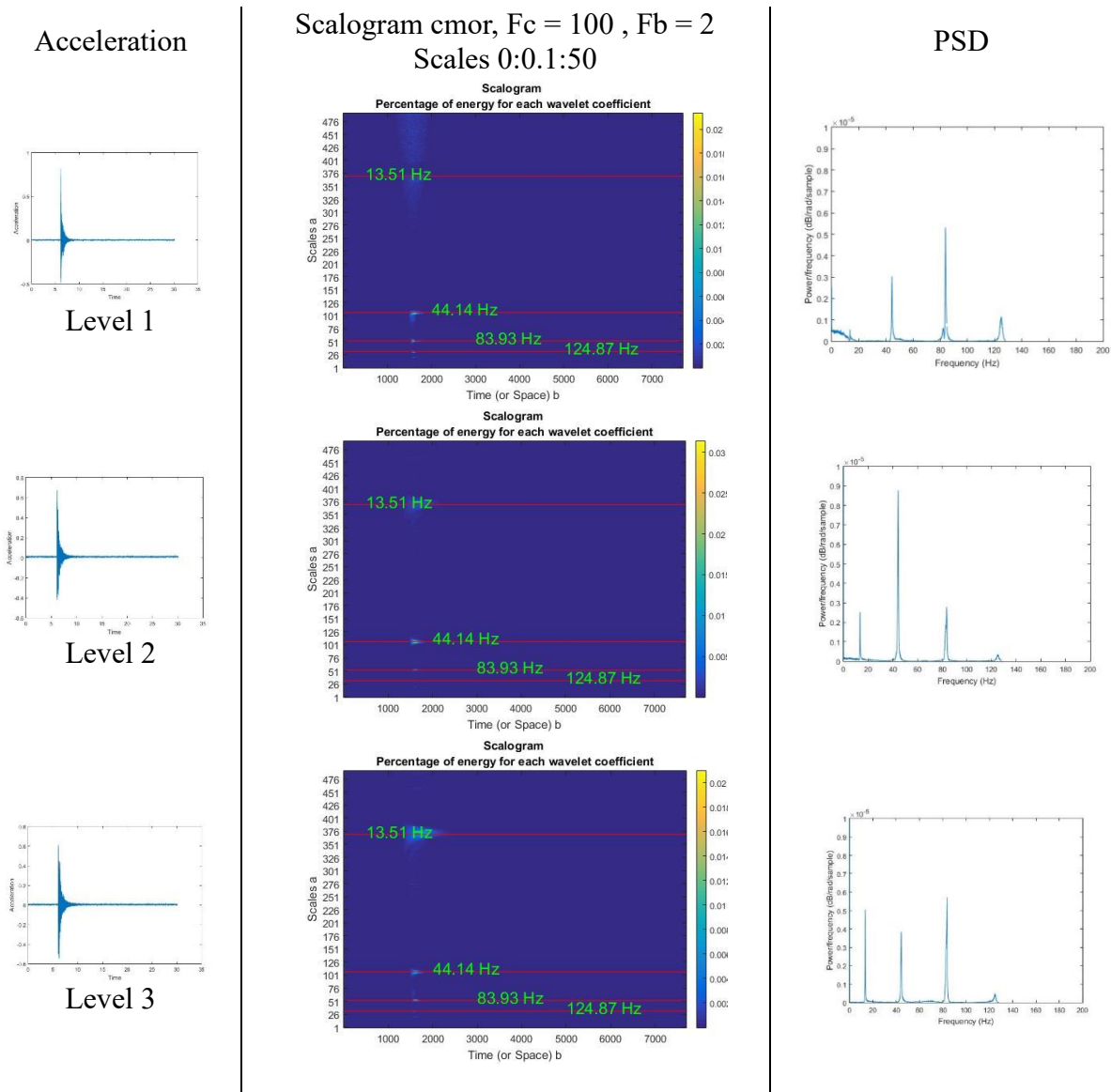
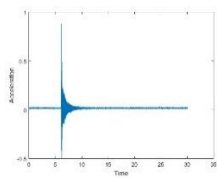


Figure 5.44 Modal properties along the width

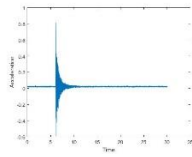
5.8.5 Modal identification along length by use of CWT in MATLAB

Modified Complex Morlet wavelet has been used for time – frequency analysis. The preliminary estimation of frequency can be estimated by use of PSD. The wavelet center frequency (f_c) and bandwidth (f_b) have been adjusted to have the better resolution. The ridge detection of Scalogram technique is used for modal properties identification. The details of Wavelet are shown in the Figure 5.45.





Level 4



Level 5

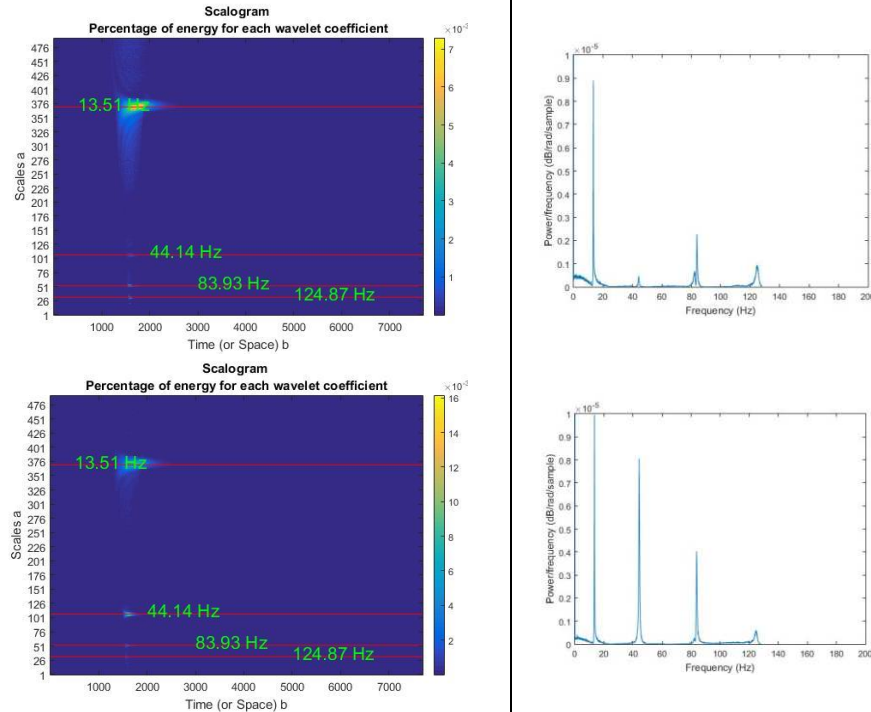


Figure 5.45 Ridge detection for frequency along the length

To find the Mode shape, the coefficient of wavelet at each peak is required. Table 5.8 shows the coefficient at each channel. The level 1 data is used as the reference data, so others data follows the reference data.

Table 5.8 Mode shape calculation

	Coeff. (32,1608)	Coeff. (52,1611)	Coeff. (107,1646)	Coeff. (370,1676)
Ground level	0	0	0	0
Level 1	0.08334	0.1408	0.1215	0.04126
Level 2	-0.0452	0.1008	0.2182	0.0671
Level 3	-0.0415	-0.1365	0.1465	0.0957
Level 4	0.0777	-0.0846	-0.0511	0.1288
Level 5	-0.0419	0.1252	-0.2112	0.1391

After finding the coefficient, Figure 5.46 indicates the frequency and mode shapes of the frame along the length.

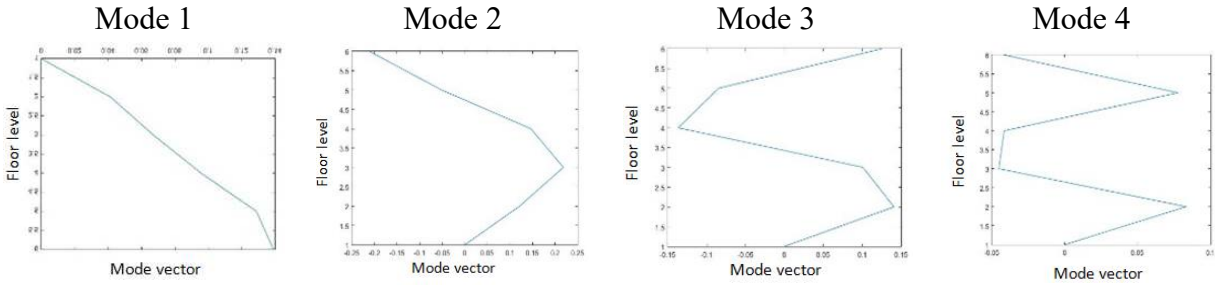


Figure 5.46 Mode shape along the length

5.8.6 Modal identification in short span by use of CWT in MATLAB

The analysis is repeated for another direction, the same scale cannot detect the first mode (last scale), and so the scale has changed to cover all modes. The detail of the wavelet properties is shown in Figure 5.47.

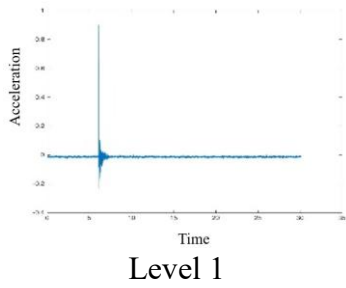
After that, the mode shape can be calculated based on equation 3.59. The wavelet coefficient is shown in Table 5.9. The level 1 data is considered as a reference data.

Table 5.9 Mode shape calculation

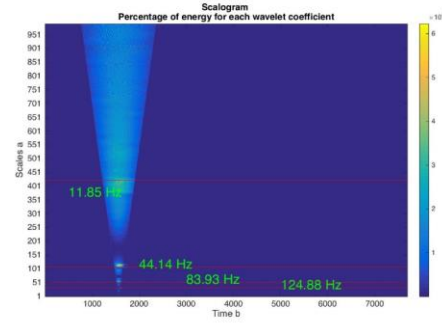
	Coeff. (32,1594)	Coeff. (52,1597)	Coeff. (107,1596)	Coeff. (423,1584)
Ground level	0	0	0	0
Level 1	0.0248	0.0349	0.0301	0.0162
Level 2	-0.0016	0.0129	0.0330	0.0230
Level 3	-0.0241	-0.0152	0.0350	0.0285
Level 4	0.0285	-0.0129	0.0044	0.0441
Level 5	-0.0058	0.0117	-0.0242	0.0510

Then, the mode shapes along the width are plotted in the Figure 5.48.

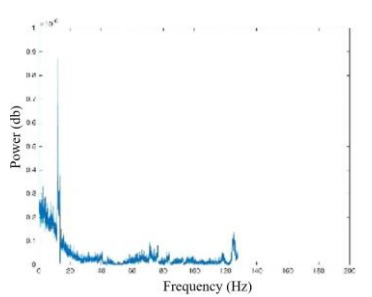
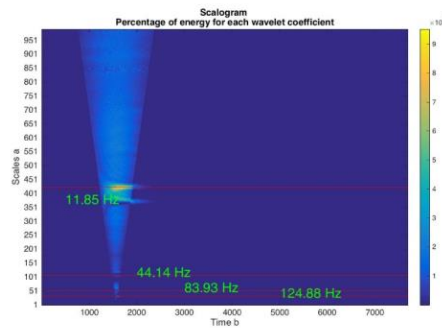
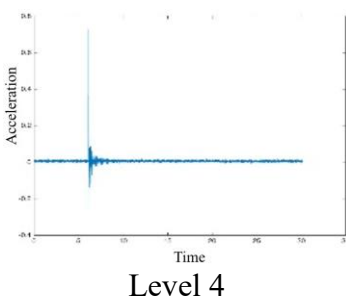
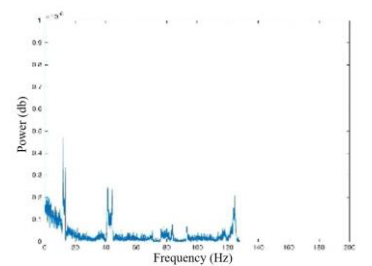
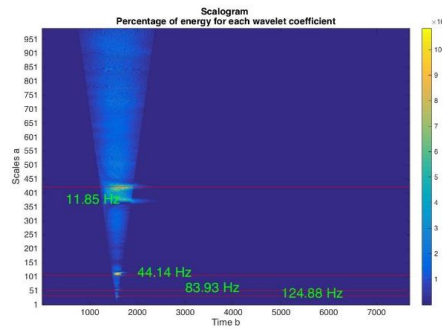
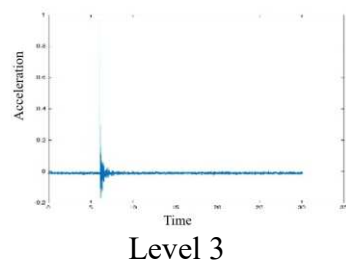
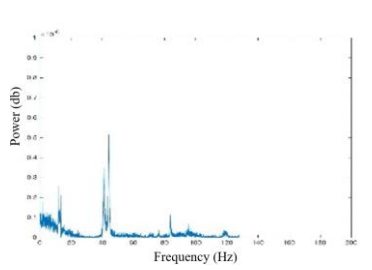
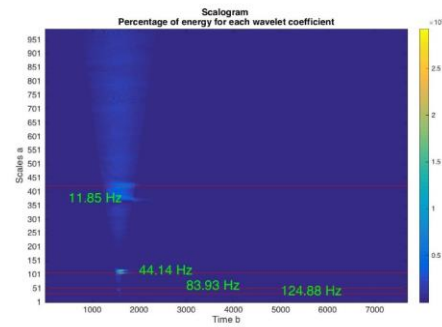
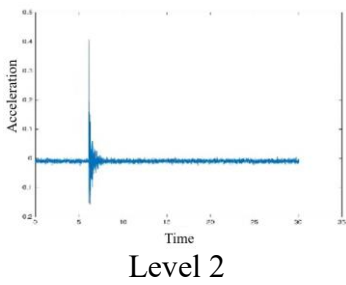
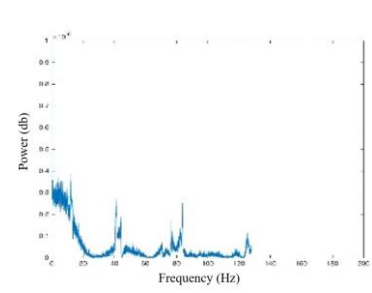
Acceleration



Scalogram cmor, $F_c = 100$, $F_b = 2$ Scales 0:0.1:100



PSD



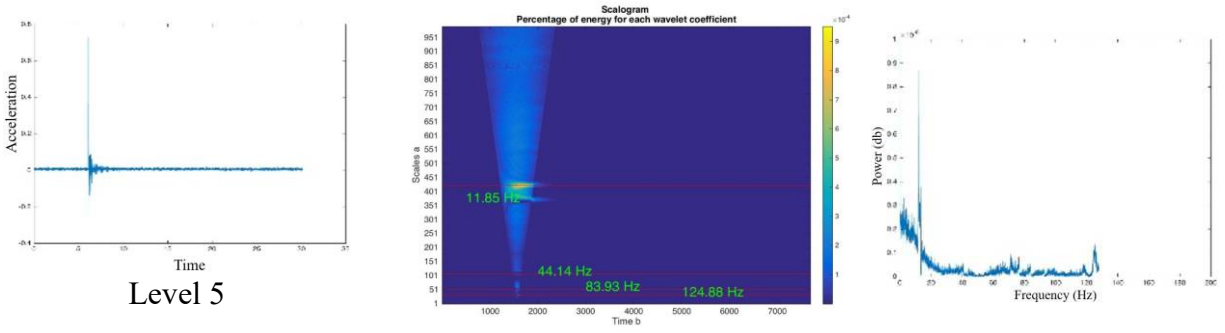


Figure 5.47 Ridge detection for frequency along the width

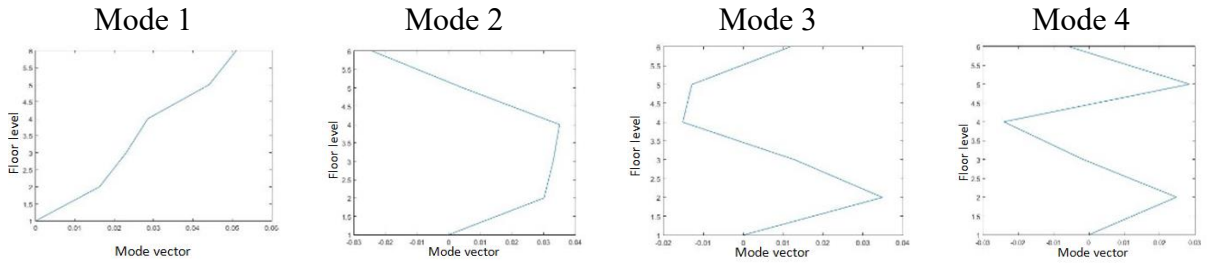


Figure 5.48 Mode shape along the width

5.8.7 Modal identification along length by use of FDD and SSI in ARTeMIS

In addition to the MATLAB software, the data has been analyzed in ARTeMIS in FDD and SSI methods along long span of five storey frame. Figure 5.49 shows the frequencies and corresponding mode shapes in FDD and SSI in ARTeMIS.

As it was mentioned, MAC values indicate the independency of the modes. It was applied to FDD and SSI results in ARTeMIS to see their independency from each other. Figure 5.50 shows the MAC results in ARTeMIS.

Table 5.10 illustrates the identified frequencies in different domains in MATLAB and ARTeMIS along long span of the frame.

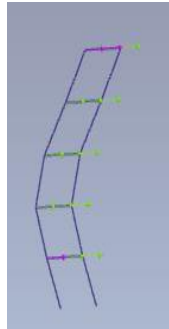
Table 5.10 Four frequencies of five storey frame using different techniques in MATLAB and ARTeMIS

	FDD – MATLAB	SSI – MATLAB	CWT- MATLAB	FDD- ARTeMIS	SSI-ARTeMIS
1 st Frequency	13.5 Hz	13.44 Hz	13.51 Hz	13.375 Hz	13.362 Hz
2 nd Frequency	44.25 Hz	44.31 Hz	44.14 Hz	44.125 Hz	44.158 Hz
3 rd Frequency	83.75 Hz	83.48 Hz	83.93 Hz	83.625 Hz	83.504 Hz
4 th Frequency	124.8 Hz	124.68 Hz	124.87 Hz	125.25 Hz	125.176 Hz

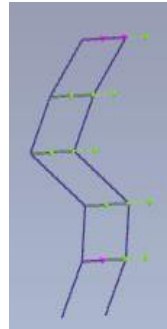
FDD



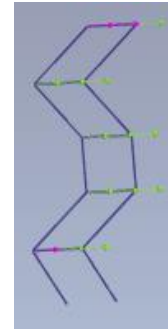
1st Frequency = 13.375 Hz



2nd Frequency = 44.125 Hz

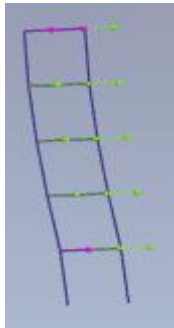


3rd Frequency = 83.625 Hz

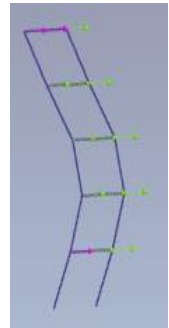


4th Frequency = 125.25 Hz

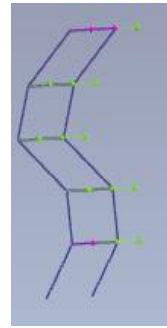
SSI



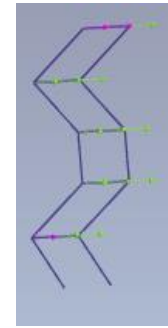
1st Frequency = 13.362 Hz



2nd Frequency = 44.158 Hz



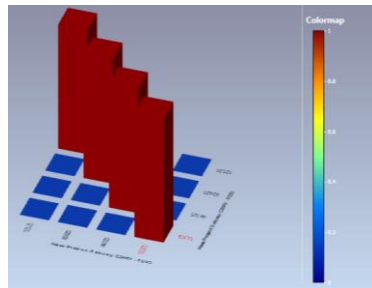
3rd Frequency = 83.504 Hz



4th Frequency = 125.176 Hz

Figure 5.49 FDD and SSI outputs for 5 storey building in ARTeMIS

MAC-FDD



MAC-SSI

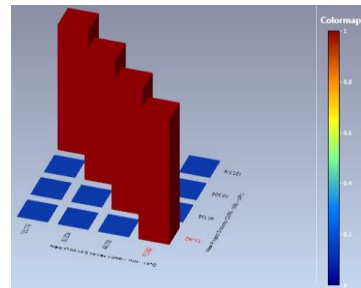


Figure 5.50 MAC values in FDD and SSI in ARTeMIS

5.9 Other contributions

Some industrial collaborations are done to apply some of the techniques developed in this thesis and conducted ambient vibration technique on a number of practical structures. However, due to confidentiality of the projects, they could not be discussed in details. Figure 5.51 shows some sample modes from the tested structures.


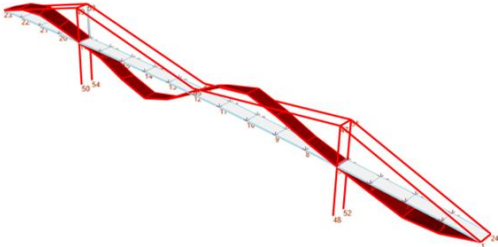
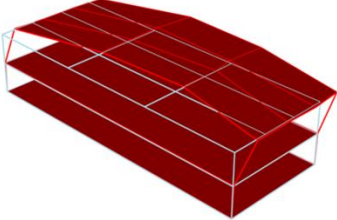
3 rd lateral bending mode of a Tower	2 nd bending mode a bridge	Flexibility Test of a building
		

Figure 5.51 Sample results of collaborated projects

5.10 Summary

As a summary, modal analysis has been applied in different cases using different domains to verify the accuracy of the result. It includes frequency domain, time domain and time-frequency analysis which the common algorithm in each domain has been applied in order to extract the modal properties. Then, the efficiency of RDT has been considered in ambient test in cantilever beam in ambient and forced vibration tests. In addition, two merging techniques (PoSER and PreGER) have been applied in hypothetical frame using MATLAB and ARTEMIS. Then, the developed merging technique called RDT-PreGER is applied to show its efficiency rather than other existing algorithms for merging the data.

Chapter 6. Finite Element Model Updating and Vibration-based Damage Detection

6.1 Overview

The FE model updating is a reliable method to correlate the real model and FE model. It leads to have same outputs in both FE model and real model. As it was mentioned in chapter 2, there are two main categories in model updating namely physics-based and data-driven method. In this research, hybrid method is developed using FE model results and Data-Driven technique using Neural Network. In addition, physics-based method using MUM is implemented to calibrate FE model.

In damage detection, Visual and non-destructive inspection have been the traditional damage identification methods. However these methods have limits that damaged parts of the structure are accessible. Vibration characteristics of a structure, such as frequency, mode shape and damping, are directly affected by the physical characteristics of the structure like mass and stiffness. Damage reduces the stiffness of the structure and changes its vibration characteristics. Therefore, the location and severity of damage can be detected by measuring and monitoring of vibration characteristics. Most of literature deals with the application of theoretical damage identification or laboratory test. Applications on real structures such as bridges or buildings are very rare. There are many analytical methods to identify damage from changes of dynamic parameters (Humar et al., 2006).

6.2 Finite Element Model Updating

6.2.1 Finite Element Model Updating in PSCB Bridge

a. Finite Element Model

The PSCB Bridge has been modeled in M-FEM compiler in MATLAB software. The details of FE model are shown in Appendix B. Figure 6.2 illustrates that the frequencies computed from initial finite element (FE) model have some differences with experimentally obtained frequencies. The parameters of the FE model are adjusted through the model updating process to correlate the analytical and experimental values of the frequencies.

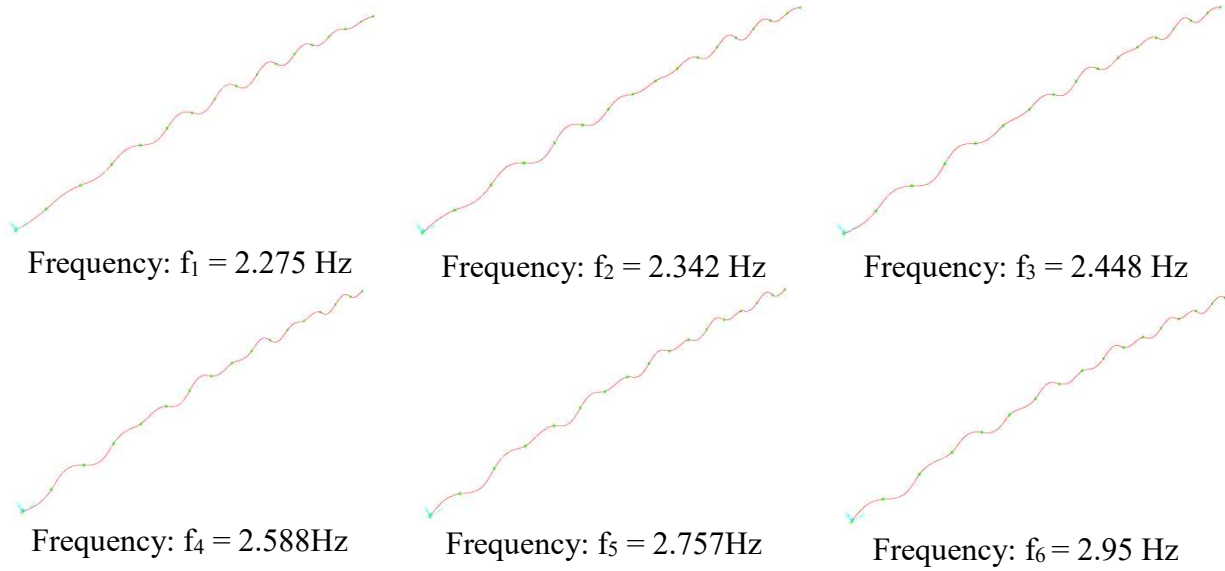


Figure 6.1 Initial Modal properties of PSCB Bridge in SAP 2000

b. PSCB model updating by hybrid method

The Artificial Neural Network (ANN) is used here for model updating of the PSCB Bridge. To reduce the number of parameters, the spans are divided into two groups. In the ANN architecture, the number of input, type of input, number of neuron, percentage of learning, validating and simulating and the type of algorithm (that Levenberg-Marquardt is suitable in this case study) are important to increase the accuracy and reduce the error. In PSCB Bridge, the stiffness of the groups elements are changed up to $\pm 50\%$. Due to small number of groups (only two), the variation of input is chosen with large number of data. For this reason, the changing stiffness has been selected $\pm 50\%$. It is well known that the more the input data used in training the network, better the results in extracting more reliable output. The actual damage may not be as high as 50%. However, it is important to capture the whole range of damage including relative high damage. The frequencies are used as an input and the stiffness changes are as an output. The data is divided in multiple groups with 70% for training, 15% for validation and 15% for testing. Figure 6.2 shows the details of the ANN in PSCB Bridge. Whereas the number of frequencies for PSCB are six, the number of input layer is shown six as well. The number of output layer is related to stiffness adjustment factor for two chosen groups.

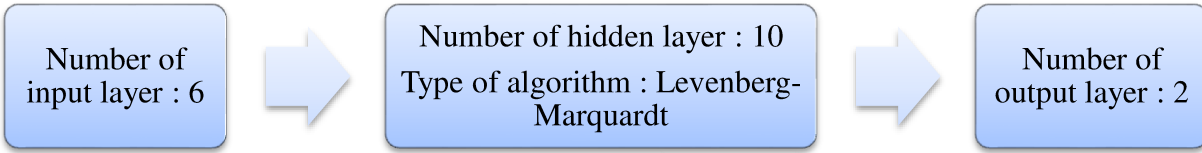


Figure 6.2 Neural Network Details for PSCB Bridge

After creating the Network, the target is utilized to show the modifier factor for each group that is indicated in Table 6.1.

Table 6.1 Stiffness modifier by NN in PSCB Bridge

Group Name	Modifier stiffness Factor
Group 1 (plus)	1.20
Group 2 (minus)	1.23

After applying this modifier stiffness factor, the updated frequencies are computed by FE software.

Table 6.2 shows the initial and update data for PSCB Bridge by use of Neural Network.

Table 6.2 Initial and update modal properties of PSCB Bridge by hybrid model

Bending Mode	Test	Initial Model		Updated Model	
	Frequency (Hz)	Frequency (Hz)	Error (%)	Frequency (Hz)	Error (%)
1	2.47	2.275	-7.89	2.424	1.86
2	2.56	2.342	-8.51	2.458	3.98
3	2.68	2.448	-8.66	2.670	1.47
4	2.83	2.588	-8.55	2.782	1.70
5	2.99	2.757	-7.78	3.005	-2.01
6	3.19	2.950	-7.52	3.212	-0.69

Table 6.2 indicates the updated modal properties using the hybrid method. It shows there are still some errors between updated FE and measured model. So, the input data of network need to be increased in order to train it better. It results in vanishing errors in updated FE model. However, the current updated FE model differences have been reduced rather than initial ones in all modes.

c. PSCB model updating by MUM

The PSCB Bridge is modeled in a MATLAB-based Finite Element program, M-FEM (Bagchi et al. 2006) for structural model updating and vibration damage detection. The model includes of 782 beam-column elements and 1565 nodes. Table 6.3 shows the difference between initial model and experimental value, the maximum difference is 5.93%.

MUM is a physics-based method using the perturbation of the system matrices in the dynamic equations of motion (Kabe 1985) and implemented in M-FEM to determine the changes in the stiffness of structure in order to correlate the test data and analysis data through an iterative technique developed in Bagchi (2005). When a small perturbation is applied, the eigenvalue equation for the target system or updated model of the structure tries to balance the equation by modifying the stiffness and mass. In this research, the mass is considered generally unchanged, the stiffness should be modified to update the model. The stiffness adjustment factor is shown in Figure 6.3.

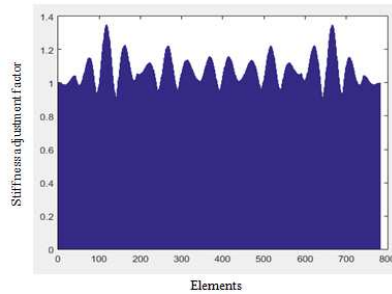


Figure 6.3 Stiffness adjustment factor in PSCB Bridge

Accordingly, M-FEM updates the initial values of frequencies and attempts to reach the experimental value. Table 6.3 indicates the initial and updated frequencies by MUM.

Table 6.3 PSCB bridge initial and updated frequencies (M-FEM)

Bending Mode	Test	Initial Model		Updated Model	
	Frequency (Hz)	Frequency (Hz)	Error (%)	Frequency (Hz)	Error (%)
1	2.47	2.333	-5.55	2.47	0.00
2	2.56	2.408	-5.93	2.56	0.00
3	2.68	2.527	-5.70	2.68	0.00
4	2.83	2.685	-5.11	2.83	0.00
5	2.99	2.877	-3.77	2.99	0.00
6	3.19	3.097	-2.92	3.19	0.00

Table 6.3 illustrate the initial and updated FE models in comparison with real model. It shows that there are no differences between updated FE model and real measurement using MUM technique in PSCB Bridge. So, it means that any change in updated FE model shows the behavior in real structure.

After finding the stiffness factor of each group and running the model the stiffness adjustment factor is closer to one. There are 12 iterations that have been done and the new stiffness adjustment factor has been shown in Figure 6.4.

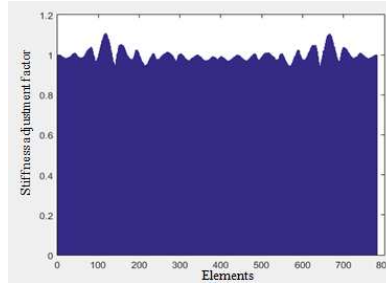


Figure 6.4 Stiffness adjustment factor in PSCB Bridge in Iteration #12

6.2.2 Finite Element Modal updating in Voided Slab Bridge

a. Finite Element model

The Voided Slab Bridge has been modeled in M-FEM compiler in MATLAB software. The details of FE Model are in Appendix C. The voided slab bridge is modeled using frame elements. The model comprises a total of 2461 frame elements. First three modes are considered for model updating. The details of first three modes are displayed in Figure 6.5.

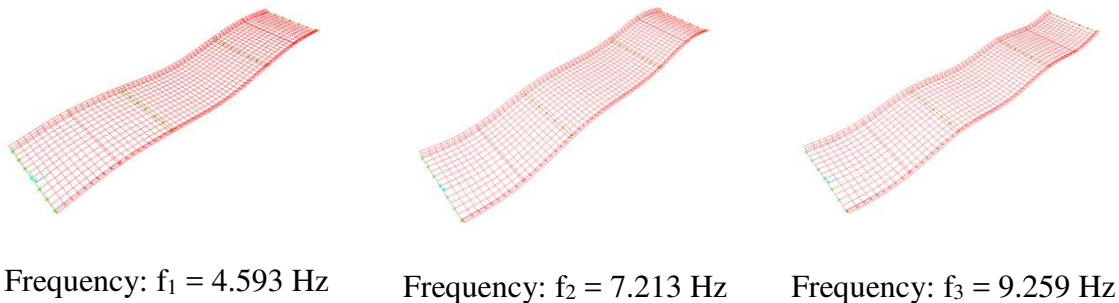


Figure 6.5 Initial mode shapes and corresponding frequencies of Voided Slab Bridge in SAP 2000

b. Voided Slab model updating by hybrid method

In Voided Slab Bridge, 8 groups have been considered in NN. Then, by changing the stiffness to $\pm 20\%$, the input data has been created for the network. The number of hidden layers have been chosen in such as way they provide better correlation between input and output (which mostly choose using trial and error). The number of input corresponding with number of cases with different stiffness modification. The input is the frequencies of the structure in different cases, and

the output is the stiffness modification factor in all group (it might be applied for certain groups). In this bridge, there are 25 cases which have been generated with different stiffness modification factor. Figure 6.6 indicates the input, output and hidden layers of NN in Voided Slab Bridge.

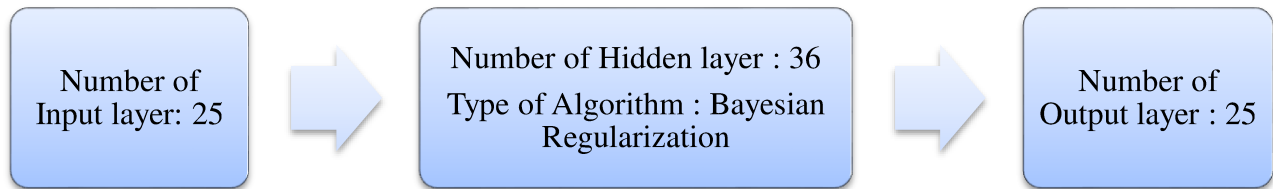


Figure 6.6 Neural Network Details for Voided Slab Bridge

Then the network is created in order to define the specific target. To reach to the target values which are measured frequencies, the network provides the proper coefficients which are stiffness adjustment factors for all groups. Table 6.4 indicates the details of modifier factor for Voided Slab Bridge.

Table 6.4 Stiffness modifier by NN in Voided Slab Bridge

Group Name	Modifier stiffness Factor
Group 1	1.036
Group 2	1.009
Group 3	1.012
Group 4	1.004
Group 5	1.000
Group 6	1.010
Group 7	1.002
Group 8	1.010

SAP 2000 have been used to compare the updated values with experimental ones which is shown is Table 6.5.

Table 6.5 Initial and update modal properties of Voided Slab Bridge by hybrid model

Bending Mode	Test	Initial Model		Updated Model	
	Frequency (Hz)	Frequency (Hz)	Error (%)	Frequency (Hz)	Error (%)
1	5.27	4.59	-12.85	4.95	6.072
2	7.45	7.21	-3.181	7.35	1.343
3	9.60	9.26	-3.550	9.46	1.458

c. Voided Slab Bridge model updating by MUM

The Voided Slab Bridge is modeled by M-FEM. The analytical values of the dynamic properties are compared with experimental result to compute their differences. Then, the perturbation is applied to the stiffness to correlate the output data. The stiffness adjustment factor for voided slab bridge is shown in Figure 6.7.

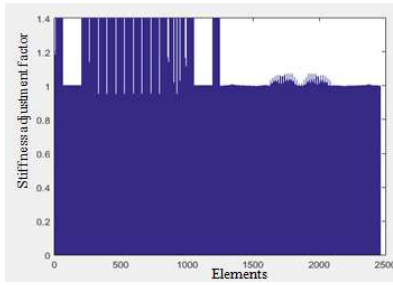


Figure 6.7 Stiffness adjustment factor voided Slab Bridge

As it is mentioned in Table 6.6, the maximum difference between initial analytical and experimental outputs is 11.80%, which is related to first bending mode. After applying the model updating in M-FEM the maximum difference is reduced to 0.11% in the first bending mode. The details of initial and updated modal properties for voided slab bridge are indicated in Table 6.6.

Table 6.6 Voided Slab Bridge initial and updated frequencies (MUM)

Bending Mode	Test	Initial Model		Updated Model	
	Frequency (Hz)	Frequency (Hz)	Difference (%)	Frequency (Hz)	Difference (%)
1	5.27	4.648	-11.80	5.264	-0.11
2	7.45	7.383	-0.90	7.449	-0.01
3	9.60	9.620	0.21	9.595	-0.05

The fourth iteration with new stiffness modifier factor shows that the c factor has approximately close to 1 as it is shown in Figure 6.8.

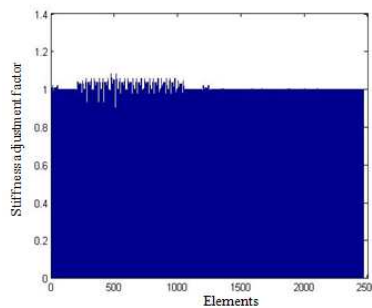


Figure 6.8 Stiffness adjustment factor voided Slab Bridge

6.2.3 Finite Element Model Updating in Steel Box Bridge (STB Bridge)

a. Finite Element Model

M-FEM compiler is used to get the initial frequencies and bending modes. The details of FE Model are in Appendix D. First six modes are considered for STB Bridge, first four modes are bending modes and others are torsion modes. The Initial modes and corresponding frequencies are illustrated in Figure 6.9.

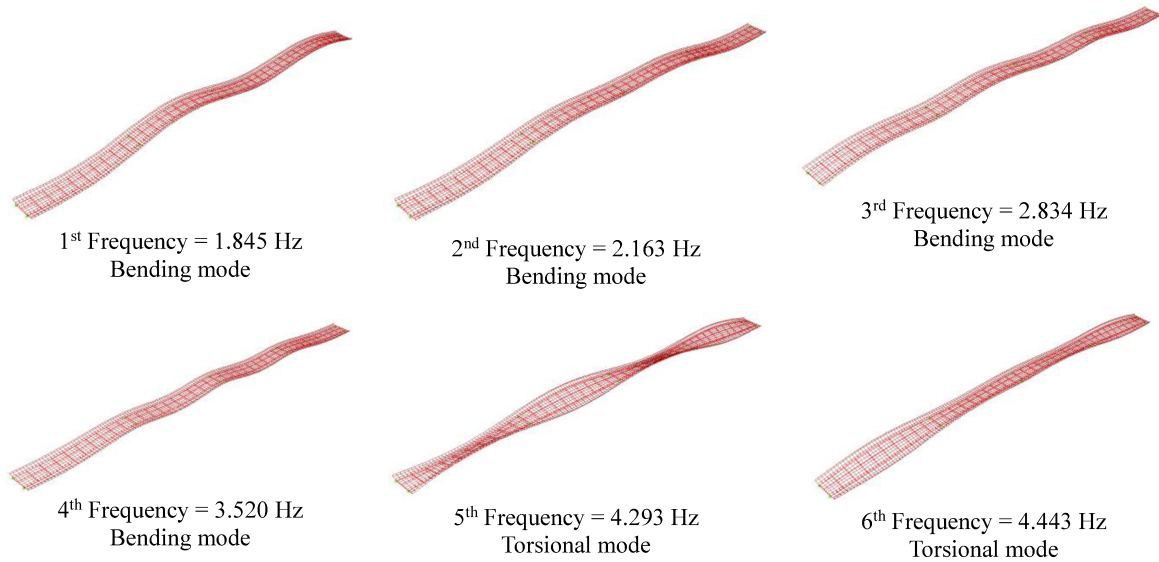


Figure 6.9 Modal properties of STB Bridge in SAP2000

b. STB bridge model updating by hybrid method

To apply model updating method using ANN in the STB Bridge, four groups are considered. To create the input data for ANN, the change in the stiffness is made in the range of $\pm 30\%$ in each group. Figure 6.10 shows the details of the layers in ANN, type of algorithm, and the number of hidden layers.

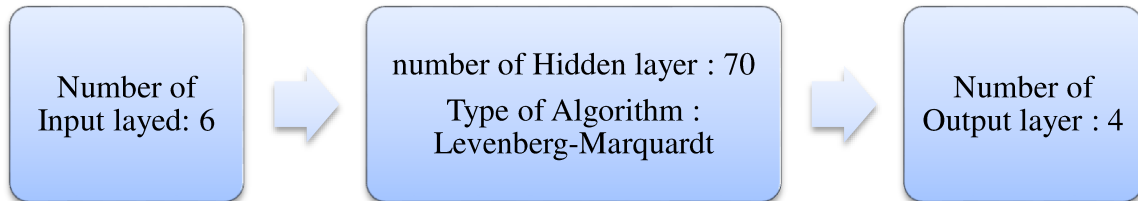


Figure 6.10 Neural Network Details for STB Bridge

The data is divided into groups containing 60% for training, 20% for validation and 20% for testing with Levenberg-Marquardt algorithm. Table 6.7 illustrates the stiffness modifiers by hybrid in STB Bridge.

Table 6.7 Stiffness adjust factor for STB Bridge by hybrid method

Group Name	Modifier stiffness Factor
Group 1	1.124
Group 2	2.362
Group 3	0.789
Group 4	0.210

The stiffness adjustment factors show that group 1 and 2 need to add stiffness and other two required stiffness reduction. The factor in group 2 is quiet impossible because it means that stiffness should be 2.36 time of current stiffness in group 2. So, it needs to be trained with more numbers of input data in such a way that can update with better factor. After applying the stiffness modifier in SAP 2000, the updated values display in Table 6.8.

Table 6.8 Initial and update modal properties of STB bridge by hybrid method

Bending Mode	Test	Initial Model		Updated Model	
	Frequency (Hz)	Frequency (Hz)	Difference (%)	Frequency (Hz)	Difference (%)
1	1.92	1.845	-3.912	1.90	1.042
2	2.23	2.163	-3.024	2.22	0.448
3	2.87	2.834	-1.241	2.91	-1.394
4	3.62	3.520	-2.762	3.61	0.276
5	4.68	4.294	-8.248	4.32	7.692
6	4.78	4.443	-7.050	4.48	6.276

c. STB bridge model updating by MUM

To do the correlation and find the stiffness adjustment factor, C, the experimental values are introduced as a target and tried to match the analytical value to experimental data by applying modifier factor to the stiffness. The stiffness adjustment factors are shown in Figure 6.11.

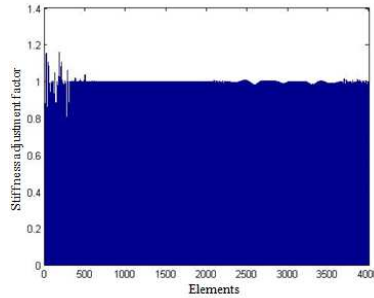


Figure 6.11 Stiffness adjustment factor in STB Bridge in iteration #4

After applying the correlations, the maximum difference between analytical frequency and experimental one is changed from 9.96% to 0.09%. The detail of model updating of STB Bridge by use of M-FEM is displayed in Table 6.9.

Table 6.9 Model updating details of STB Bridge by MUM

Bending Mode	Test	Initial Model		Updated Model	
	Frequency (Hz)	Frequency (Hz)	Difference (%)	Frequency (Hz)	Difference (%)
1	1.92	1.901	-1.00	1.92	0.00
2	2.23	2.265	1.55	2.23	0.00
3	2.87	3.037	5.83	2.872	0.07
4	3.62	3.867	6.83	3.622	0.06
5	4.68	5.146	9.96	4.684	0.09
6	4.78	5.177	8.31	4.780	0.00

The new stiffness modifier factor has been applied to STB data. The new stiffness adjustment factor is shown in Figure 6.12 in four iterations.

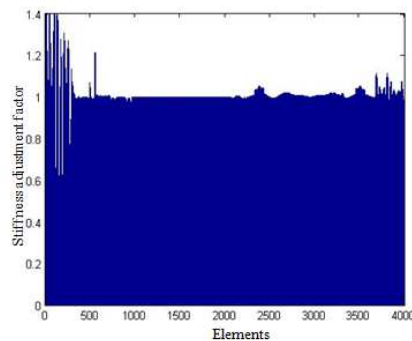


Figure 6.12 Stiffness adjustment factor in STB Bridge in iteration #4

6.2.4 Finite Element Model Updating in Three storey steel frame

a. Finite Element Model

The M-FEM program used to model the frame, and Figure 6.13 shows the natural frequency and corresponding mode shape of the frame. The details of M-FEM input is in Appendix F.

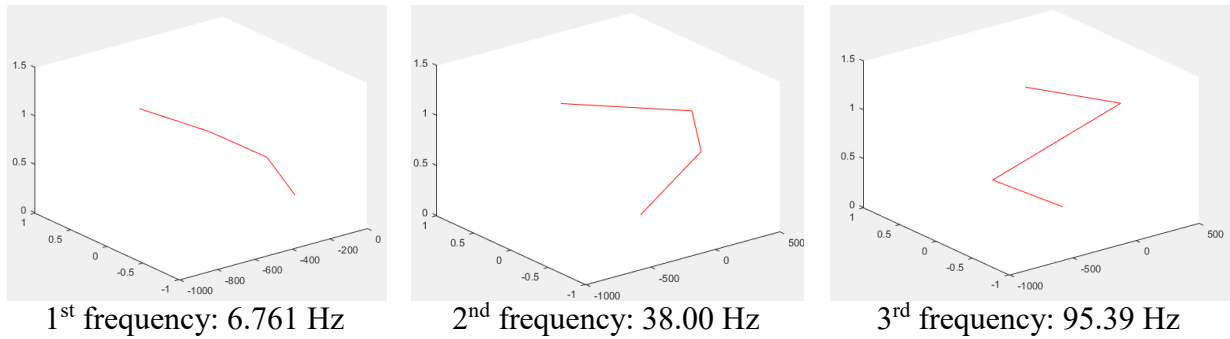


Figure 6.13 Modal properties of three storey Finite Element model

b. Three-storey steel scaled frame model updating by hybrid method

Each floor defined as one group, the stiffness variation is kept at $\pm 30\%$ and corresponding vibration properties are computed, which are used in creating the network. The levenberg-Marquardt network is trained with 70% of the data, 15% for verification and 15% for testing. After arranging the network, the output of updated model is reported in Table 6.10.

Table 6.10 Model updating three storey frame by hybrid method

Mode	Measured frequency (Hz)	Initial frequency (Hz)	Difference	Update frequency (Hz)	Difference
1	7.25	6.761	-6.74%	7.244	-0.08%
2	37.75	38.00	0.66%	37.73	-0.05%
3	94.00	95.39	1.48%	93.93	0.07%

c. Three-storey steel scaled frame model updating by MUM

The MUM is applied by use of MATLAB compiler which is called M-FEM. The measured frequency and finite element output have been adjusted by applying the stiffness adjustment factor, the updated model is shown in Table 6.11 in 5 iterations.

Table 6.11 Model updating three storey by MUM

Mode	Measured frequency (Hz)	Initial frequency (Hz)	Difference	Update frequency (Hz)	Difference
1	7.25	6.761	-6.74%	7.25	0.00%
2	37.75	38.00	0.66%	37.75	0.00%
3	94.00	95.39	1.48%	94.00	0.00%

Consequently, the comparison between stiffness adjustment factor in two methods shows the MUM have better result and more accurate result than neural network. The value of stiffness adjust factor is shown in Table 6.12.

Table 6.12 Stiffness adjust factor for three storey scaled frame by hybrid method and MUM

Method	Matrix Updated Method	Hybrid Method
Group 1	1.09703	1.21881
Group 2	0.97386	0.99109
Group 3	0.66198	0.65842

6.2.5 Finite Element Model Updating in Cantilever steel beam

a. Finite Element model

The beam has been modelled in M-FEM compiler in different mass conditions. Figure 6.13 indicates the beam with its first three frequency and corresponding mode shape.

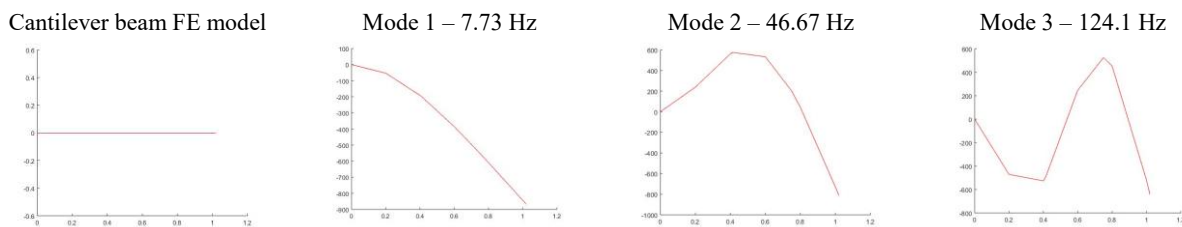


Figure 6.14 FE model of Cantilever beam and its corresponding modal properties

b. Matrix Update Method (MUM)

The beam was divided into eight elements with nodes coinciding with the location of the sensors and masses. The FE model was updated for the case with no additional masses, and the updated model was verified for different cases of mass variation. Figure 6.15 shows the updated model when there is no additional mass. Then, the other results have been verified in different conditions.

It means that the updated FE model has been used in different conditions mass variations. The stiffness adjustment factors are almost one in most of the updated FE models.

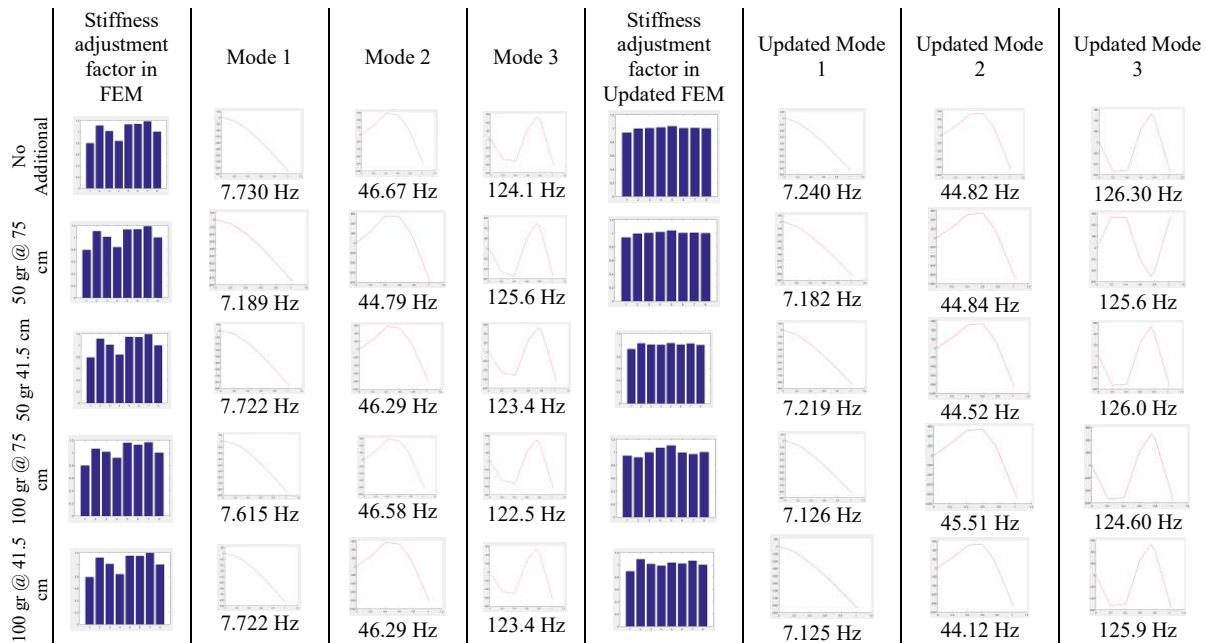


Figure 6.15 Model updating in cantilever steel beam in different conditions

6.3 Vibration-based Damage Detection in PSCB Bridge

The PSCB Bridge is used for comparing of various damage detection through computer simulation studies because there is no damage by visual inspections and frequencies are higher than FEM model. The bridge is assumed that damage reduces the stiffness of element 166, 167 (span 4) and 566, 567 (span 12) by 20% and that of element 366, 367 (span 8) by 30%. Computer simulation based on a FEM of the bridge provides both undamaged and damaged vibration characteristics.

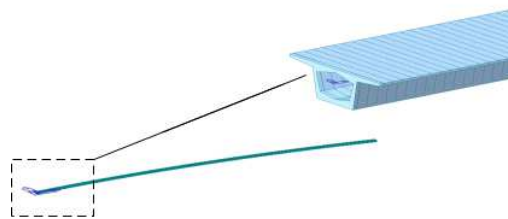


Figure 6.16 FEM of the PSCB Bridge

Changing frequency is the effect of structural property changes such as mass, stiffness and damping. However, this technique has significant practical limitations for application for real structures. There are two reasons. First, very precise frequency measurements are required to

detect small levels of damage. Second, environmental elements, especially temperature, have an important effect on frequency changes. If higher modal frequencies are used, this method may be useful because these modes are associated with local responses. However, it is difficult to excite and extract these higher local modes.

In this research, different methods have been used to detect damage. To simulate the damage, the updated FE model of PSCB Bridge (which is updated in previous section) is considered and applied the modification stiffness factor in six elements. The damaged element is shown in Figure 6.17. The details of SAP2000 model is in Appendix E.

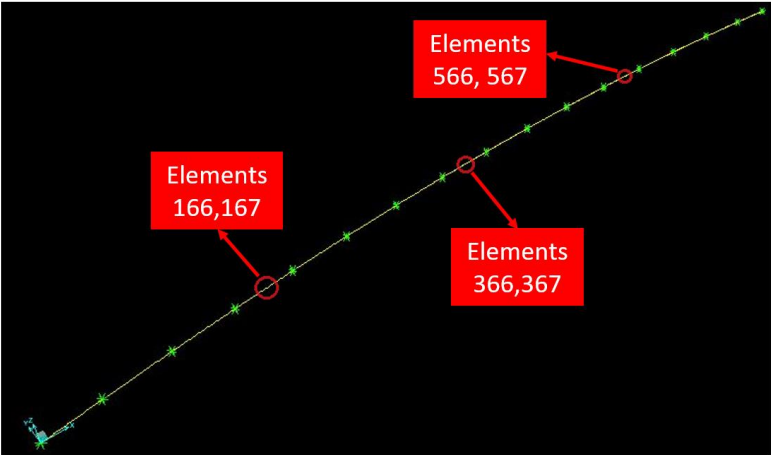


Figure 6.17 Damage applied in specified element (a) Elements 166,167, 566, 567 are 20% stiffness reduction (b) Elements 366,367 are 30% stiffness reduction

In this research, two main damage detection categories are used in order to identify damage called baseline methods and baseline free technique.

6.3.1 Method based on frequency changes

Table 6.13 shows the frequencies of undamaged and damaged bridge. It is clear that there is a reduction in frequencies after damage, but the differences are very subtle and location of damage cannot be identified.

Table 6.13 Frequencies of undamaged and damaged bridge

Mode No.	undamaged (Hz)	damaged (Hz)	Difference (%)
1 st	2.275	2.268	0.32
2 nd	2.342	2.337	0.22
3 rd	2.448	2.441	0.27
4 th	2.588	2.587	0.06
5 th	2.757	2.752	0.21
6 th	2.950	2.945	0.17

6.3.2 Method based on mode shape changes

When damages are subtle, mode shape method is not available because MAC values are close to 1. By the way, MAC shows that the numbers of mode shapes that we have chosen are correct and matched with real modes (Table 6.14).

Table 6.14 MAC values

Mode no.	1 st	2 nd	3 rd	4 th	5 th	6 th
1 st	0.99970	0.00007	0.00012	0.00000	0.00001	0.00002
2 nd	0.00007	0.99982	0.00000	0.00000	0.00004	0.00004
3 rd	0.00012	0.00000	0.99907	0.00042	0.00031	0.00004
4 th	0.00000	0.00000	0.00044	0.99930	0.00024	0.00001
5 th	0.00001	0.00004	0.00030	0.00026	0.99931	0.00001
6 th	0.00002	0.00004	0.00004	0.00001	0.00001	0.99981

6.3.3 Mode shape curvature method

Figure 6.18 shows the mode shape curvature for Modes 1 and 3, before and after damage. It is evident that the modal curvature has significantly increased in spans 4, 8 and 12 (166, 167, 366, 367, 566, 567), which already have been damaged.

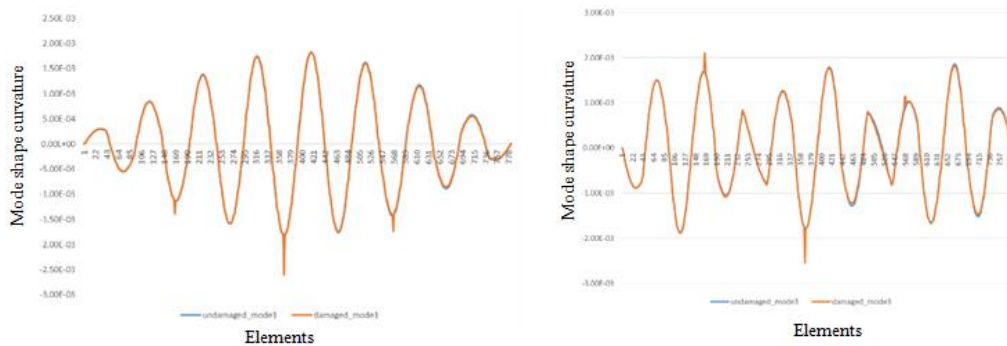


Figure 6.18 Modal curvatures of mode 1 and mode 3

6.3.4 Method base on change in flexibility matrix

The flexibility differences δ_j obtained from Equation 2.9, are plotted in Figure 6.19. It is apparent that span 4, 8 and 12 (166, 167, 366, 367, 566, and 567) have been affected by damage.

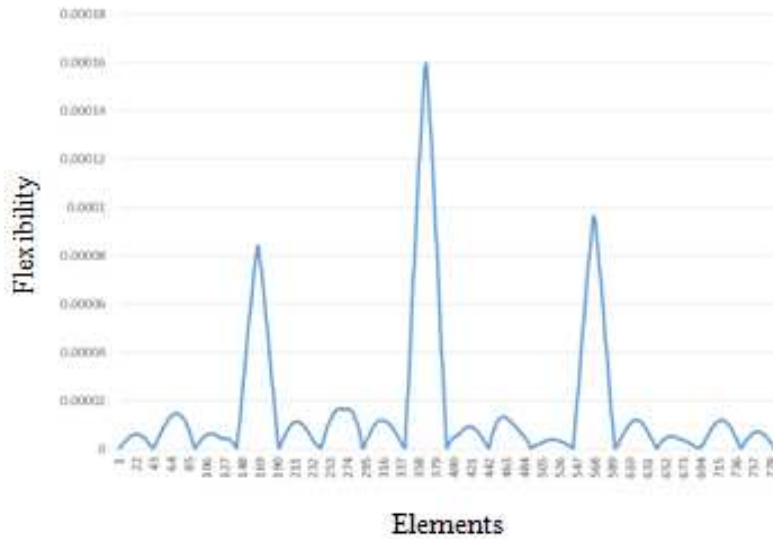


Figure 6.19 Maximum differences of flexibility matrices of damaged and undamaged bridge

6.3.5 Methods based on changes in uniform flexibility shape curvature

The uniform flexibility shape curvature differences obtained from the flexibility matrix using Equation 2.11 are plotted in Figure 6.20. It is apparent that span 4, 8 and 12 (166, 167, 366, 367, 566, and 567) have been affected by the damage.

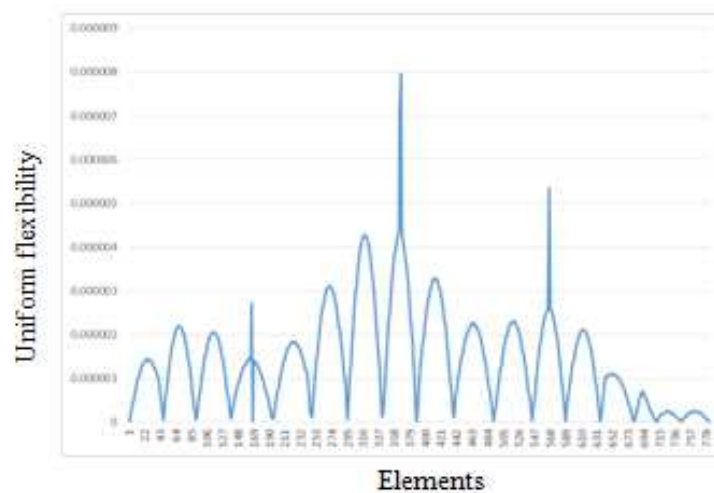


Figure 6.20 Differences in uniform flexibility curvatures of damaged and undamaged bridge

6.3.6 Damage index method

The damage index method is applied to detect damage for the PSCB Bridge. Six mode shapes are used for this method. Using Equation 2.16, damage indices are obtained for the elements and are plotted in Figure 6.21. It is apparent from the plot that damage is expected in spans 4, 8 and 12 (166, 167, 366, 367, 566, and 567).

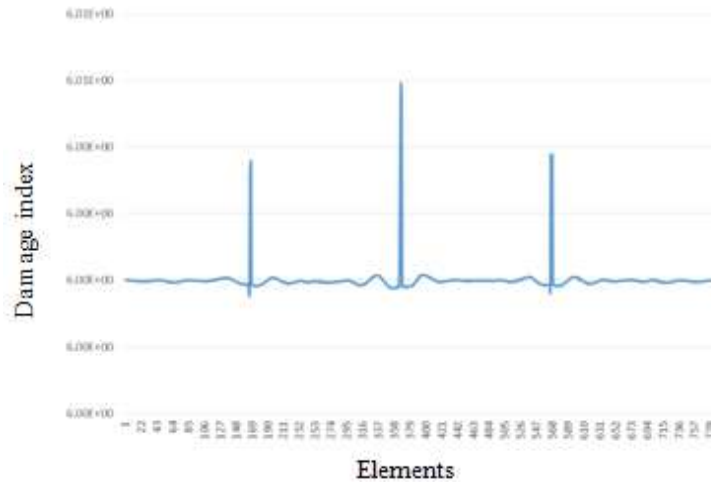


Figure 6.21 Damage indices calculated from equation

6.3.7 Wavelet Transform

The Continuous Wavelet Transform (CWT) is used as a baseline free technique for damage detection. The baseline free method is useful technique when there is no access to the initial data of the structure to evaluate its performance. Then, the final data is the only data to assess the structure. It should be noted that there is no baseline-free method in true sense. Here, the abnormality in the final data pattern is used as an indication for anomaly or damage. In this case, baseline free method can be applied to detect any malfunction or abrupt change in data. In this research, the Gaussian wavelet has been used with order 2 to find the damage in baseline free data. The damage data only used to localize the damage in the bridge. The 1st damaged mode shape is considered as an input for wavelet.

Figure 6.22 shows the wavelet coefficient in damage mode 1 with different color types. It illustrates that wavelet is able to localize the damage by use of the wavelet coefficient in damage elements. As can be seen, damage elements have sharp spikes in wavelet coefficient plot.

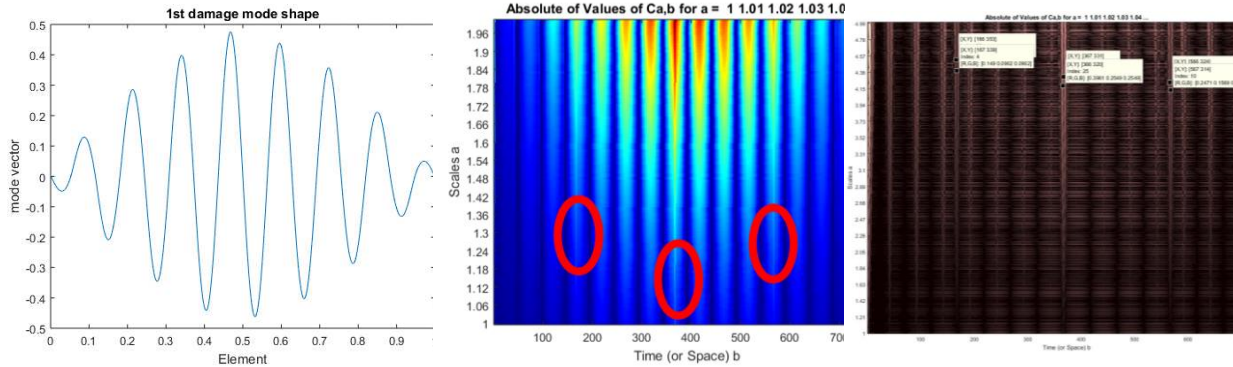


Figure 6.22 (a) 1st damaged mode shape in PSCB Bridge (b) Damage Detection in Wavelet plot color type 1 (c) Damage Detection in Wavelet plot color type 2

a. Sensitivity Analysis

The sensitivity has been applied in three different cases to detect damage using CWT baseline free technique. The intensity level of damage has been decreased from Damage State (DS) 1 to DS3 to evaluate the accuracy and sensitivity of CWT in presence of slight damage. Table 6.15 shows the details of defined damaged in SAP2000 using stiffness reduction factor in specified elements.

Table 6.15 Stiffness reduction in specified element in different damage states

Element Numbers	DS1	DS2	DS3
366, 367	30% Reduction	20% Reduction	10% Reduction
166, 167	20% Reduction	10% Reduction	5% Reduction
566, 567	20% Reduction	10% Reduction	5% Reduction

The same CWT algorithm using Gaussian mother wavelet has been applied in 1st damaged mode shape only. Figure 6.23 shows the wavelet coefficient plot in three different damage states.

As it shows the CWT algorithm can localize the DS1 in all three parts clearly in two different types of colors. DS1 has the highest level of damage among of these damage states. When DS1 move to DS3, the severity of damage become lower and it need a very sensitive and accurate algorithm to identify the perturbation. In DS2, the algorithm still can localize the damage but it is little vague for first and last sections in color type 2. In DS3, only color type 1 is capable to identify the damage in one of three sections only. Due to the damage level is very subtle in DS3 (5% in first and third

sections and 10% in middle section) and CWT is not sensitive to identify damage efficiently.

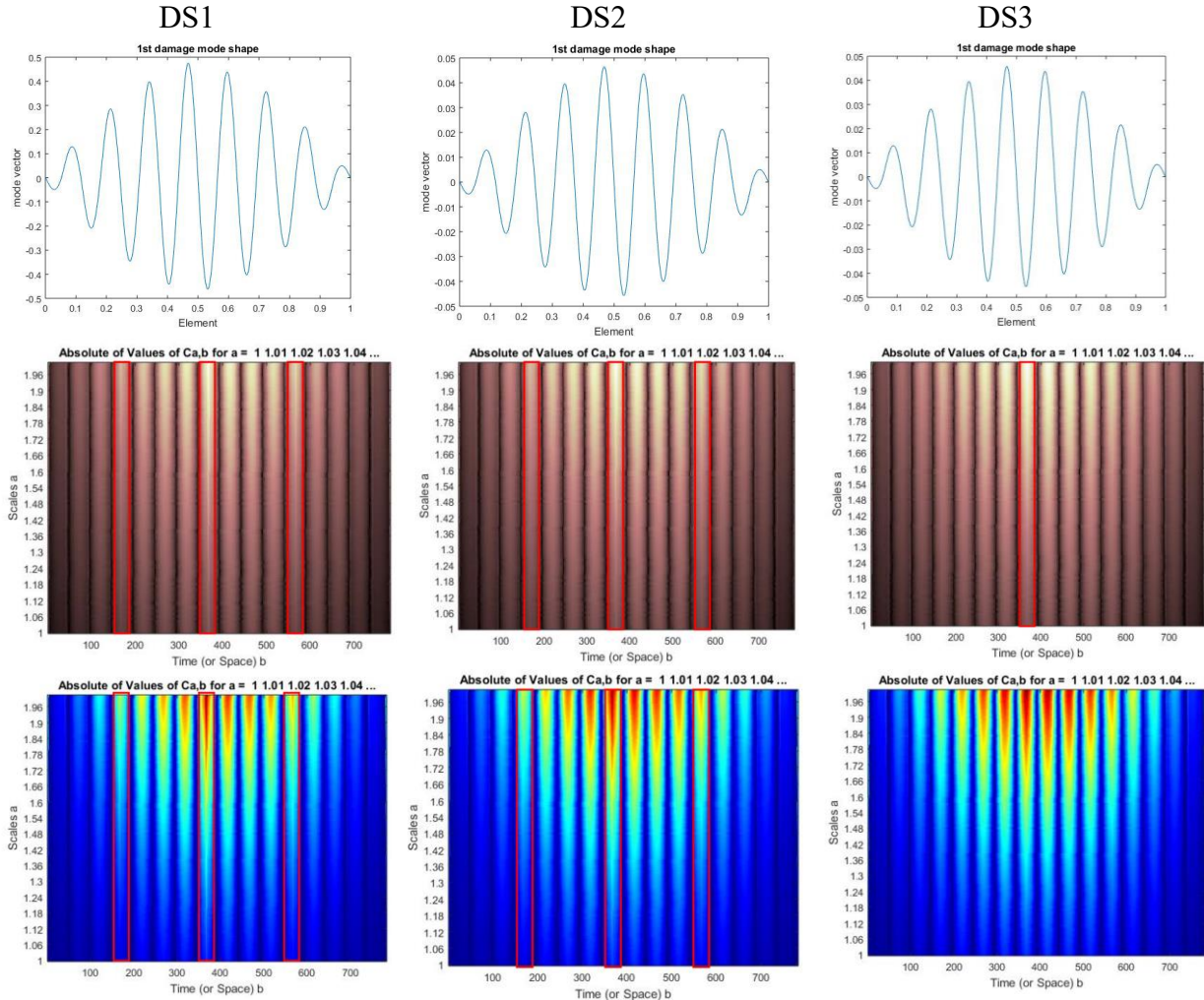


Figure 6.23 wavelet coefficient in three different damage states

6.4 Summary

In this chapter, the FE model updating has been applied in several case studies in two different classification methods such as physics-based (by use of MUM) and hybrid method (by use of FE models and NN). In, hybrid methods, the changing frequency and corresponding modal properties were collected from FE software (e.g. SAP2000, MFEM, etc.) to train the network for further input. In addition, the matrix updated method was used in one case study in a normal condition, and then the updated model was compared in different additional mass variation with real model

to verify the updated FE (Physics-Based Technique). Then the developed hybrid method in FE model using Neural Network and Physics-Based Method have been compare with exciting Matrix Updated Method in different cases to verity its efficiency. The developed FE model updating method is applied as follows; The FE model output require to create an input for Neural Network input. In this research, the updating FE model just changing the stiffness of elements. Then, the initial FE model has certain frequencies. After that, by changing the stiffness in some elements find the corresponding frequencies. It is clear the more the volume of data used in training of NN, the better the performance. The network is trained using frequencies as an input and corresponding stiffness variation factor as an output. When the network is trained well, for any input, it can provide the output which is stiffness variation factor in all elements. So, the real measurement of frequency can be provided and get the stiffness variation factor for all element to reach to this frequency. Physics-based vs NN methods provide a comparison. Since data-driven method, after training, does not require a FE model, it is simpler for practical application.

In addition, baseline and baseline free damage detection methods have been applied in pre-defined damage to an updated FE model of the PSCB Bridge. It showed that some of the techniques like damage index method is able to quantify the level of damage in addition to damage localization. Moreover, Wavelet transform as a baseline free technique is able to localize the damage using the first mode shape only. It is very helpful to use a baseline free method in case there is no access to the original or intact model. Furthermore, in SHM, usually the output (e.g. mode shape) is available, not the input data (e.g. applied load or excitation) to detect damage. At the end, the sensitivity analysis has been implemented in CWT to evaluate its efficiency in presences of low level damage.

Chapter 7. Summary and Conclusions

7.1 Summary

For system identification, the multi setup merging is the common method in large structure for operational modal analysis. In this process, the numbers of collected data from sensor are too large which can affect the processing time. In last decades, pre-merging multi setups methods were developed which could result in reducing the computational effort in modal analysis. However, it can also be large when the analysis has been recorded for long time which can also be contaminated by noise especially in operational modal analysis that makes a barrier for modal identification. So, the new technique is developed to tackle these kinds of limitations and problems in multi-setups merging. The new technique which called RDT-PreGER, was provided for time-consuming and noise contamination problems in multi-setups analysis. It has been indicated that RDT-PreGER is able to reduce the number of data in a large structure and remove the noise in operational data. It converts the ambient data to free decay data which can detect the modal properties clearly.

Regarding the noise reduction, finite element frame model of a structure was simulated with white Gaussian noise as an ambient excitation. One of the effective methods to reduce the noise level in an ambient vibration signals it to pass it through the Singular Value Decomposition (SVD) algorithm. It can separate the modes in such a way that the topmost curve of SVD has the lowest noise level and bottommost curve has the largest. Additional techniques can be employed to enhance SVD results, such as low-pass filtering and wavelet noise reduction. Therefore, two scenarios have been considered in the finite element model: a combination of low-pass filter and SVD, and Wavelet and SVD. The simulation results were then compared according to the Signal to Noise Ratio (SNR) in SVD. Finally, the techniques have been applied to the vibration test data obtained from the laboratory test on a steel frame.

There exist a number of methods for updating finite element models and identifying the system parameters like stiffness and mass, based on the dynamic response of a structure. These methods are categorized as Physics-based and Data-driven methods. Another objective of this research was to develop the Hybrid method by use of Neural Network in Data-Driven and SAP 2000 and M-FEM in Physic-based Method. They update their model through the data from ambient vibration tests. The MUM was applied in a Physics-based method and the NN was used in Data-driven

methods for updating or correlating the FE models. The MUM correlates the models by solving the inverse problem through constrained optimization. In hybrid method, the NN was applied to find the correlations between the structural frequencies and changes in the sectional properties of the bridge segments. The outputs of these models were compared to certain target frequencies based on the measured data in order to adjust the section properties of the bridge elements.

Furthermore, the damage detection techniques on PSCB Bridge have been studied. To detect damage in the bridge, frequency based and mode shape based methods were proposed. The mode shape based method includes MAC, Mode shape curvature, flexibility Matrix, uniform flexibility shape curvature, damage index method.

7.2 Conclusions

Based on the work presented in the study, the following conclusions are made.

- In system Identification, the pre-merging technique with RDT helps reduce the amount of data and error in modal identification. The frequency domain algorithm showed the similar result of pre merging along and pre merging with RDT. Also, RDT can remove the noise in ambient vibration test by averaging the time segments in certain trigger value.
- Among all merging techniques, PreGER is the fastest method especially with large number of setups. So, using RDT results in reducing the amount of data and enhancing the performance of the system identification process. It can have better result with more accuracy by noise reduction which was shown in five storey finite element model.
- In noise reduction, the results indicated that Wavelets with fourth order Daubechies (db4) and eighth order of Symlets (sym8) algorithms achieve better result rather than low pass filter. On the other hand, low pass filter gives better result than both types of wavelets when only one level of decomposition is used for data corresponding to each floor. The computed SNR of the data denoised using db4 and sym8 wavelets with four levels of decompositions produces accurate output in comparison to low pass filter and other types of wavelets in most additive SNRs. Moreover, low pass filter worked more efficiently than the single level decomposition of wavelets.

- In model updating, the hybrid technique shows better results by selecting the proper number of element group. It has been compared with perturbation technique in physic-based method which is called Matrix Updated Method in different case studies.

7.3 Contribution

There are two main contributions here. The first one is developing the merging technique in system identification. The second one is a hybrid method in FE model updating. The overall contributions are as follows;

- Developed a hybrid method in FE model updating.
- Developed an efficient frequency domain method in multi setup merging.
- Studied on Frequency domain, Time domain and Time-Frequency Analysis technique in modal identification
- Studied on an efficient scheme for noise reduction in vibration data.
- Studied the existing methods for damage detection and identified an effective one for practical use.

7.4 Limitations and Scope for Future Work

The new method in system identification was tested with one reference sensor; it should be tested for more than one sensor when the torsion mode is required. In addition, the developed RDT-PreGER was implemented in frequency domain, it can be developed using time domain methods. Regarding the hybrid method, it is more efficient to link a FE model (e.g. SAP 2000) to data-driven model (e.g. MATLAB) directly to run the model with different stiffness to implement the input matrix for neural network. Field tests of large structures in different climatic conditions should be done to further determine the efficacy of the proposed methods.

As a note to the future direction for SHM, it could be mentioned that modal analysis and model updating are important tools for SHM. There are many challenges to make the FE model to represent a real structure because of the lack information about the structural details, reliable measurements, and robust techniques for correlation between the real structure and FE model. There is a scope for further development in these areas. Modal properties can be monitored periodically or continuously in order to check the condition of the structure. In addition, there is a

need for development of innovative sensors that will work under operational and extreme load conditions without the requirement to external modifications to vibration signals from the structure using large scale exciter. All of these techniques help us to have a smart and safe community with no sudden collapse. It is also anticipated that the data-driven methods will provide a more practical diagnostic mechanism.

References

- Adeli, H. and Jiang, X., 2006. Dynamic fuzzy wavelet neural network model for structural system identification. *Journal of Structural Engineering*, 132(1), pp.102-111.
- Adeli, H. and Kim, H., 2004. Wavelet-hybrid feedback-least mean square algorithm for robust control of structures. *Journal of Structural Engineering*, 130(1), pp.128-137.
- Allemang, R.J. and Brown, D.L., 1982, November. A correlation coefficient for modal vector analysis. In *Proceedings of the 1st international modal analysis conference (Vol. 1, pp. 110-116)*. Orlando: Union College Press.
- Allemang, R.J., 2003. The modal assurance criterion—twenty years of use and abuse. *Sound and Vibration*, 37(8), pp.14-23.
- Alvin, K.F., Robertson, A.N., Reich, G.W. and Park, K.C., 2003. Structural system identification: from reality to models. *Computers & structures*, 81(12), pp.1149-1176.^[17]_[SEP]
- Andersen, P., 1997. Identification of civil engineering structures using vector ARMA models (Doctoral dissertation,). *Aalborg University, Denmark*
- Asmussen, J.C. and Brincker, R., 1996, February. Estimation of frequency response functions by random decrement. In *proceedings SPIE international society for optical*, pp. 246-252, Denmark
- Bagchi, A., 2005. Updating the mathematical model of a structure using vibration data. *Journal of Vibration and Control*, 11(12), pp.1469-1486.
- Barai, S.V. and Pandey, P.C., 1995. Vibration signature analysis using artificial neural networks. *Journal of Computing in Civil Engineering*, 9(4), pp.259-265.
- Baruch, M. and Itzhackj, I.Y.B., 1977. Orttiogonalization of Measured Modes. *AIAA journal*, 16(4).
- Berman, A. and Nagy, E.J., 1983. Improvement of a large analytical model using test data. *AIAA Journal*, 21(8), pp.1168-1173.
- Bodeux, J.B. and Golinval, J.C., 2001. Application of ARMAV models to the identification and damage detection of mechanical and civil engineering structures. *Smart Materials and Structures*, 10(3), p.479.
- Brincker, R. and Rodrigues, J., 2005. Application of the random decrement technique in operational modal analysis. In *Proc., 1st Int. Operational Modal Analysis Conf. (IOMAC)*, Denmark.
- Brincker, R., Jensen, J.L. and Krenk, S., 1990. Spectral Estimation by the Random Dec Technique. *Dept. of Building Technology and Structural Engineering, Aalborg University*.

- Brincker, R., Krenk, S. and Jensen, J.L., 1991. Estimation of Correlation Functions by the Random Decrement. *In Proceedings of the Florence Modal Analysis Conference* (pp. 783-788).
- Brincker, R., Ventura C. E., 2015. Introduction to Operational Modal Analysis John Wiley & Sons Ltd , United Kingdom.
- Brincker, R., Zhang, L. and Andersen, P., 2000, February. Modal identification from ambient responses using frequency domain decomposition. *Proc. of the 18th International Modal Analysis Conference (IMAC), San Antonio, Texas.*
- Brock, J.E., 1968. Optimal matrices describing linear systems. *AIAA Journal*, 6(7), pp.1292-1296.
- Chen, C.H., 2005. Structural identification from field measurement data using a neural network. *Smart Materials and Structures*, 14(3), p.S104.
- Cole Jr, H.A., 1971. On-line analysis of random vibrations. *9th Structural Dynamics and Materials Conference.*
- Cole Jr, H.A., 1973. On-line failure detection and damping measurement of aerospace structures by random decrement signatures. *Nielsen Engineering and research, INC.*
- Cornwell, P., Farrar, C.R., Doebling, S.W. and Sohn, H., 1999. Environmental variability of modal properties. *Experimental techniques*, 23(6), pp.45-48.
- Doebling, S.W., Farrar, C.R. and Prime, M.B., 1998. A summary review of vibration-based damage identification methods. *Shock and Vibration Digest*, 30(2), pp.91-105.
- Doebling, S.W., Farrar, C.R., Prime, M.B. and Shevitz, D.W., 1996. Damage identification and health monitoring of structural and mechanical systems from changes in their vibration characteristics: a literature review.
- Donoho, D.L. and Johnstone, I.M., 1995. Adapting to unknown smoothness via wavelet shrinkage. *Journal of the American Statistical Association*, 90(432), pp.1200-1224.
- Entezami, A. and Shariatmadar, H., 2014. Damage localization in shear buildings by direct updating of physical properties. *International Journal of Advanced Structural Engineering (IJASE)*, 6(2), p.4.
- Ewins, D.J., 2003. Modal testing: theory, practice and application (mechanical engineering research studies: engineering dynamics series). *Research Studies Press Ltd, England.*
- Farrar, C.R., Doebling, S.W., Cornwell, P.J. and Straser, E.G., 1996. Variability of modal parameters measured on the Alamosa Canyon Bridge (No. LA-UR-96-3953; CONF-970233-7). *Los Alamos National Lab., NM (United States).*
- Farshchin, M. (2015). Frequency Domain Decomposition (FDD), *MATLAB.*

- Felber, A.J., 1993. Development of a hybrid bridge evaluation system (*Doctoral dissertation, University of British Columbia*).
- Fox, C.H.J., 1992. The location of defects in structures-A comparison of the use of natural frequency and mode shape data. *In 10th International Modal Analysis Conference (Vol. 1, pp. 522-528)*.
- Friswell, M.I. and Mottershead, J.E., 1995. Finite Element Modelling. *In Finite Element Model Updating in Structural Dynamics (pp. 7-35)*. Springer Netherlands.
- Gul, M., 2009 Investigation Of Damage Detection Methodologies For Structural Health Monitoring. *Doctoral thesis, University of central florida, US*.
- HasançEbi, O. and Dumlupınar, T., 2013. Linear and nonlinear model updating of reinforced concrete T-beam bridges using artificial neural networks. *Computers & Structures, 119, pp.1-11*.
- Hsu, D.S., Yeh, I.C. and Lian, W.T., 1993. Artificial neural damage detection of existing structure. *In Proc., 3rd ROC and Japan Seminar on Natural Hazards Mitigation (pp. 423-436)*. Taiwan: Tainan.
- Humar, J. Bagchi, A. and Xu, H. 2006. Performance of vibration-based techniques for the identification of structural damage. *SAGE Journal of Structural Health Monitoring, 5(3): 215–241*.
- Ibrahim, S.R., 1977. Random decrement technique for modal identification of structures. *Journal of spacecraft, 14(11), pp.696-700*.
- Jaishi B, Ren WX., 2005. Structural finite element model updating using ambient vibration test results. *Journal of Structural Engineering 131 (4):617-628*
- Jaishi, B. and Ren, W.X., 2005. Structural finite element model updating using ambient vibration test results. *Journal of Structural Engineering, 131(4), pp.617-628*.
- James III, G.H., Carne, T.G. and Lauffer, J.P., 1993. The natural excitation technique (NExT) for modal parameter extraction from operating wind turbines (No. SAND--92-1666). *Sandia National Labs, Albuquerque, NM (United States)*.
- Jiang, X. and Mahadevan, S., 2008. Bayesian wavelet method for multivariate model assessment of dynamic systems. *Journal of Sound and Vibration, 312(4), pp.694-712*.
- Kabe, A. M., 1985. Stiffness matrix adjustment using mode data, *AIAA Journal 23(9), 1431–1436*.
- Kammer, D., 1988. Optimum approximation for residual stiffness in linear system identification. *AIAA Journal, 26(1), pp.104-112*.
- Kang, J.S., Park, S.K., Shin, S. and Lee, H.S., 2005. Structural system identification in time domain using measured acceleration. *Journal of Sound and Vibration, 288(1), pp.215-234*.

- Kijewski, T. and Kareem, A., 2003. Wavelet transforms for system identification in civil engineering. *Computer Aided Civil and Infrastructure Engineering*, 18(5), pp.339-355.
- Kölling, M., Resnik, B. and Sargsyan, A., 2014. Application of the random decrement technique for experimental determination of damping parameters of bearing structures. *BHS Berlin, Germany*.
- Lardies, J. and Gouttebroze, S., 2002. Identification of modal parameters using the wavelet transform. *International Journal of Mechanical Sciences*, 44(11), pp.2263-2283.
- Li, C., Smith, S.W. and Smith, S.W., 1995. Hybrid approach for damage detection in flexible structures. *Journal of Guidance, Control, and Dynamics*, 18(3), pp.419-425.
- Lim, Ch. A. 2016. Application of Vibration Based Damage Identification and Modal Identification, Concordia University, Montreal. Canada.
- Link, S. and El-Sayed, M.A., 1999. Spectral properties and relaxation dynamics of surface plasmon electronic oscillations in gold and silver nanodots and nanorods. 8410-8426.
- Manuel, F. 2012. Operational modal analysis for testing and monitoring^[11] of bridges and special structures. *Doctoral dissertation, University of Porto*.
- Mohl, B., Wahlberg, M. and Madsen, P.T., 2003. Ideal spatial adaptation via wavelet shrinkage. *The Journal of the Acoustical Society of America*, 114, pp.1143-1154.
- Møller, N., Herlufsen, H. and Gade, S., 2005, April. Stochastic Subspace Identification Techniques in Operational Modal Analysis. *In 1st IOMAC Conference, Denmark*.
- Morsy, R., Marzouk, H., Haddara, M. and Gu, X., 2017. Multi-channel random decrement smart sensing system for concrete bridge girders damage location identification. *Engineering Structures*, 143, pp.469-476.
- Ndambi, J.M., Peeters, B., Maeck, J., De Visscher, J., Wahab, M.A., Vantomme, J., De Roeck, G. and De Wilde, W.P., 2000. Comparison of techniques for modal analysis of concrete structures. *Engineering Structures*, 22(9), pp.1159-1166.
- Neild, S.A., McFadden, P.D. and Williams, M.S., 2003. A review of time-frequency methods for structural vibration analysis. *Engineering Structures*, 25(6), pp.713-728.
- Parloo, E. 2003. Application of Frequency-Domain System Identification Techniques in the Field of Operational Modal Analysis. *PhD Thesis, Vrije Universiteit Brussel, Belgium*.
- Peeters, B. and De Roeck, G., 2001. One-year monitoring of the Z24-Bridge: environmental effects versus damage events. *Earthquake engineering & structural dynamics*, 30(2), pp.149-171.
- Piombo, B.A.D., Fasana, A., Marchesiello, S. and Ruzzene, M., 2000. Modelling and identification of the dynamic response of a supported bridge. *Mechanical Systems and Signal Processing*, 14(1), pp.75-89.

- Qian, S., 2002. Introduction to time-frequency and wavelet transforms. *Prentice Hall, United States*.
- Qin, Q., Li, H., Qian, L.Z. and Lau, C.K., 2001. Modal identification of Tsing Ma bridge by using improved eigensystem realization algorithm. *Journal of sound and vibration*, 247(2), pp.325-341.
- Rainieri, C., Fabbrocino, G., 2014. Operational Modal Analysis of Civil Engineering Structures. Springer, New York, Heidelberg, Dordrecht, London.
- Rhee, W., 2000. Linear and nonlinear model reduction in structural dynamics with application to model updating. *Doctoral dissertation, Texas Tech University*.
- Ricles, J.M., 1991. Nondestructive structural damage detection in flexible space structures using vibration characterization. *Texas A and M Univ., NASA*.
- Rizzo, P. and di Scalea, F.L., 2005. Ultrasonic inspection of multi-wire steel strands with the aid of the wavelet transform. *Smart Materials and Structures*, 14(4), p.685.
- Rodrigues, J., Brincker, R. and Andersen, P., 2004, January. Improvement of frequency domain output-only modal identification from the application of the random decrement technique. *In Proc. 23rd Int. Modal Analysis Conference, Deaborn, MI*.
- Rodrigues, J., Brincker, R. and Andersen, P., 2004, January. Improvement of frequency domain output-only modal identification from the application of the random decrement technique. *In Proc. 23rd Int. Modal Analysis Conference, Deaborn, MI*.
- Sabamehr, A., and Bagchi, A. 2015. "Updating the mathematical models of bridges using data-driven techniques", IWSHM, Stanford University, CA, USA.
- Sabamehr, A., Roy, T.B., Mirshafiei, M. and Bagchi, A. 2017. "Comparative Study on different methods for noise reduction in the ambient vibration signal of structures for modal identification", CSCE conference, Vancouver, British Columbia, CA.
- Sabamehr, A., Roy, T. B., Patel, S. S., Bagchi, A., Tirca, L., Panigrahi, S. K. and Chourasia, A. Operational Modal Analysis of a five storey scaled frame Structure in Frequency, Time and Time-Frequency Domai, *Journal of vibration and control*.
- Sabamehr, A., Bagchi, A., Tirca, L., Panigrahi, S. K. and Chourasia, A., 2017. Model Updating and Parameter Identification of a Steel Cantilever Beam using Forced and Ambient Vibration Responses in Differen, *IOMAC, Ingolstadt, Germany*.
- Sato, T. and Sato, M., 1997. Structural identification using neural network and Kalman filter algorithms. *Doboku Gakkai Ronbunshu*, 1997(563), pp.1-10.
- Smith, S.W., 1992, April. Iterative use of direct matrix updates: connectivity and convergence. *In Proc. of the 33rd AIAA Structures, Structural Dynamics and Materials Conference (pp. 1797-1806)*.

Sohn, H., Dzwonczyk, M., Straser, E.G., Kiremidjian, A.S., Law, K.H. and Meng, T., 1999. An experimental study of temperature effect on modal parameters of the Alamosa Canyon Bridge. *Earthquake engineering & structural dynamics*, 28(8), pp.879-897.

Staszewski, W.J., 1997. Identification of damping in MDOF systems using time-scale decomposition. *Journal of sound and vibration*, 203(2), pp.283-305.

Stubbs, N., 1995. Field verification of a nondestructive damage localization and severity estimation algorithm. *IMAC XIII – 13th International Modal Analysis Conference. Nashville, US.*

Tsai, C.H. and Hsu, D.S., 2002. Diagnosis of reinforced concrete structural damage base on displacement time history using the back-propagation neural network technique. *Journal of Computing in Civil Engineering*, 16(1), pp.49-58.

Turi, E.Y., 2007. Output only Modal Analysis. (Master dissertation). *Blekinge Institute of Technology, Karlskrona, Sweden.*

Urgessa, G.S., 2011. Vibration properties of beams using frequency-domain system identification methods. *Journal of Vibration and Control*, 17(9), pp.1287-1294.

Welch, P.D., 1967. The use of fast Fourier transform for the estimation of power spectra: A method based on time averaging over short, modified periodograms. *IEEE Transactions on audio and electroacoustics*, 15(2), pp.70-73.

Wijesundara, K.K., Negulescu, C., Monfort, D. and Foerster, E., 2012, September. Identification of modal parameters of ambient excitation structures using continuous wavelet transform. *In 15th World Conference on Earthquake Engineering: 15th WCEE, Portugal.*

Xu, B., Wu, Z.S. and Yokoyama, K., 2003. Response time series based structural parametric assessment approach with neural networks. *In Proceedings of the First International Conference on Structural Health Monitoring and Intelligent Infrastructure, Tokyo, Japan (Vol. 1, pp. 601-609).*

Yan, B., Miyamoto, A. And Goto, S., 2004. A comparison of wavelet transform and Hilbert-Huang transform for modal parameter extraction of structure. *Journal of Applied Mechanics*, 7, pp.1167-1178.

Yan, B.F., Miyamoto, A. and Brühwiler, E., 2006. Wavelet transform-based modal parameter identification considering uncertainty. *Journal of Sound and Vibration*, 291(1), pp.285-301.

Yang, J.N., Lei, Y., Pan, S. and Huang, N., 2003. System identification of linear structures based on Hilbert–Huang spectral analysis. Part 1: normal modes. *Earthquake Engineering & Structural Dynamics*, 32(9), pp.1443-1467.

Yi, T.H., Li, H.N. and Zhao, X.Y., 2012. Noise smoothing for structural vibration test signals using an improved wavelet thresholding technique. *Sensors*, 12(8), pp.11205-11220.

Zimmerman, D.C. and Kaouk, M., 1992. Eigenstructure assignment approach for structural

damage detection. *AIAA Journal (USA)*, 30(7), pp.1848-1855.

Zimmerman, D.C. and Kaouk, M., 1994. Structural damage detection using a minimum rank update theory. *Transactions-American Society of Mechanical Engineers Journal of Vibration and Acoustics*, 116, pp.222-222.

Zimmerman, D.C. and Simmermacher, T., 1994. Model refinement and system health monitoring using data from multiple static loads and vibration tests. *Paper No. AIAA-94-1714-CP*.

Appendix A – FE model of five storey frame

The frame has been modeled as a massless frame with concentrated mass in center of mass which is located in the middle of each floor.

Total number of Nodes: 24

Total number of Elements: 45

Type of bridge modeling: 3D frame with shell

Material and Sectional Properties:

Modulus of Elasticity (E) = 24855578 KN/m²

Poisson ratio (U) = 0.2

Weight per Unit Volume = 0 KN/m³

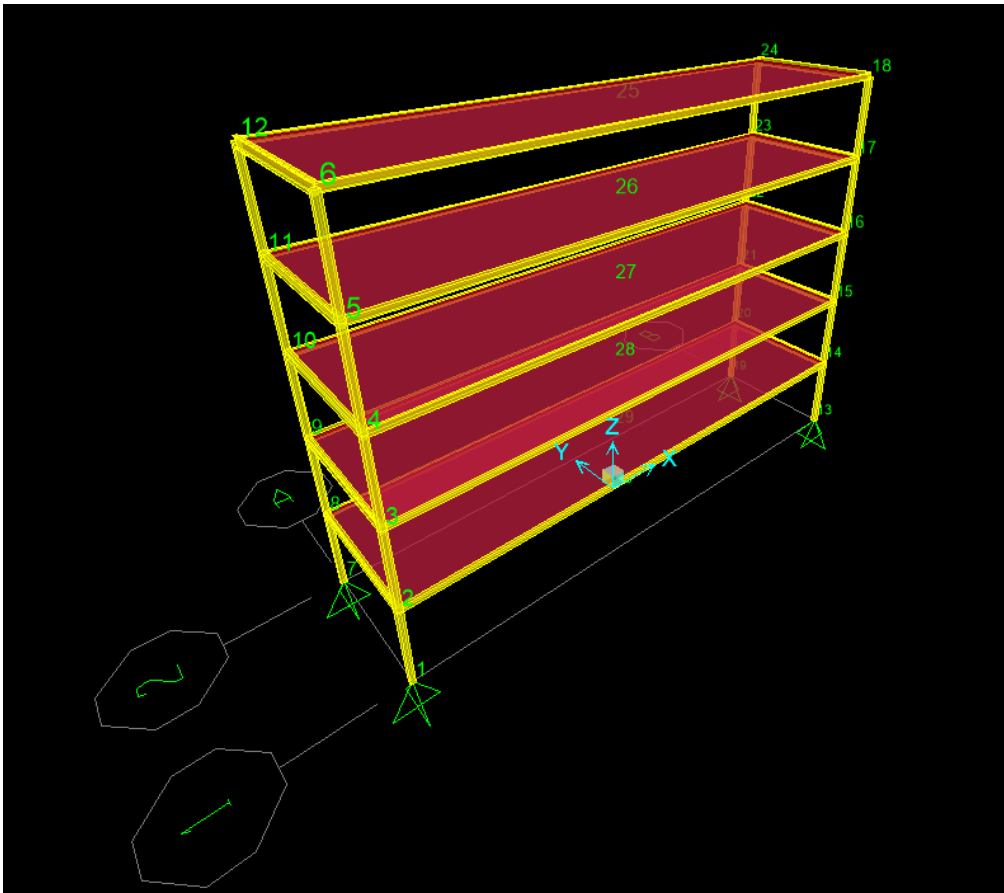
Shear Modulus (G) = 10356491 KN/m²

No.	Cross sectional area (m ²)	Moment of Inertia about axis 2 (m ⁴)	Moment of Inertia about axis 3 (m ⁴)	Torsional constant (m ⁴)
18x18	0.0324	8.748E-05	8.748E-05	1.478E-08
20x10	0.02	6.667E-05	1.667E-05	4.578E-05

Thin – Shell with 0.05 m thickness.

Support Conditions:

All supports type (Continuous beam) = Restraint in u2, u3 and r1 (local coordinate in SAP2000).



Appendix B - FE model of PSCB Bridge

Total number of Nodes: 1565

Total number of Elements: 782

Type of bridge modeling: Continuous longitudinal Bridge

Material and Sectional Properties:

Modulus of Elasticity (E) = 27388993 KN/m²

Poisson ratio (U) = 0.167

Weight per Unit Volume = 24.5166 KN/m³

Shear Modulus (G) = 11734787 KN/m²

Cross sectional area = 9537140 mm²

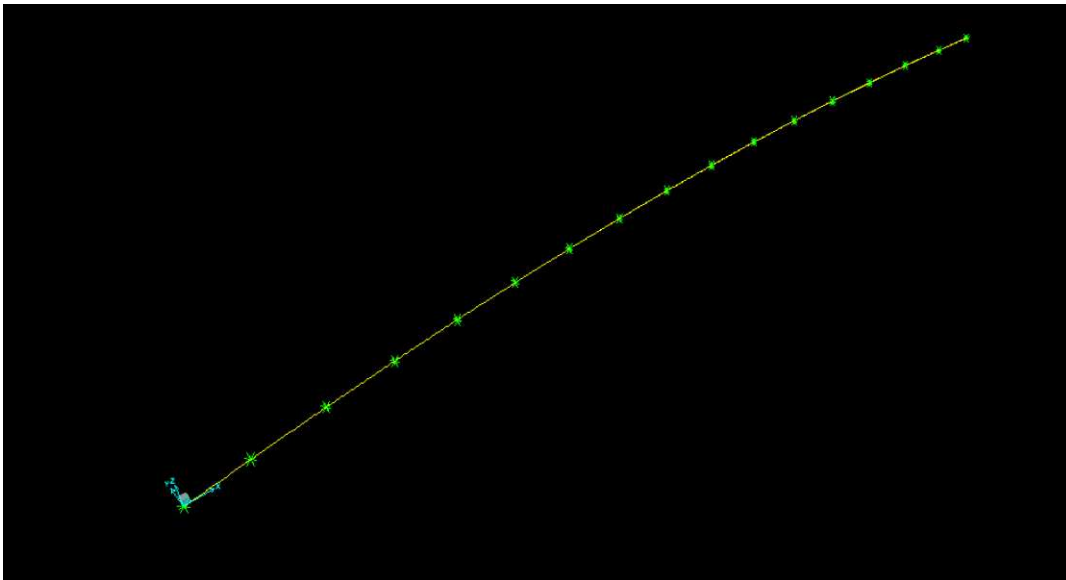
Moment of Inertia about axis 2 = 6.586E+13 mm⁴

Moment of Inertia about axis 3 = 1.173E+13 mm⁴

Torsional constant = 2.207E+13 mm⁴

Support Conditions:

All supports type (Continuous beam) = Restraint in u2, u3 and r1 (local coordinate in SAP2000).



Appendix C – FE model of Voided Slab Bridge

Total number of Nodes: 1358

Total number of Element: 2461

Type of bridge modeling: 3D without shell

Material and Sectional Properties:

Modulus of Elasticity (E) = 26700000 KN/m²

Poisson ratio (U) = 0.167

Weight per Unit Volume = 24.5166 KN/m³

Shear Modulus (G) = 11439589

There are 109 different cross sections which have been used in this bridge. All are rounded surface cross sections.

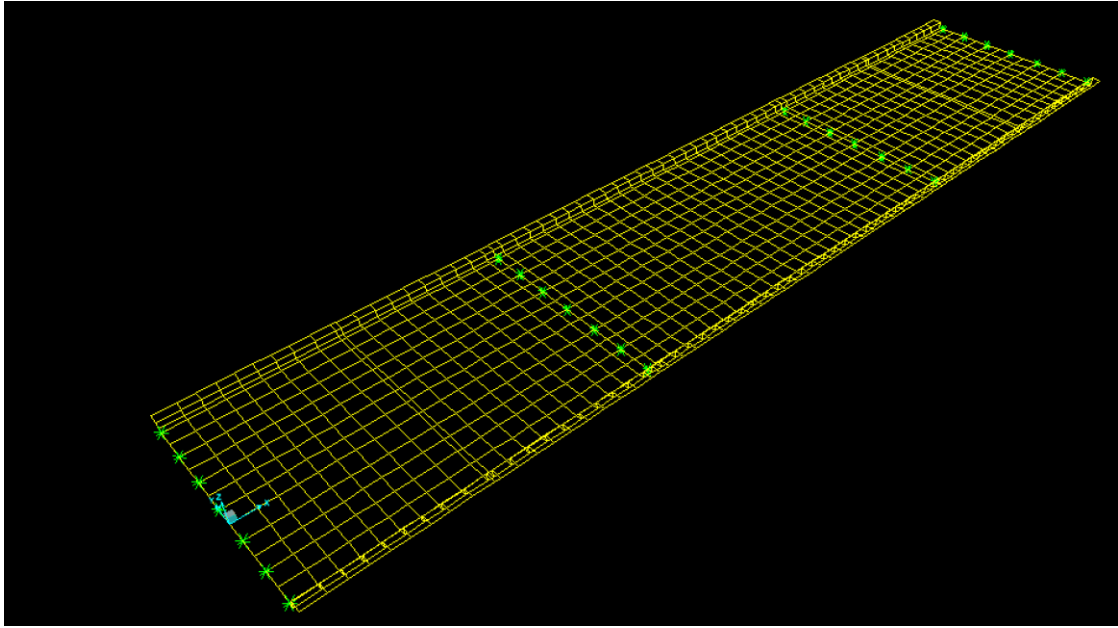
No.	Cross sectional area (m ²)	Moment of Inertia about axis 2 (m ⁴)	Moment of Inertia about axis 3 (m ⁴)	Torsional constant (m ⁴)
1	100	833.333	833.333	1406.25
2	1.32	0.1331	0.1584	0.244741
3	0.819893	0.0550684	0.138497	0.035266
4	0.841893	0.0572867	0.14647	0.0374161
5	0.885893	0.0617234	0.162761	0.0422458
6	1.4135	0.142528	0.194501	0.278375
7	0.941594	0.067333	0.183916	0.0495784
8	0.974594	0.0706605	0.197011	0.0544141
9	1.01868	0.0751114	0.21504	0.0615899
10	1.05168	0.0784389	0.229003	0.0674745
11	1.08468	0.0817664	0.243375	0.0737406
12	1.1287	0.0862069	0.263211	0.0827644
13	1.1617	0.0895344	0.278614	0.0900816
14	1.1947	0.0928619	0.294492	0.0975675
15	1.738	0.175248	0.361562	0.401262
16	1.76	0.177467	0.375467	0.409558
17	1.2277	0.0961894	0.310864	0.105498
18	1.1837	0.0917527	0.289146	0.0950956
19	1.1507	0.0884252	0.273428	0.0876435
20	1.11768	0.0850939	0.258176	0.0804047
21	1.07368	0.0806572	0.238538	0.0716383
22	1.04068	0.0773297	0.224305	0.06545
23	1.00768	0.0740022	0.210472	0.0597666
24	0.963594	0.0695514	0.192608	0.0527747
25	0.930594	0.0662239	0.179626	0.04803

26	0.897594	0.0628964	0.166969	0.0437388
27	0.852893	0.0583959	0.150498	0.0385368
28	0.01	8.33E-06	8.33E-06	1.41E-05
29	0.375	0.0488281	0.0028125	0.00954947
30	0.3	0.025	0.00225	0.00730015
31	1.05	0.0669922	0.126	0.148622
32	0.800463	0.04065	0.11609	0.0498069
33	0.818046	0.0418932	0.122469	0.0518266
34	0.853046	0.0443511	0.135667	0.0559651
35	1.12437	0.0717375	0.154716	0.166526
36	0.896796	0.0473988	0.153055	0.0618207
37	0.923046	0.0492157	0.163989	0.0655798
38	0.95808	0.0516301	0.179183	0.0710322
39	0.98433	0.0534296	0.191054	0.0752915
40	1.01058	0.0552227	0.203349	0.0798218
41	1.04558	0.0576042	0.220425	0.0860302
42	1.07183	0.0593839	0.233761	0.0908055
43	1.09828	0.0611712	0.247589	0.0960462
44	1.3825	0.0882064	0.287606	0.231496
45	1.4	0.0893229	0.298667	0.235851
46	1.12453	0.0629411	0.261875	0.101136
47	1.08953	0.0605802	0.242935	0.094346
48	1.06308	0.0587912	0.229264	0.0891378
49	1.03683	0.0570097	0.216081	0.0844697
50	1.00183	0.0546257	0.199202	0.0782983
51	0.97558	0.0528305	0.18705	0.0738922
52	0.94933	0.0510287	0.175318	0.0696142
53	0.914296	0.048611	0.160301	0.0642913
54	0.888046	0.0467913	0.149495	0.0606333
55	0.861796	0.0449627	0.139063	0.057089
56	0.826796	0.0425095	0.125711	0.0528218
57	1.8	0.3375	0.216	0.445685
58	1.30093	0.163578	0.196179	0.136587
59	1.39093	0.180453	0.229616	0.155043
60	1.39093	0.180453	0.229616	0.155043
61	1.9275	0.361406	0.265228	0.517707
62	1.46593	0.194515	0.259167	0.172664
63	1.51109	0.202995	0.277704	0.184459
64	1.57109	0.214245	0.303377	0.200927
65	1.61609	0.222683	0.323396	0.214484
66	1.66109	0.23112	0.344098	0.228769
67	1.72109	0.24237	0.372803	0.248644
68	1.76616	0.250829	0.395197	0.264672
69	1.81116	0.259266	0.418343	0.281465
70	2.37	0.444375	0.493039	0.790698

71	2.4	0.45	0.512	0.810685
72	1.85616	0.267704	0.442273	0.298662
73	1.79616	0.256454	0.410542	0.275849
74	1.75116	0.248016	0.387651	0.259359
75	1.70609	0.239558	0.365506	0.243548
76	1.64609	0.228308	0.33712	0.223777
77	1.60109	0.21987	0.316649	0.209962
78	1.55609	0.211433	0.296851	0.196741
79	1.49593	0.20014	0.271447	0.180322
80	1.45093	0.191703	0.253127	0.168918
81	1.40593	0.183265	0.235399	0.158321
82	1.34593	0.172015	0.212634	0.145486
83	1.56	0.2197	0.1872	0.33969
84	1.17	0.0926859	0.1404	0.187861
85	1.44875	0.170247	0.179693	0.294631
86	1.49625	0.175829	0.197954	0.313177
87	0.3855	0.00289125	0.0530456	0.00986442
88	1.34685	0.118641	0.192611	0.247337
89	1.37769	0.121358	0.206149	0.257563
90	1.41882	0.12498	0.225167	0.271301
91	1.44966	0.127697	0.240173	0.281672
92	1.48051	0.130414	0.255832	0.292094
93	1.52163	0.134037	0.277749	0.306057
94	1.58	0.131667	0.328693	0.319475
95	0.96	0.0288	0.2048	0.0880289
96	1.57	0.130833	0.322491	0.316214
97	1.53	0.1275	0.298465	0.303194
98	1.47	0.1225	0.26471	0.283748
99	1.43	0.119167	0.243684	0.270852
100	1.4	0.116667	0.228667	0.261222
101	1.37	0.114167	0.214279	0.251634
102	1.33	0.110833	0.196053	0.238926
103	1.3	0.108333	0.183083	0.229461
104	1.27	0.105833	0.170699	0.22006
105	1.23	0.1025	0.155072	0.207646
106	1.2	0.1	0.144	0.198439
107	1.55248	0.136754	0.294983	0.316573
108	1.58332	0.139471	0.312917	0.327123
109	1.5	0.125	0.28125	0.293457

Support Conditions:

All supports type (green color points in Figure below) = Restraint in u3 and r1 (local coordinate in SAP2000)



Appendix D – FE model of STB Bridge

Total number of Nodes: 3789

Total number of Element: 3982

Type of bridge modeling: 3D with surface

Material and Sectional Properties:

There are 17 different materials which are summarized as follows;

No.	Modulus of Elasticity (E) (KN//m ²)	Shear Modulus (G) (KN//m ²)	Poisson ratio (U)	Mass per Unit Volume (Kg/m ³)
1	2.06E+11	7.92E+10	0.3	8710.575
2	2.06E+11	7.92E+10	0.3	8710.575
3	2.06E+11	7.92E+10	0.3	8710.575
4	2.06E+11	7.92E+10	0.3	8710.575
5	2.06E+11	7.92E+10	0.3	8710.575
6	2.06E+11	7.92E+10	0.3	8710.575
7	2.06E+11	7.92E+10	0.3	8710.575
8	2.06E+11	7.92E+10	0.3	8710.575
9	2.06E+11	7.92E+10	0.3	8710.575
10	2.06E+13	1.03E+13	0	0
11	2.06E+11	7.92E+10	0.3	8710.575
12	2.06E+13	1.03E+13	0	0
13	2.06E+13	1.03E+13	0	0
14	2.40E+10	1.03E+10	0.167	3300.214
15	2.06E+11	7.92E+10	0.3	8710.575
16	2.26E+10	9.69E+09	0.167	2500.163
17	2.26E+10	9.69E+09	0.167	2500.163

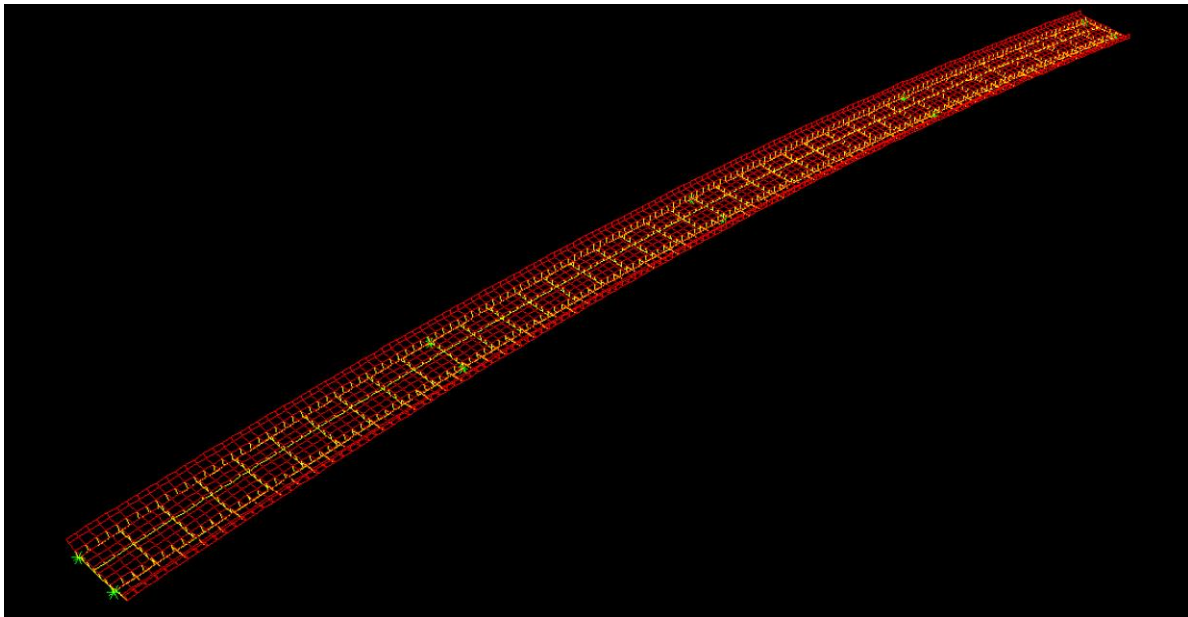
There are 17 different cross sections which have been used in this bridge.

No.	Cross sectional area (m ²)	Moment of Inertia about axis 2 (m ⁴)	Moment of Inertia about axis 3 (m ⁴)	Torsional constant (m ⁴)
1	0.104	0.0932	0.0897	0.1228
2	0.021	0	0.0062	0

3	0.7854	0.0491	0.0491	0.0982
4	0.0125	0	0.0011	0
5	0.109	0.0958	0.096	0.1285
6	0.7854	0.0491	0.0491	0.0982
7	0.7854	0.0491	0.0491	0.0982
8	0.013	0.0001	0.0007	0
9	0.119	0.101	0.1071	0.1364
10	0.124	0.1036	0.112	0.1393
11	0.108	0.095	0.0942	0.1228
12	0.134	0.1088	0.1269	0.1532
13	0.154	0.1192	0.1519	0.1672
14	0.104	0.0932	0.0897	0.1228
15	0.2	0	0	0
16	0.2	0	0	0
17	0.15	0	0	0

Support Conditions:

All supports type (green color points in Figure below) = Restraint in u2, u3 and r1 (local coordinate in SAP2000).



Appendix E - FE model of Three Storey Scaled Steel Frame

Total number of Nodes: 5

Total number of Elements: 3

Type of modeling: Linear model

Material and Sectional Properties:

Modulus of Elasticity (E) = $2E+11$ KN/m²

Poisson ratio (U) = 0.3

Mass per Unit Volume = 7849.0474 Kg/m³

Shear Modulus (G) = $7.69E+10$ KN/m²

Cross sectional area = $5.12E-4$ m²

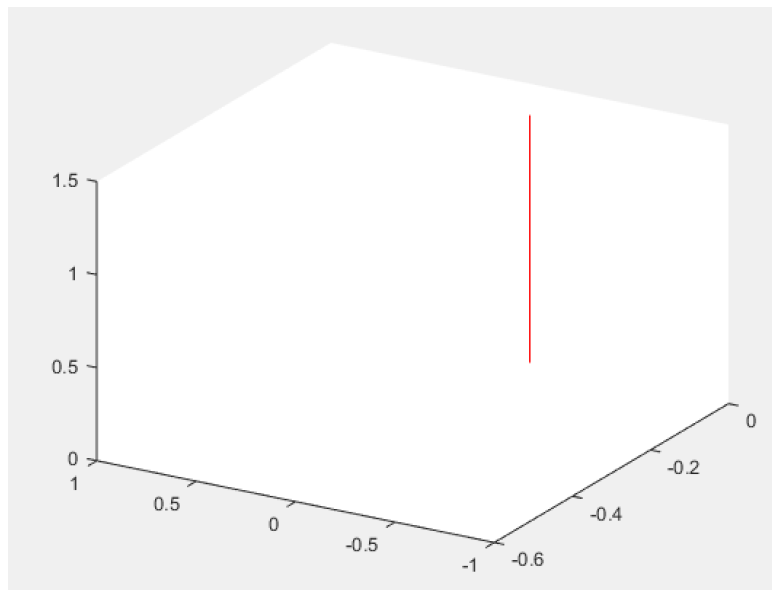
Moment of Inertia about axis 2 = $1.01E-08$ m⁴

Moment of Inertia about axis 3 = $1.01E-08$ m⁴

Torsional constant = $4.567E-09$ m⁴

Support Conditions:

Modelled like horizontal cantilever beam.



Appendix F - FE model of Steel Cantilever Beam

Total number of Nodes: 10

Total number of Elements: 8

Type of modeling: Linear model

Material and Sectional Properties:

Modulus of Elasticity (E) = $1.999\text{E}+11$ KN/m²

Poisson ratio (U) = 0.3

Mass per Unit Volume = 7849.0474 Kg/m³

Shear Modulus (G) = $7.69\text{E}+10$ KN/m²

Cross sectional area = $6.5\text{E}-4$ m²

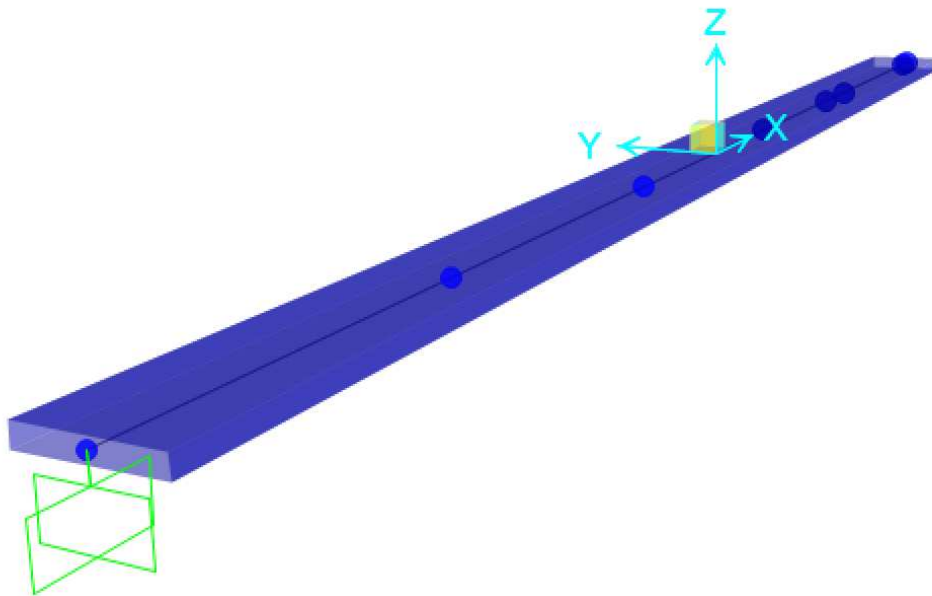
Moment of Inertia about axis 2 = $2.289\text{E}-07$ m⁴

Moment of Inertia about axis 3 = $5.417\text{E}-09$ m⁴

Torsional constant = $2.343\text{E}-07$ m⁴

Support Conditions:

Modelled like cantilever beam.



Appendix G – Publications

Journal papers

- **Sabamehr, A.**, Lim, Ch., and Bagchi, A. “System Identification and Model Updating of Highway Bridges using Ambient Vibration Tests”, *Journal of Civil in structural Health Monitoring* (accepted).
- **Sabamehr, A.**, and Bagchi, A. “Developing a new approach in Modal Analysis through Random Decrement Technique”, *Journal of Structural Health Monitoring* (under Review).
- **Sabamehr, A.**, and Bagchi, A. “System Identification and Modal Calibration of Three story Steel Scaled Frame”, *Journal of Engineering Structures* (under Review).
- **Sabamehr, A.**, Lim, Ch., and Bagchi, A. “Reference-Based and Reference-Free Methods in Vibration Based Damage Detection Techniques for the Bridge”, *Journal of Sensors* (under Review).
- **Sabamehr, A.**, Roy, T. B., Patel, S. S., Bagchi, A., Tirca, L., Panigrahi, S. K. and Chourasia, A. “Operational Modal Analysis of a five story scaled frame Structure in Frequency, Time and Time-Frequency Domain”, *Journal of vibration and control* (under Review).

Conference papers

- Soltani, A., **Sabamehr, A.**, and Bagchi, A. “System Identification and Vibration Based Damage Detection in a Concrete Shear Wall system”, SPIE, Denver, Colorado, US, March 2018.
- **Sabamehr, A.**, Mirshafiei, F. and Bagchi, A. “Development of New Technique in Multi Setups merging of Vibration Test system Identification”, SHMII-8- Brisbane, Australia, December 2017.
- Hakimtoroghi, N., **Sabamehr, A.**, Mirshafiei, M. and Bagchi, A. “Comparative study on two different types of sensors for measuring vibration response of structure”, SHMII-8- Brisbane, Australia, December 2017.
- **Sabamehr, A.**, Bagchi, A., Tirca, L., Panigrahi, S. K. and Chourasia, A. “Effectiveness of the Random Decrement Technique in Modal Identification of Structures using Ambient Vibration Response”, IWSHM, Stanford, CA, US, September 2017.

- **Sabamehr**, A., Bagchi, A., Tirca, L., Panigrahi, S. K. and Chourasia, A. “Model Updating and Parameter Identification of a Steel Cantilever Beam using Forced and Ambient Vibration Responses in Different”, IOMAC, Ingolstadt, Germany, May 2017.
- **Sabamehr**, A. and Bagchi. “A comparative study on book shelf steel structure based on frequency domain, time domain and time-frequency plane modal analysis, SPIE, Portland, Oregon, US, March 2017.
- Banerji, S. Roy, T. B., **Sabamehr**, A. and Ashutosh Bagchi. “Experimental validation of a structural damage detection method based on Marginal Hilbert Spectrum”, SPIE, Portland, Oregon, US, March 2017.
- **Sabamehr**, A. and Bagchi, A. “Pre and Post merging of Multi setup Vibration Test of Eight Story Full Scale Frame Building”, CSCE conference, Vancouver, British Columbia, CA, May 2017.
- **Sabamehr**, A., Roy, T. B., Mirshafiei, M. and Bagchi, A. “Simplified procedure for estimating building mass for prediction of seismic response”, CSCE conference, Vancouver, British Columbia, CA, May 2017.
- **Sabamehr**, A. and Bagchi, A. “Model update methods for vibration based damage detection in three story book shelf”, OMICS Steel Conference, Las Vegas, USA, September 2016.
- **Sabamehr**, A., Bagchi, A. and Tirca, L. “Modal Testing and System identification of a three story steel frame”, 8th European workshop on Structural Health Monitoring (EWSHM), Bilbao, Spain, July 2016.
- Lim, Ch., **Sabamehr**, A. and Bagchi, A. “system Identification and Damage Detection Techniques in Prestress concrete Box Bridge”, CSCE conference, London, Ontario, CA, May 2016.
- **Sabamehr**, A. and Bagchi, A. “Updating the mathematical models of bridges using data-driven techniques”, the International on Structural Health Monitoring Stanford University (IWSHM), CA, USA, September 2015.
- **Sabamehr**, A. and Bagchi, A. “Investigation of Various Types of Base Isolator on Seismic Behavior of a Box Girder Continuous Bridge”, Forensic Engineering 7th Proceeding ASCE, USA, November 2015.

Poster presentation

- **Sabamehr**, A. and Bagchi, A. “The effect of using nanosilica in permeability and compressive strength of Concrete under condition of Caspian Sea”, Edmonton, Canada, IC-IMPACT 2016, May 2016 (Oral Presentation).
- Banerji, S., **Sabamehr**, A. and Bagchi, A. “Fire resistance by Nanoclay coating on fibre reinforced polymer for structural strengthening”, Edmonton, Canada, IC-IMPACT 2016, May 2016 (Oral Presentation).
- **Sabamehr**, A. and Bagchi, A. “Updating the mathematical models of bridges using data-driven techniques”, Toronto, Canada, IC-IMPACT 2015, June 2015 (Oral Presentation).
- **Sabamehr**, A. and Bagchi, A. “Performance of Different Base Isolation Systems in a Continuous Box Girder Bridge”, the 21st Annual CEGSS conference, McGill University, May 2014 (Oral Presentation).

Awards

- Excellence in Collaboration and Creativity award in IC-IMPACT Summer Institute, 2016
- Top 15 posters in Annual General Meeting of IC-IMPACTS Annual Conference, 2016
- Mentorship group Competition Award in IC-IMPACTS Annual Conference, 2016
- Avtar Pall Graduate Award in Earthquake Engineering, Winter, 2016
- Excellence in Collaboration and Creativity award in IC-IMPACTS Summer Institute, 2015
- Partial Tuition Scholarship for International student Award in Concordia University, Winter 2014